AD_____

Award Number: DAMD17-02-1-0455

TITLE: Tumor-Host Interaction in Breast Cancer Bone Metastasis

PRINCIPAL INVESTIGATOR: Janet Price, Ph.D.

CONTRACTING ORGANIZATION: The University of Texas M.D. Anderson Cancer Center
Houston, TX 77030

REPORT DATE: January 2006

TYPE OF REPORT: Final

PREPARED FOR: U.S. Army Medical Research and Materiel Command
Fort Detrick, Maryland 21702-5012

REPORT DOCUMENTATION PAGE

Form Approved
OMB No. 0704-0188

1. REPORT DATE *(DD-MM-YYYY)*	**2. REPORT TYPE**	**3. DATES COVERED** *(From - To)*
01-01-2006	Final	15 MAY 2002 - 15 DEC 2005

4. TITLE AND SUBTITLE
Tumor-Host Interaction in Breast Cancer Bone Metastasis

5a. CONTRACT NUMBER

5b. GRANT NUMBER
DAMD17-02-1-0455

5c. PROGRAM ELEMENT NUMBER

6. AUTHOR(S)
Janet Price, Ph.D.

E-mail: jprice@mdanderson.org

5d. PROJECT NUMBER

5e. TASK NUMBER

5f. WORK UNIT NUMBER

7. PERFORMING ORGANIZATION NAME(S) AND ADDRESS(ES)

The University of Texas M.D. Anderson Cancer Center
Houston, TX 77030

8. PERFORMING ORGANIZATION REPORT NUMBER

9. SPONSORING / MONITORING AGENCY NAME(S) AND ADDRESS(ES)
U.S. Army Medical Research and Materiel Command
Fort Detrick, Maryland 21702-5012

10. SPONSOR/MONITOR'S ACRONYM(S)

11. SPONSOR/MONITOR'S REPORT NUMBER(S)

12. DISTRIBUTION / AVAILABILITY STATEMENT
Approved for Public Release; Distribution Unlimited

13. SUPPLEMENTARY NOTES

14. ABSTRACT

The proposal will test the hypothesis that bone represents a unique microenvironment favoring the survival and growth of metastatic breast cancer cells. Further, that cells in breast cancer bone metastases are specialized populations of cancer cells, endowed with properties that promote their growth in bone. The presence of breast cancer cells can disrupt the normal balance of bone turnover and promote osteoclast activity. Understanding the biology of breast cancer bone metastasis and the contribution of cancerderived factors, such as platelet-derived growth factor (PDGF) will lead to new approaches for control or prevention of this significant clinical problem. Expression analyses will be performed using cDNA arrays, testing samples from breast cancer cell lines growing in different conditions – *in vitro* and *in vivo* (direct injection into bone or mammary fatpad, and/or metastases from different organs in mice). The arrays will be used to identify cytokines and receptors, and genes involved in specific pathways (Cell cycle regulation, cell death, metastasis, and invasion, signal transduction, angiogenesis). One of the factors known to promote bone resorption is PDGF, and the consequences of release of PDGF by metastatic breast cancer cells will be determined *in vitro* using immortalized osteoblasts.

15. SUBJECT TERMS
Metastasis; tumor-host interactions; cytokines; growth factors

16. SECURITY CLASSIFICATION OF:			**17. LIMITATION OF ABSTRACT**	**18. NUMBER OF PAGES**	**19a. NAME OF RESPONSIBLE PERSON**
					USAMRMC
a. REPORT	**b. ABSTRACT**	**c. THIS PAGE**			**19b. TELEPHONE NUMBER** *(include area code)*
U	U	U	UU	52	

Standard Form 298 (Rev. 8-98)
Prescribed by ANSI Std. Z39.18

Table of Contents

Tumor-host interactions in breast cancer bone metastasis

INTRODUCTION:

Breast cancer is the most common cancer (after non-melanoma skin cancer) of women in the United States of America. Twenty percent of women with early stage, node-negative breast cancer may subsequently develop metastatic disease, while as many as 90% of women with locally advanced, or with extensive lymph node involvement will develop metastases [2]. In addition to the axillary lymph nodes, other sites where breast cancer metastases are found include the liver, lungs and brain. However, the most common site of breast cancer metastasis is the bone [3-5]. Breast cancer metastases in bone predominantly present as osteolytic lesions. Such lesions can have serious complications, including hypercalcemia, pain, pathologic fractures and central nervous compromise (spinal cord or nerve root compression)[6]. Bone metastases are the most common cause of pain for cancer patients, resulting from either mechanical or chemical stimulation of pain receptors in the periosteum or endosteum. Pressure effects, microfractures and cytokine release also contribute to the pain [7]. Patients with bone as the first site of relapse of breast cancer can have a significantly longer survival than patients with liver as the first site (20 months vs. 3 months median survival after relapse) [6]. However, the prolonged course of a disease with such complications as bone pain and pathological fractures severely reduces a patient's quality of life, and can make heavy demands on health care resources. There is increasing support for the idea that certain properties of breast cancer cells contribute to the high incidence of bone metastases of this disease. One observation is the correlation between expression of parathyroid hormone related protein (PTHrP) and breast cancer bone metastasis [8]. PTHrP has been shown to be upregulated in breast cancer cells exposed to TGF-β1[9]. This may serve to enhance PTHrP expression locally, since the bone matrix is a rich source of a variety of growth factors, including insulin-like growth factors I and II (IGF-I, IGF-II) and TGF-β[10,11].

In healthy adult bone there is a continuous process of turnover with a balance maintained between resorption and new bone formation. In post-menopausal women or in conditions of estrogen depletion the balance of normal bone turnover can become uncoupled. Osteoblast function is reduced while osteoclast function is maintained, leading to net bone loss. Multiple cytokines and hormones are involved in osteoblast stimulation of osteoclastogenesis. Many of these, for example PTHrP, IL-6, IL-11 and M-CSF, are expressed by tumor cells [12]. Another key factor is the TNF-like cytokine osteoprotegerin ligand (OPGL), also known as RANKL (receptor activator of NF-κB ligand) or ODF (osteoclast differentiation factor). The receptor RANK is expressed by osteoclasts. The action of OPGL is antagonized by a soluble "decoy" form of the receptor, osteoprotegerin (OPG), which is also expressed by osteoblasts [13] suggesting a finely tuned system for the local control of osteoclast activation. Exposure of osteoblasts to cytokines and other factors (including PTHrP) that promote bone resorption can stimulate expression of OPGL and reduce levels of OPG [14,15]. Bone resorption leads to the local release of matrix-bound factors and cytokines that normally stimulate osteoblasts to form new bone [10], yet could also promote the survival and growth of breast cancer cells. As noted above, TGF-β, which is abundant in bone matrix, can increase PTHrP production by metastatic breast cancer cells. In a preliminary study we found that TGF-β treatment of breast cancer cells increased the release of PDGF, another factor which can stimulate bone resorption. Others have shown that the media from cultures of resorbing bone are chemotactic and growth stimulatory for rat and human breast cancer cells [16,17]. Breast cancer bone metastases are commonly found in sites of active bone

remodeling, predominantly in trabecular bone, suggesting that the growth and survival of metastatic cells are promoted in areas of remodeling one.

A report by Kang et al [18] was published in 2003, since the last annual report, describing studies with a very similar goal to those of this award, to identify genes important for bone metastasis of breast cancer. Their study used gene expression array analysis of variants of the MDA-MB-231 breast cancer cell line that had been isolated from bone metastases generated from the left heart injection into nude mice. Among the set of genes identified were CXCR4 and Connective tissue growth factor (CTGF). CXCR4 is a chemokine receptor for CXCL12/Stromal derived factor 1-α (SDF1α), and expression of the receptor has been shown to contribute to the metastatic dissemination of breast cancer cells in SCID mice [19]. CTGF is a reported to act as an angiogenic factor and has been linked to malignant progression of breast cancers [20]. In other studies in the laboratory, CTGF was shown to have increased expression in lung metastasis derived variants of the GI101A breast cancer cell line [21]. Thus, the increased expression of CTGF may be more associated with metastatic potential, rather than specifically with bone metastasis ability.

The hypothesis tested in this work is that bone represents a unique microenvironment favoring the survival and growth of metastatic breast cancer cells. Further, that cells in breast cancer bone metastases are specialized populations of cancer cells, endowed with properties that promote their growth in bone. The presence of breast cancer cells can disrupt the normal balance of bone turnover and promote osteoclast activity. Understanding the biology of breast cancer bone metastases and the contribution of cancer cell-derived factors, such as platelet-derived growth factor (PDGF), will lead to new approaches for control or prevention of this significant clinical problem.

BODY:

Specific Aim #1: Gene expression comparisons of breast cancer cells growing *in vivo* and *in vitro*

Analyses of gene expression were proposed using two breast cancer cell lines, injected into nude mice to generate tumors, in the mammary fatpad (as previously described [22]), and into the tibia, which is a model for growth of cancer in the bone [23,24]. The two cell lines used for the analyses were SUM 149, a line from an inflammatory breast cancer [25], and MDA-MB-435 [22]. Tumor tissues were recovered from mammary fatpad and bone tumors, and total RNA isolated for analyses of gene expression. The total RNA from the tumors were used for expression array analyses using two array formats, interrogating the expression of genes involved in metastasis, and of inflammatory cytokines and receptors. This latter array was chosen as it included genes that are reported to be important for activation of osteoclasts, and essential part of the vicious cycle of human breast cancer metastasis. For the two cell lines the analyses with the arrays and/or real time PCR compared expression of the sets of genes in the original cell line grown *in vitro*, cells from tibia tumors in nude mice (selected), and propagated *in vitro*, and tissue recovered from tibia tumors in nude mice. These genes measured by PCR were for validation of the array results, and selected based on previous literature and reports of potential involvement in bone metastasis.

The data shown in tables in Appendix 1 (Tables A1-A4) are values for which sufficient hybridization to the arrays were detected. Genes scored as "absent" (average density <1.5-fold mean value of local backgrounds of lower than 75% of non-bleeding spots) were excluded from

the tables. Relatively few of the remaining genes were differentially expressed in the cells growing in the bone (*in vivo*) or in cells selected from the bone tumors, relative to expression of the original cells propagated *in vitro* (Fig 1). For the SUM149 series there is a parallel comparison of *in vivo* and selected cells, revealing 5 genes in the inflammatory cytokine and receptors series, and 4 genes in the metastasis-associated series that showed a consistent alteration in both samples compared with the original cells, using a 2-fold change in expression as a cut-off. Only few genes were consistently altered in bone tumors from both breast cancer cell lines. Based on the results from the array analyses, three additional gene targets were included in the real-time PCR analyses; these were IL-11, cathepsin K and MMP-11 (stromelysin-3).

Figure 1: Genes altered in the bone tumors of breast cancer cells

	SUM 149	MDA-MB-435
Cytokines and receptors	CCL11 (0.325 x) IL1R1 (4.07 x) IL-6 (5.4 x) IL-8RB (0.37 x) PF4 (0.02 x)	BCL6 (2.15 x) CCL15 (2.2 x) CCL20 (0.3 x) CEBPB (0.4 x) IL-11 (5.9 x) LTB4R (0.4 x) TNFRSF1B (0.3 x) XCL1 (4.0 x)
Metastasis-associated	Cathepsin K (12.9 x) GPNMB (5.6 x) MCAM (3.9 x) MMP-11 (5.4 x)	COL4A2 (3.3 x) Cathepsin K (2.0 x) Fibronectin 1 (2.7 x) MMP-11 (3.2 x) uPAR (4.1 x) S100A4 (3.6 x)

Fold expression is relative to the value of expression in the original parent cell line grown in vitro.

results shown in Tables 1 and 2 demonstrate that for many of the genes tested by real time PCR expression was induced in the breast cancer cells growing in the bone, compared with cells propagated in tissue culture. The results confirmed findings from the arrays, notable the increase in cathepsin K and MMP-11 expression in both breast cancer cell lines, and the increase in IL-6 in SUM 149, and increased expression of IL-11 in MDA-MB-435 bone tumors.

For some genes expression was induced in the tumor tissue samples and the high expression was retained in the cell line established from bone tumors (VEGF, CSF-1, IL-11,

OPG, CXCR4, cathepsin K, MMP-11, MMP-7 for MDA-MB-435; IL-6, IL-8, RANK, CTGF, cathepsin K, MMP-11 for SUM 149). This suggests that increased expression of these genes may contribute to the ability of the breast cancer cells to survive and/or grow in the bone environment. Sustained higher expression in the cells isolated from the tumor may indicate that these cells arose from sub-populations within the original, heterogeneous tumors that had the ability to grow in the bone. These selected cell populations will be used for analyses of what regulates expression of the genes that are increased in the process of bone tumor growth. This knowledge may then be applied to efforts to control the growth of breast cancer in bone metastases. Key targets of this effort would be cathepsin K and MMP-11, as increased expression is seen in both of the tumor variants we have tested. Some genes that only show increased expression in the bone tumors, not the selected cell line (PTHrP, PDGF-Rα and -Rβ, VEGF in SUM 149) represent genes that are subject to environmental regulation, yet the higher expression is not sustained when cells recovered from the bone are grown in tissue culture. Key environmental factors in regulating expression include hypoxia [26]and TGF-β, a cytokine abundant in bone matrix [9,11].

A previous annual report included information on RANKL expression in SUM 149 bone tumors. Analyses on additional samples failed to confirm this finding, and all other data shows that the breast cancer cells tested do not express detectable levels of RANKL, consistent with the findings of Thomas et al [15]. RANKL is required for activation of osteoclasts [13], and high osteoclast activity is seen in SUM 149 tibia tumors (Fig. 2), indicated by TRAP staining.

Figure 2: Section of SUM 149 tumor in tibia of nude mouse, stained for presence of red-staining tartrasine-resistant acid phosphatase (TRAP), indicating activated osteoclasts (Magnification x 200)

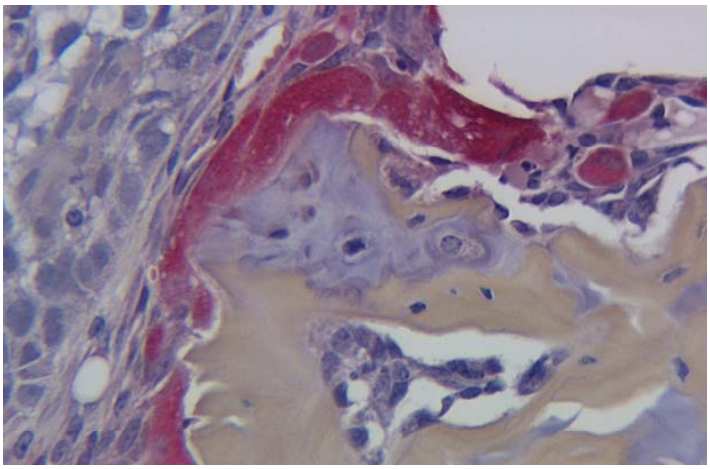

As no RANKL detection was detected in the tumor cells, the RANKL is likely contributed by osteoblasts (see Objective 2). Many of the other factors expressed by the breast cancer cells growing in the bone can contribute to stimulation of osteoblasts and osteoclasts, to promote osteoclast activation , including PTHrP, CSF-1, IL-6, IL-11 and MMP-7. A recent publication has reported that MMP-7, which is produced by osteoclasts as well as cancer cells, can process RANKL to a soluble form that can promote osteoclast activation [27]. Thus the expression of MMP-7 can contribute to the development of osteolysis of bone metastases. MMP-7 is one of the family of MMPs that is reported to be expressed by cancer cells, rather than primarily in stromal cells [28,29].

One factor that we hypothesized to be an important player in tumor-host interactions of breast cancer bone metastasis is the platelet-derived growth factor (PDGF) family of growth factors. PDGFs are among the cytokines and growth factors released by breast cancer cells that have the potential for promoting bone resorption [30,31,31]. The PDGFs form a family of disulfide binding dimeric isoforms; at present there are four known isoforms, A, B, C, and D, and two of these (C and D) require proteolytic activation [32,33]. PDGF A and B can form either homo- or heterodimers, and different cell types differ in expression of the PDGF isoforms. The two specific receptors, PDGF α- and β-receptor are members of the tyrosine kinase receptor super-family. Ligand binding promotes dimerization of receptor subunits, and triggers tyrosine-specific phosphorylation, initiating a signal transduction cascade and ultimately phenotypic changes [34,35]. PDGFs are potent bone mitogens which stimulate proliferation of osteoblasts, and also increase bone resorption, probably by increasing osteoclast number [30,30,36]. Osteoblasts express receptors for PDGF, and respond to the factors with various phenotypic changes, including upregulation of IL-6 [37]. There is less information on the actions of PDGFs directly on osteoclasts, although there is one report that these cells express PDGF receptors [31].

We previously reported the expression of PDGFs, and the induction of PDGF receptors in the tumors of MDA-MB-435 growing in the mammary fatpad and the bone of nude mice, detected by immunohistochemistry. While the ligand and receptor are present in the tumors from both sites, there is substantially more activation of the receptor in the bone tumors than in the mammary fatpad tumors. These data are included in a publication (Chelouche Lev et al, *Inhibition of Platelet-Derived Growth Factor Receptor Signaling Restricts the Growth of Human Breast Cancer in the Bone of Nude Mice*, Appendix) that investigated the consequence of blocking the activation of PDGF-receptors with the small molecule inhibitor STI571. Blockade of the PDGF receptor signaling was found to inhibit the development of the osteolytic tumors in nude mice, and reduce bone lysis. The observation that the breast cancer cells were expressing the receptor *in vivo* was an unexpected one, and thus the interpretation of the effects of the tyrosine kinase inhibitor is that of blocking possible autocrine and paracrine interactions initiated by the cancer cell-derived PDGF.

The RT-PCR data presented in Table 1 and 2 confirms the immunohistochemistry findings of induction of PDGF-receptors in the tumors. The mechanism(s) for this induction is not known. TGF-β, a cytokine released from bone matrix by the action of osteoclasts [10] has been reported to increase expression of PDGF in breast cancer cells [38], and we have confirmed this *in vitro* by ELISA measurements of supernatant from breast cancer cells treated with TGF-β, and PDGFs are reported to regulate the expression of the cognate receptors in some cells [39], again by unknown mechanism(s).

Comparison of gene expression patterns in breast cancer cells growing in bone and mammary fatpad tumors

To determine whether the induction in gene expression in breast cancer cells growing in vivo was specific to the bone environment, samples from mammary fatpad (mfp) tumors were included in real time PCR analyses. Due to technical problems in preparation of total RNA from the mfp tumors, only samples of MDA-MB-435 tumors were used. Multiple attempts to prepare RNA from SUM 149 tumors were unsuccessful, for reasons not yet resolved. When purity of these samples was checked on denaturing gels, very little undegraded RNA was seen; hence the following analyses were restricted to the MDA-MB-435 tumor line. Table 3 reports the results

of the PCR analyses, for selected genes that showed induced expression in the bone tumors of MDA-MB-435 series. There was minimal alteration in expression of CSF-1 and MMP-7 in the mfp tumors, while for VEGF the induction was similar, or greater than that seen in bone tumors. For IL-11, PTHrP, Cathepsin K and MMP-11, expression was increased in the mfp tumors, but not to the same level as that seen in bone tumors, notably for PTHrP. These results suggest that similar environmental factors may be regulating expression of these genes in the two sites of growth, and that the increase seen in the expression of some genes is not a reflection of a bone-environment specific modulation. However, MMP-7 showed only minimal increase in expression in the mfp tumors, while this was substantially increased in the bone tumors (and the bone-selected MDA-MB-435 variant cell line, Table 1). This data adds more support to further investigation of the role of MMP-7 in the development of osteolytic bone lesions, and the role of the environment in regulation of its expression by breast cancer cells. This is a direction of research that will be pursued in continuing studies.

Expression of the chemokine receptor CXCR4 in breast cancer cells.

As noted above, the report from Kang et al [18] reported that the chemokine receptor CXCR4 was increased in clones of the MDA-MB-231 cell line that was selected for ability to form bone metastases. Expression of CXCR4 was measured in a panel of breast cancer cell lines, and reported in a publication (Cabioglu et al, *CXCL-12/Stromal cell-derived factor1α transactivates HER2/neu in breast cancer cells by a novel pathway involving src kinase activation*, Appendix [1]). This investigation reported that cells with high HER2 expression also often show high CXCR4 expression, consistent with the report of Li et al [40]. Also, that SDF-1α, the ligand for CXCR4, can stimulate activation of HER2, and thus contribute to the malignant progression of breast cancer cells. SDF-1α is abundantly expressed in the bone marrow stroma and by osteoblasts, and would thus be a microenvironmental factor important in the regulation of breast cancer growth in bone marrow and bone. A further publication arising from this research (Cabioglu et al, *Chemokine receptor CXCR4 expression in breast cancer as a potential predictive marker of isolated tumor cells in bone marrow*, Appendix [41]), reported that high CXCR4 expression in breast cancer may be a potential marker in predicting isolated tumor cell in bone marrow. However, the real time PCR analyses of bone tumor samples did not show a consistent induction or selection of CXCR4 expression in breast cancer cells (Table 1 and 2). The finding of Kang et al [18]may thus suggest that the finding from MDA-MB-231 cell system does not necessarily reflect all breast cancers. However, the lack of change in expression may not necessarily indicate that the CXCR4 receptor does not have an important role in the development of bone and bone marrow metastases. We have determined that the SUM 149 cell line expresses relatively high levels of CXCR4, and responds to SDF1α stimulation with induced migration that can be blocked by the CXCR4 inhibitor AMD3100 (Fig 3.). Medium collected from cultures of human immortalized osteoblasts (hFOB) and bone marrow stromal cells (BMS) were very effective in stimulating migration; high levels of SDF1α were measured in the conditioned media by ELISA (> 6 μg/ml in media from confluent cultures).

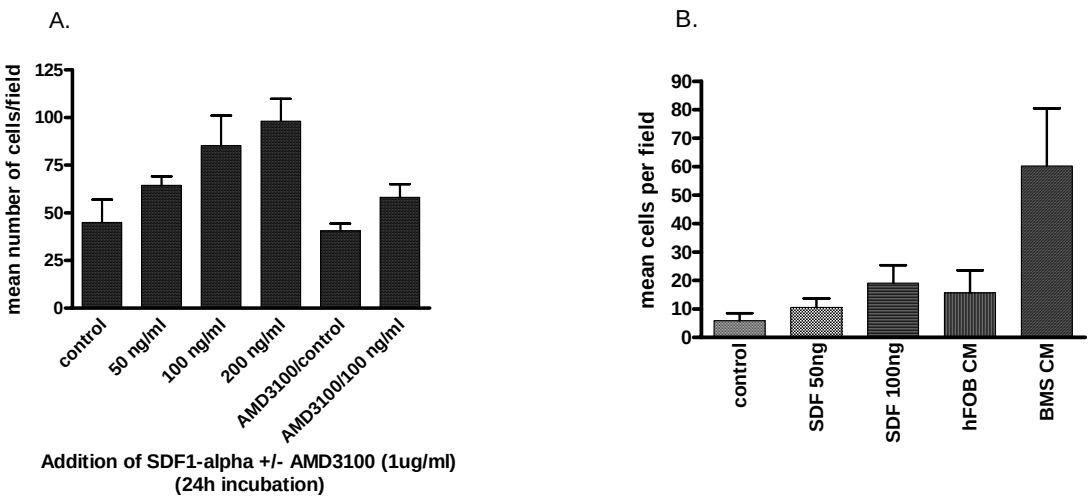

Fig.3 Stimulation of SUM149 migration with the chemokine SDF1α/CXCL12. A: A dose dependent increase in migration of cells that can be blocked in the presence of AMD3100. B: Migration increased in the response to conditioned media collected from osteoblasts (hFOB) and bone marrow stromal cultures (BMS). Migration assays are performed as described by Cabioglu et al [1].

Ongoing studies with the SUM149 cells will continue to investigate the role of CXCL12, as a factor released by bone marrow stromal cells and osteoblasts, in promoting the growth and survival of breast cancer cells capable of forming bone tumors.

Specific Aim #2 PDGF-mediated regulation of osteoblast expression of osteolytic cytokines

This aim employed a SV40-large T antigen transformed hFOB1.19 human fetal osteoblast cell line. These cells, grow actively at 34^{o}C, and grow slowly and differentiate at the permissive temperature of 39^{o} C [42]. Studies of PDGF receptor phosphorylation have been performed in cells at the permissive temperature, i.e. differentiated phenotype. In the previous report we described the results of PDGF stimulated phosphorylation of receptors in the cells, and stimulation of the receptors by medium collected from breast cancer cells.

Colony-formation assays were attempted to test the effect of PDGF on the hFOB1.19 cells; however, these produced no conclusive results, possibly as the cells grow poorly when plated at very low density used for such assays. As an alternate assay, the cells were plated at a higher density in 6-well plates, in serum-free medium supplemented with 1 or 5 ng/ml PDGF-BB. Over 3 weeks of culture, the numbers of cells surviving in the plates were significantly higher in the wells supplemented with PDGF compared with the control, although the numbers did not increase, suggesting that PDGF may act to promote the survival of osteoclasts (see annual report for 2003-2004). PDGF-treatment of the hFOB cells, when in differentiated state and in the absence of other growth factors showed increased phosphorylation of Akt (Fig. 4). This is consistent with the increased survival of the osteoblasts, since the Akt signaling pathway is

Fig.4: Activation of PDGF-Rβ and phospho-Akt in hFOB osteoblasts treated with PDGF-BB

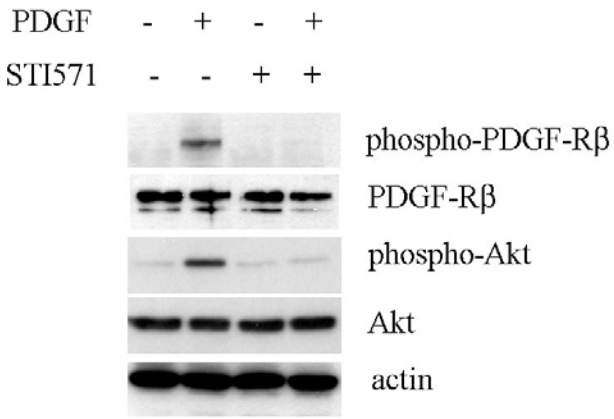

Fig 4 legend: Cultures of hFOB1.19 cells were serum-starved for 24 h, then stimulated with PDGF-BB (10 ng/ml) with or without STI571 (1.0μM). Lysates were used for immunoblot analysis of phospho-PDGF-Rβ and phospho-Akt activity, which was inhibited in the presence of STI-571

reported to enhance survival of cells [43]. Including the small molecule tyrosine kinase inhibitor STI571 (Gleevec), which inhibits signaling of PDGF-receptors (and also c-Abl and c-Kit kinases) abrogated the stimulation of Akt phosphorylation. We show in the publication appended to this report (Chelouche Lev et al.[44]) show that STI571 can also abrogate PDGF-receptor signaling in breast cancer cells growing in the bone of mice, and reduce the growth and osteolysis. The result shown in Fig 4 demonstrates that the inhibitor can also have effects in the normal cells present in the bone environment, and that are presumably being stimulated by the ligands (PDGFs) released by the tumor cells [44].

The effect of PDGF on expression of RANKL, OPG, MCSF and IL-6 was measured using quantitative RT-PCR. Total RNA was isolated from hFOB1.19 cells grown in the presence of 1 or 10 ng/ml PDGF BB, at 8 h incubation. Consistent with previous annual reports we found a transient increase in expression of RANKL and IL-6 (Fig. 5). The data do not unequivocally

Fig 5: Stimulation of osteoclast activating cytokine expression in hFOB1.19 cells

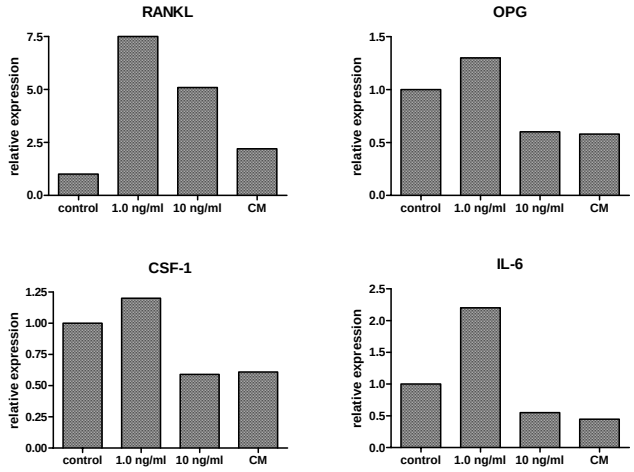

Expression of RANKL, OPG, CSF_1 and IL_6 measured by real time PCR in samples of cDNA from hFOB1.19 cells treated for 8 h with PDGF-BB.

identify PDGF as the factor in the breast cancer conditioned medium that is responsible for modulating the cytokines in the cells. Experiments using a neutralizing antibody to remove PDGF from the conditioned medium did not give consistent results, and the presence of the antibody alone appeared to stimulate receptor phosphorylation in the osteoblasts (although the antibody had been reported to be capable of PDGF depletion in published reports). An alternative approach being used in current experiments was to use the tyrosine kinase inhibitor STI571. The experiment described in Fig 5 was repeated but with the addition of 1.0 μM STI571. No difference was seen in the expression of CSF-1 and OPG, which were not substantially altered in the presence of PDGF-BB, (data not shown). However, the addition of STI571 abrogated the increase in RANKL and IL-6 expression (Fig, 6). Results shown are representative of repeated experiments, and will be included in a report that is being prepared for publication, on the role of PDGF in promoting osteoclast activation, related to the potential of

Fig. 6: Abrogation of PDGF-induced cytokine regulation with STI571

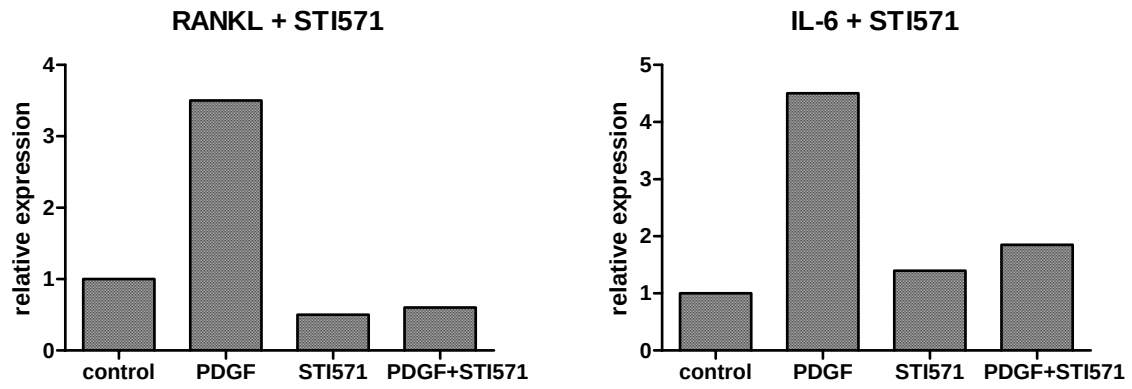

the inhibitor STI571 for reducing the osteolysis in bone tumors (as reported in our publication, Chelouche Lev et al, 2005.)

To demonstrate that the induction of RANKL and IL-6 expression in hFOB1.19 cells had an effect on the ability of the osteoblasts to activate osteoclasts, the immortalized cell line RAW 264.7 was used as a substitute for bone marrow derived cultures. Experiments that used bone marrow derived cells have failed to give reproducible results, presumably related to technical problems in the preparation and/or propagation of the primary cells. The immortalized line, RAW 264.7 was thus substituted for the experiments, and is used widely in similar studies of osteoclast activation. RAW 264.7 cells were incubated in the presence of RANKL (50 ng/ml) as a positive control for osteoclast activation, and the test conditions were PDGF-BB, and conditioned medium from hFOB1.19 cells with or without PDGF-BB pre-treatment. After 5 days incubation the cell cultures were fixed and stained for the presence of tartrasine-resistant acid phosphatase (TRAP), a marker of activated osteoclasts. Cells that were positive for TRAP and with > 3 nuclei were scored in triplicate cultures. The results are shown in Fig. 7, demonstrating that the medium from the osteoblast cultures that have been stimulated with PDGF can promote the differentiation of RAW 264.7, similar to the effect of recombinant

RANKL. Conditioned medium from the unstimulated-hFOB1.19 cells can increase the numbers of positive cells, but the increase was not statistically significant (P = 0.08, Student's t-test).

Fig. 7: Stimulation of differentiation of RAW 264.7 cells by conditioned media from osteoblast cells treated with PDGF

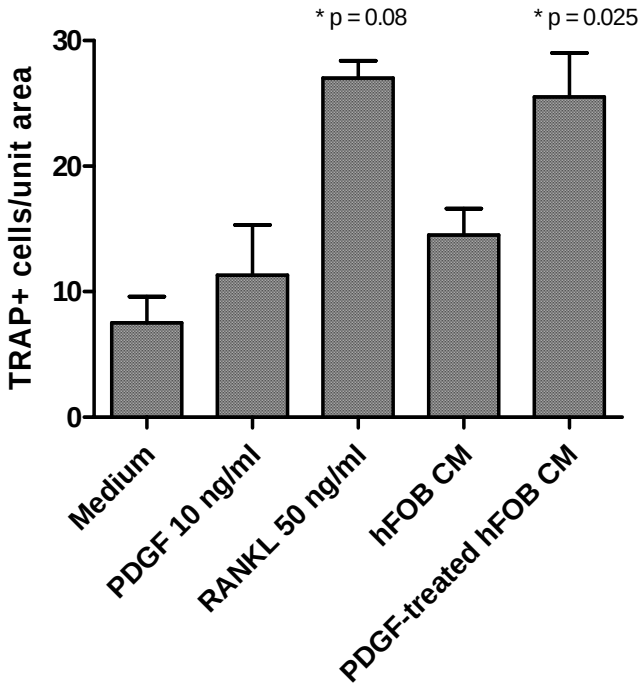

The results suggest that the PDGF-stimulation of osteoblasts in culture can promote release of factors that drive the differentiation of RAW 264.7 cells to activated osteoclasts. Continuing experiments, using depletion with neutralizing antibodies are seeking to confirm that RANKL and IL-6 in the conditioned medium are key active factors. The technical problems noted above with culture of primary bone marrow cells has delayed progress in completing this part of the objective, in addition to the studies investigating co-cultures of breast cancer cells with the osteoblasts and osteoclasts. As demonstrated in Fig. 7, we have now the appropriate conditions for an in vitro assay of osteoclast differentiation and activation, which will be used to complete the studies.

KEY RESEARCH ACCOMPLISHMENTS

- Demonstration of differential expression of multiple genes, including PDGF-Rβ, PTHrP, MMP-11, MMP-7, Cathepsin K, in breast cancer cells growing *in vivo* (in both bone and mammary fatpad tumors) compared with cells grown in tissue culture.
- Demonstration that induction of MMP-7 in breast cancer cells is noted in tumors growing in the bone, rather than in the mammary fatpad, suggesting that specific regulating factors in the bone microenvironment.

- The inhibition of breast cancer bone tumor growth by inhibition of PDGF-receptor signaling, using a small molecule inhibitor.
- Demonstration that PDGF and conditioned medium from breast cancer cells can regulate the expression of RANKL in immortalized osteoblasts.

REPORTABLE OUTCOMES

- Thesis, entitled "PDGF expression by breast cancer cells, and its role in regulating osteolytic cytokine expression in osteoblasts", presented by Claudia P. Miller to the faculty of the University of Texas Health Science Center at Houston Graduate School of Biomedical Sciences, in partial fulfillment of the requirement for the degree of Master of Science. August 2003.
- Oral presentation at The IVth International Conference on Cancer-Induced Bone Diseases, San Antonio, Dec 7-9, 2003; Title "Inhibition of Platelet-Derived Growth Factor Receptor Restricts the Growth of Breast Cancer Cells in the Bone but not in the Mammary Fatpad", D. Chelouche Lev, S.J. Kim, A. Onn, V. Stone, D.Y. Nam, S. Yazici, I.J. Fidler, and J. E. Price.
- Oral presentation at the Era of Hope DOD BCRP meeting, June 2005; title "Cytokines and growth factors involved in host-tumor interactions in breast cancer bone metastasis", J.E. Price, C. Miller, D. Chelouche Lev, S.J. Kim, S. Yazici, and I.J. Fidler.
- Publication: "Inhibition of Platelet-Derived Growth Factor Receptor Signaling Restricts the Growth of Human Breast Cancer in the Bone of Nude Mice ", D. Chelouche Lev, S.J. Kim, A. Onn, V. Stone, D.Y. Nam, S. Yazici, I.J. Fidler, and J. E. Price. *Clinical Cancer Research*, 11: 306-314, 2005.
- Publication: "Chemokine receptor CXCR4 expression in breast cancer as a potential predictive marker of isolated tumor cells in bone marrow" N. Cabioglu, A. Sahin, M. Doucet, E. Yavuz, A. Igci, E.O. Yildirim, E. Aktas, S. Bilgic, B. Kiran, G. Deniz, and J.E. Price. *Clinical and Experimental Metastasis*, 22: 39-46, 2005.
- Publication: "CXCL-12/Stromal cell-derived factor-1α transactivates HER2-neu in breast cancer cells by a novel pathway involving src kinase activation", N, Cabioglu, J. Summy, C. Miller, N.U. Parikh, A.A. Sahin, S. Tuzlali, K. Pumiglia, G.E. Gallick, and J.E. Price. *Cancer Research*, 65: 6493-6497, 2005.

LIST OF PERSONNEL RECEIVING PAY FROM THE RESEARCH EFFORT:
Janet E. Price, D.Phil, P.I.
Galina Kiriakova, Research Assistant.
Neslihan Cabioglu, MD, Ph.D., post-doctoral fellow.

CONCLUSIONS:

This grant tested the hypothesis that the bone represents a unique microenvironment favoring the survival and growth of metastatic breast cancer cells. The results demonstrate that the *in vivo* environment can regulate the expression of various genes, some of which are reported in the literature to promote osteoclast activation or to be important for bone metastasis (including PTHrP, IL-6, IL-11 and cathepsin K). The increased expression of some genes was maintained in new variants of breast cancer cell lines established from bone tumors generated in nude mice by –direct injection of the original cells. These represent selected sub-populations of breast

cancer cells, capable of growing in the bone environment. The results and the variant cell lines provide the basis for further investigation of microenvironmental regulation of genes, including (MMP-11 and cathepsin K) in breast cancer that may impact the progression of bone metastases. A notable finding was that the regulation of the protease MMP-7 in bone tumors and not in mammary fatpad tumors. The mechanism of this environmental regulation of MMP-7 will be the focus of further investigations, using the same models and approached developed in this project.

Increased expression of the PDGFs and PDGF-receptors, with the demonstration of activation of the receptors in the bone but not the mammary fatpad tumors, was another example of environmental regulation of genes in breast cancer cells. With the availability of the tyrosine kinase inhibitor STI571, which inhibits PDGF-R activation, we demonstrated that blockade of PDGF-R signaling can reduce the growth of breast cancer cells within the bone. However, the growth of the breast cancer cells was not completely inhibited. The other data from this study has demonstrated that multiple genes are regulated by the microenvironment of the bone, and inhibition of the signaling generated by only one may not successfully retard tumor growth. The model we have developed may, however, identify common pathways of regulation present within the bone environment, which could be targeted for to control of breast cancer bone metastasis growth.

REFERENCES:

1. Cabioglu, N., Summy, J., Miller, C., Parikh, N. U., Sahin, A. A., Tuzlali, S., Pumiglia, K., Gallick, G. E., and Price, J. E. CXCL-12/Stromal cell-derived factor-1α transactivates HER2-neu in breast cancer cells by a novel pathway involving src kinase activation. Cancer Res, *65*: 6493-6497, 2005.

2. Hagemeister, F. B., Buzdar, A. V., Luna, M. A., and Blumenschein, M. Causes of death in breast cancer: a clinicopathological study. Cancer, *46*: 162-167, 1980.

3. Viadana, E., Cotter, R., Pickren, J. W., and Bross, I. An autopsy study of metastatic sites of breast cancer. Cancer Res, *33*: 179-181, 1973.

4. Theriault, R. L. and Hortobagyi, G. N. Bone metastasis in breast cancer. Anti-Cancer Drugs, *3*: 455-462, 1992.

5. Colleoni, M., O'Neill, A., Goldhirsch, A., Gelber, R. D., Bonetti, M., Thurlimann, B., Price, K. N., Castiglione-Gertsch, M., Coates, A. S., Lindtner, J., Collins, J., Senn, H. J., Cavalli, F., Forbes, J., Gudgeon, A., Simoncini, E., Cortes-Funes, H., Veronesi, A., Fey, M., and Rudenstam, C. M. Identifying breast cancer patients at high risk for bone metastases. J.Clin.Oncol., *18*: 3925-3935, 2000.

6. Rubens, R. D. Bone metastases - the clinical problem. Eur.J.Cancer, *34*: 210-213, 1998.

7. Houston, S. J. and Rubens, R. D. Metastatic bone pain. Pain Reviews, *1*: 138-152, 1994.

8. Powell, G. J., Southby, J., Danks, J. A., Stillwell, R. G., Hayman, J. A., Henderson, M. A., Bennett, R. C., and Martin, T. J. Localization of parathyroid hormone-related protein in breast cancer metastases: Increased incidence in bone compared with other sites. Cancer Res, *51*: 3059-3061, 1991.

9. Yin, J. J., Selander, K., Chirgwin, J. M., Dallas, M., Grubbs, B. G., Wieser, R., Massague, J., Mundy, G. R., and Guise, T. A. TGF-β signaling blockade inhibits PTHrP secretion by breast cancer cells and bone metastases development. J.Clin.Invest., *103*: 197-206, 1999.

10. Mohan, S. and Baylink, D. J. Bone growth factors. Clin.Orthop.Res., *263*: 30-48, 1991.

11. Chirgwin, J. M. and Guise, T. A. Molecular mechanisms of tumor-bone interactions in osteolytic metastases. Crit.Rev.Eukaryotic Gene Exp., *10*: 159-178, 2000.

12. Pederson, L., Winding, B., Foger, N. T., Spelsberg, T. C., and Oursler, M. J. Identification of breast cancer cell line-derived paracrine factors that stimulate osteoclast activity. Cancer Res, *59*: 5849-5855, 1999.

13. Lacey, D. L., Timms, E., Tan, H.-L., Kelley, M. J., Dunstan, C. R., Burgess, T., Elliott, R., Colombero, A., Elliott, G., Scully, S., Hsu, H., Sullivan, J., Hawkins, N., Davy, E., Capparelli, C., Eli, A., Qian, Y.-X., Kaufman, S., Sarosi, I., Shalhoub, V., Senaldi, G., Guo, J., Delaney, J., and Boyle, W. J. Osteoprotegerin ligand is a cytokine that regulate osteoclast differentiation and activation. Cell, *93*: 165-176, 1998.

14. Horwood, N. J., Elliott, J., Martin, T. J., and Gillespie, M. T. Osteotropic agents regulate the expression of osteoclast differentiation factor and osteoprotegerin in osteoblastic stromal cells. Endocrinology, *139*: 4743-4746, 1998.

15. Thomas, R. A., Guise, T. A., Yin, J. J., Elliott, J., Horwood, N. J., Martin, T. J., and Gillespie, M. T. Breast cancer cells interact with osteoblasts to support osteoclast formation. Endocrinology, *140*: 4451-4458, 1999.

16. Manishen, W. J., Sivananthan, K., and Orr, F. W. Resorbing bone stimulates tumor cell growth. A role for the host microenvironment in bone metastasis. Am.J.Pathol., *123*: 39-45, 1986.

17. Orr, F. W., Sanchez-Sweatman, O. H., Kostenuik, P., and Singh, G. Tumor-bone interactions in skeletal metastasis. Clin.Orthop.Rel.Res, *312*: 19-33, 1995.

18. Kang, Y., Siegel, P. M., Shu, W., Drobnjak, M., Kakonen, S. M., Cordon-Cardo, G., Guise, T. A., and Massague, J. A multigenic program mediating breast cancer metastasis to bone. Cancer Cell, *3*: 537-549, 2003.

19. Muller, A., Homey, B., Soto, H., Ge, N., Catron, D., Buchanan, M. E., McClanahan, T., Murphy, E., Yuan, W., Wagner, S. N., Barrera, J. L., Mohar, A., Verastegui, E., and Zlotnik, A. Involvement of chemokine receptors in breast cancer metastasis. Nature, *410*: 50-56, 2001.

20. Xie, D., Nakachi, K., Wang, H., Elashoff, R., and Koeffler, H. P. Elevated levels of connective tissue growth factor, WISP-1, and CYR61 in primary breast cancers associated with more advanced features. Cancer Res, *61*: 8917-8923, 2001.

21. Kluger, H. M., Chelouche Lev, D., Kluger, Y., McCarthy, M. M., Kiriakova, G., Camp, R. L., Rimm, D. L., and Price, J. E. Using a xenograft model of human breast cancer metastasis to find genes associated with clinically aggressive disease. Cancer Res, *65*: 5578-5587, 2005.

22. Price, J. E., Polyzos, A., Zhang, R. D., and Daniels, L. M. Tumorigenicity and metastasis of human breast carcinoma cell lines in nude mice. Cancer Res., *50*: 717-721, 1990.

23. Berlin, O., Samid, D., Donthineni-Rao, R., Akeson, W., Amiel, D., and Woods, V. L., Jr. Development of a novel spontaneous metastasis model of human osteosarcoma transplanted orthotopically into bone of athymic mice. Cancer Res., *53*: 4890-4895, 1993.

24. Weber, K. L., Doucet, M., Price, J. E., Baker, C., Kim, S. J., and Fidler, I. J. Blockade of epidermal growth factor receptor signaling leads to inhibition of renal cell carcinoma growth in the bone of nude mice. Cancer Res, *63*: 2940-2947, 2003.

25. Forozan, F., Veldman, R., Ammerman, C. A., Parsa, N. Z., Kallioniemi, A., Kallioniemi, O.-P., and Ethier, S. P. Molecular cytogenetic analysis of 11 new breast cancer cell lines. Br J Cancer, *81*: 1328-1334, 1999.

26. Harris, A. L. Hypoxia - a key regulatory factor in tumour growth. Nat Rev Cancer, *2*: 38-47, 2002.

27. Lynch, C. C., Hikosaka, A., Acuff, H. B., Martin, M. D., Kawai, N., Singh, R. K., Vargo-Gogola, T. C., Begtrup, J. L., Peterson, T. E., Fingleton, B., Shirai, T., Matrisian, L. M., and Futakuchi, M. MMP-7 promotes prostate cancer-induced osteolysis via the solubilization of RANKL. Cancer Cell, *7*: 496, 2005.

28. Heppner, K. J., Matrisian, L. M., Jensen, R. A., and Rodgers, W. H. Expression of most matrix metalloproteinase family members in breast cancer represents a tumor-induced host reponse. Am J Pathol, *149*: 273-282, 1996.

29. Pacheco, M. M., Mourao, M., Mantovani, E. B., Nishimoto, I. N., and Brentani, M. M. Expression of gelatinase A and B, stromelysin-3 and matrilysin genes in breast carcinomas: clinico-pathological correlations. Clin Exp Metastasis, *16*: 577-585, 1998.

30. Cochran, D. L., Rouse, C. A., Lynch, S. E., and Graves, D. T. Effects of platelet-derived growth factor isoforms on calcium release from neonatal mouse calvariae. Bone, *414*: 53-58, 1993.

31. Zhang, Z., Chen, J., and Jin, D. Platelet-derived growth factor (PDGF)-BB stimulates osteoclastic bone resorption directly: The role of receptor β. Biochem Biophys Res Commun, *251*: 190-194, 1998.

32. Li, X., Ponten, A., Aase, K., Karlsson, L., Abramsson, A., Uutela, M., Heldin, C. H., Li, H., Soriano, P., Betsholtz, C., Alitalo, K., and Eriksson, E. PDGF-C is a new protease-activated ligand for the PDGF α-receptor. Nature Cell Biol., *2*: 302-309, 2000.

33. Bergsten, E., Uutela, M., Li, X., Pietras, K., Heldin, C. H., Alitalo, K., and Eriksson, U. PDGF-D is a specific, protease-activated ligand for the PDGF β-receptor. Nature Cell Biol., *3*: 512-516, 2001.

34. Claesson-Welsh, L. Platelet-derived growth factor receptor signals. J Biol Chem, *269*: 32023-32026, 1994.

35. Dirks, R. P. H. and Bloemers, H. P. J. Signals controlling the expression of PDGF. Mol Biol Reps, *22*: 1-24, 1996.

36. Canalis, E., Varghese, S., McCarthy, T. L., and Centrella, M. Role of platelet derived growth factor in bone cell function. Growth Regul., *2*: 151-155, 1992.

37. Nakai, M., Mundy, G. R., Williams, P., Boyce, B. F., and Yoneda, T. A synthetic antagonist to laminin inhibits the formation of osteolytic metastases by human melanoma cells in nude mice. Cancer Res, *52*: 5393-5399, 1992.

38. Chen, C.-R., Kang, Y., and Massague, J. Defective repression of c-*myc* in breast cancer cells: A loss at the core of the transforming growth factor β growth arrest program. Proc Natl Acad Sci U S A, *98*: 992-999, 2001.

39. Heldin, C. H. and Westermark, B. Mechanism of action and in vivo role of platelet-derived growth factor. Physiol Rev, *79*: 1283-1316, 1999.

40. Li, Y. M., Pan, Y., Wei, Y., Cheng, X., Zhou, B. P., Tan, M., Zhou, X., Xia, W., Hortobagyi, G. N., Yu, D., and Hung, M. C. Upregulation of CXCR4 is essential for HER2-mediated tumor metastasis. Cancer Cell, *6*: 459-469, 2004.

41. Cabioglu, N., Sahin, A. A., Doucet, M., Yavuz, E., Igci, A., Yildirim, E. O., Aktas, E., Bilgic, S., Kiran, B., Deniz, G., and Price, J. E. Chemokine receptor CXCR4 expression in breast cancer as a potential predictive marker of isolated tumor cells in bone marrow. Clin Exp Metastasis, *22*: 39-46, 2005.

42. Harris, S. A., Enger, R. J., Riggs, B. L., and Spelsberg, T. C. Development and characterization of a conditionally immortalized human fetal osteoblastic cell line. J Bone Miner Res, *10*: 178-186, 1995.

43. Datta, S. R., Brunet, A., and Greenberg, M. E. Cellular survival: a play in three Akts. Genes Dev, *13*: 2905-2927, 1999.

44. Chelouche Lev, D., Kim, S. J., Onn, A., Stone, V., Nam, D. H., Yazici, S., Fidler, I. J., and Price, J. E. Inhibition of platelet-derived growth factor receptor signaling restricts the growth of human breast cancer in the bone of nude mice. Clin Cancer Res, *11*: 306-314, 2005.

Table 1: Relative expression of selected genes in MDA-MB-435 breast cancer cells growing in vitro and in bone.

Gene	435it1	it-tumor 1	it-tumor 2	comment
VEGF	2.63	3.52	2.69	induced, selected
CSF-1	3.2	2.85	3.62	induced, selected
IL-6	ND	2.9	0.23	inconsistent
IL-8	1.32	2.99	0.96	inconsistent
IL-11	6.72	6.21	12.73	induced, selected
PTHrP	ND	25.7	2.3	induced in vivo
OPG	3.5	8.5	4.1	induced, selected
RANK	minimal expression in all samples tested, including MDA-MB-435 cells			
CTGF	0.79	3.9	4.8	induced in vivo
CXCR4	8.0	3.0	ND	induced, selected
PDGFA	1.55	1.11	0.7	no change
PDGF-Rα	induced	induced	induced	induced in vivo
PDGF-Rβ	induced	induced	induced	induced in vivo
Cathepsin K	4.22	3.7	7.34	induced, selected
MMP-11	1.89	13.84	9.55	induced, selected
MMP-7	2.8	15.0	21.2	induced, selected

ND = none detected

Induced – expression increased in the tumor sample; selected – the increase in expression in maintained in the cells isolated from a bone tumor sample, and propagated in vitro.

Total RNA was reversed transcribed with random primers from the High Capacity cDNA Archive Kit (Applied Biosystems, Foster City,CA). The Gene AMP PCR system 9700 thermal cycler was used to perform the RT step using the following cycle conditions: 25°C for 10 min, 37° C for 120 min. cDNA was amplified in duplicate samples using the ABI 7000 Sequence Detection System for the expression of genes shown in the table and 18s using TaqMan® Assay Reagents (Applied Biosystems) and following

the manufacturer's recommended amplification procedure. Results were recorded as mean Ct, and relative expression was determined using the comparative Ct method. The ΔCt was calculated as the difference between the average Ct value of the endogenous control, 18s, from the average Ct value of the gene of interest. To compare the relative amount of target gene expression in different samples, human placenta RNA (Promega, Madison, WI) was used as a calibrator. The ΔΔCt was determined by subtracting the ΔCt of the calibrator from the ΔCt of the test sample. Relative expression of of the target gene is calculated by the formula, $2^{-\Delta\Delta Ct}$, which is the amount of gene product, normalized to the endogenous control and relative to a calibrator. The results were then normalized to expression in the MDA-MB-435 cells grown *in vitro.*

Table 2: Relative expression of selected genes in SUM 149 breast cancer cells growing in vitro and in bone.

Gene	149it1	it-tumor 1	it-tumor 2	comment
VEGF	1.34	8.11	13.13	induced in vivo
CSF-1	0.3	0.17	0.17	reduced
IL-6	7.7	7.3	15.4	induced, selected
IL-8	3.8	0.5	1.4	selected only
IL-11	0.62	1.14	1.7	minimal change
PTHrP	1.2	117.8	249.0	induced in vivo
OPG	0.7	173.0	128.9	induced in vivo
RANK	2.84	4.9	7.8	induced, selected
CTGF	2.3	4.5	4.8	induced, selected
CXCR4	0.38	0.33	0.41	reduced
PDGFA	0.55	3.59	2.32	induced in vivo
PDGF-Rα	induced	induced	induced	induced in vivo
PDGF-Rβ	induced	induced	induced	induced in vivo
Cathepsin K	5.6	21.9	29.2	induced, selected
MMP-11	5.69	6.4	10.4	induced, selected
MMP-7	0.29	3.2	3.8	induced in vivo

ND = none detected

Induced – expression increased in the tumor sample; selected – the increase in expression in maintained in the cells isolated from a bone tumor sample, and propagated in vitro.

Method as in table 1, relative to expression in SUM 149 cells *in vitro*. The results are representative of duplicate experiments.

Table 3: Relative expression of selected genes in MDA-MB-435 breast cancer cells growing in bone and mammary fatpad tumors

Gene	it-tumor 1	it-tumor 2	mfp-1	mfp-2	mfp-3
VEGF	3.5	2.9	3.0	9.0	3.8
CSF-1	2.8	2.6	1.6	2.6	0.9
IL-11	6.7	7.3	1.3	2.4	1.6
PTHrP	21.3	25.7	9.2	9.0	8.6
Cathepsin K	7.7	3.7	2.9	3.2	3.6
MMP-11	9.55	15.2	10.3	4.8	4.4
MMP-7	21.1	71.2	1.7	1.4	1.3

Expression is relative to expression recorded in MDA-MB-435 cells growing in culture, and determined as described in legends to Table 1.

Appendix:

Table A1: Array results for cytokines and receptors array/SUM 149 compared with bone tumors and selected cells.

Table A2: Array results for cytokines and receptors array/MDA-MB-435 compared with bone tumor

Table A3: Array results from metastasis array/SUM 149 compared with bone tumors and selected cells.

Table A4:Array results from metastasis array/MDA-MB-435 compared with bone tumor.

Publications:

"Inhibition of Platelet-Derived Growth Factor Receptor Signaling Restricts the Growth of Human Breast Cancer in the Bone of Nude Mice ", D. Chelouche Lev, S.J. Kim, A. Onn, V. Stone, D.Y. Nam, S. Yazici, I.J. Fidler, and J. E. Price. *Clinical Cancer Research*, 11: 306-314, 2005.

"Chemokine receptor CXCR4 expression in breast cancer as a potential predictive marker of isolated tumor cells in bone marrow" N. Cabioglu, A. Sahin, M. Doucet, E. Yavuz, A. Igci, E.O. Yildirim, E. Aktas, S. Bilgic, B. Kiran, G. Deniz, and J.E. Price. *Clinical and Experimental Metastasis*, 22: 39-46, 2005.

"CXCL-12/Stromal cell-derived factor-1α transactivates HER2-neu in breast cancer cells by a novel pathway involving src kinase activation", N, Cabioglu, J. Summy, C. Miller, N.U. Parikh, A.A. Sahin, S. Tuzlali, K. Pumiglia, G.E. Gallick, and J.E. Price. *Cancer Research*, 65: 6493-6497, 2005.

Table A1: Array result for cytokines and receptors/ SUM 149 compared with bone tumor and selected cells

RefSeq Num	Symbol	Description	in vivo/cell line	selected/original cells
NM_002954	**RPS27A**	**Ribosomal protein S27a**	0.61727015	0.925641008
NM_001090	ABCF1	ATP-binding cassette, sub-family	0.482423762	0.879986976
NM_001706	BCL6	B-cell CLL/lymphoma 6 (zinc fing	2.654543924	0.50626753
NM_000064	C3	Complement component 3	0.550352979	0.927030682
NM_000592	C4A	Complement component 4A	1.552207696	0.698778682
NM_002986	CCL11	Chemokine (C-C motif) ligand 11	0.325407851	0.359062808
NM_004167	CCL15	Chemokine (C-C motif) ligand 15	0.560434286	0.602454682
NM_004591	CCL20	Chemokine (C-C motif) ligand 20	1.944344854	2.782276817
NM_002989	CCL21	Chemokine (C-C motif) ligand 21	0.908832009	1.145685866
NM_005624	CCL25	Chemokine (C-C motif) ligand 25	0.500274304	0.699045352
NM_002985	CCL5	Chemokine (C-C motif) ligand 5	0.628931655	1.246659483
NM_006273	CCL7	Chemokine (C-C motif) ligand 7	0.60661779	0.711165869
NM_005194	CEBPB	CCAAT/enhancer binding protein	0.219239998	0.691064547
NM_001511	CXCL1	Chemokine (C-X-C motif) ligand	0.943183577	1.128518955
NM_001565	CXCL10	Chemokine (C-X-C motif) ligand	0.795051893	0.985540187
NM_002089	CXCL2	Chemokine (C-X-C motif) ligand	0.995929439	2.05439622
NM_002090	CXCL3	Chemokine (C-X-C motif) ligand	1.340996853	3.547026685
NM_002994	CXCL5	Chemokine (C-X-C motif) ligand	1.304085531	0.966519684
NM_003467	CXCR4	Chemokine (C-X-C motif) recept	0.368828854	0.610017696
NM_005226	EDG3	Endothelial differentiation, sphin	1.242211936	1.140664833
NM_000628	IL10RB	Interleukin 10 receptor, beta	0.458339402	0.729133714
NM_000641	IL11	Interleukin 11	1.535150471	0.657400493
NM_004512	IL11RA	Interleukin 11 receptor, alpha	4.233858024	1.196741916
NM_000882	IL12A	Interleukin 12A (natural killer cel	1.584000553	1.070431891
NM_002188	IL13	Interleukin 13	0.683369681	0.545248146
NM_001560	IL13RA1	Interleukin 13 receptor, alpha 1	0.538407627	0.581039568
NM_172175	IL15	Interleukin 15	0.585851891	0.783551737
NM_002189	IL15RA	Interleukin 15 receptor, alpha	0.227676845	2.670241957
NM_001562	IL18	Interleukin 18 (interferon-gamma	0.438846247	0.762093145
NM_000575	IL1A	Interleukin 1, alpha	0.205841843	1.66041368
NM_000576	IL1B	Interleukin 1, beta	0.619259429	2.002369769
NM_000877	IL1R1	Interleukin 1 receptor, type I	4.071019255	4.210673606
NM_004633	IL1R2	Interleukin 1 receptor, type II	12.81343185	1.654496866
NM_000577	IL1RN	Interleukin 1 receptor antagonist	1.368067356	0.468253858
NM_000600	IL6	Interleukin 6 (interferon, beta 2)	5.445325046	5.156049701
NM_000584	IL8	Interleukin 8	1.004176425	2.716235044
NM_001557	IL8RB	Interleukin 8 receptor, beta	0.375436082	0.285562706
NM_181657	LTB4R	Leukotriene B4 receptor	1.876972164	2.589320902
NM_002415	MIF	Macrophage migration inhibitory	0.625670467	0.957262697
NM_002619	PF4	Platelet factor 4 (chemokine (C-)	0.023610336	0.180688507
NM_004757	SCYE1	Small inducible cytokine subfam	1.379081314	0.295640073
NM_000582	SPP1	Secreted phosphoprotein 1 (oste	1.195170142	0.233409984
NM_000594	TNF	Tumor necrosis factor (TNF supe	1.440022233	0.404159305
NM_001065	TNFRSF1A	Tumor necrosis factor receptor s	1.190158489	0.927258816
NM_019009	TOLLIP	Toll interacting protein	1.069237127	0.646231932
NM_002995	XCL1	Chemokine (C motif) ligand 1	0.274595083	0.824389657
NM_005283	XCR1	Chemokine (C motif) receptor 1	0.336654654	0.70679471
NM_002046	**GAPDH**	**Glyceraldehyde-3-phosphate d**	0.614740068	0.656137153
NM_004048	**B2M**	**Beta-2-microglobulin**	0.300976568	0.603025487
				Table A1/report page 24

NM_007355	HSPCB	Heat shock 90kDa protein 1, b	0.614241889	0.916269727
NM_007355	HSPCB	Heat shock 90kDa protein 1, b	0.605003274	0.916211634
NM_001101	ACTB	Actin, beta	0.623150376	0.914958652
NM_001101	ACTB	Actin, beta	0.619010231	0.888976373

Table A4: Array results for metastasis associated genes/MDA-MB-435 compared with bone tumor

RefSeq Num	*Symbol*	*Description*	*in vivo/original cells*
NM_002954	**RPS27A**	**Ribosomal protein S27a**	1.653927928
NM_000038	APC	Adenomatosis polyposis coli	1.183909798
NM_001702	BAI1	Brain-specific angiogenesis inhibitor 1	1.302692408
NM_015399	BRMS1	Breast cancer metastasis suppressor 1	0.612806649
NM_001753	CAV1	Caveolin 1, caveolae protein, 22kDa	0.839546266
NM_000610	CD44	CD44 antigen (homing function and Indian blood g	0.814733496
NM_021153	CDH19	Cadherin 19, type 2	1.552349671
NM_001796	CDH8	Cadherin 8, type 2	0.675105068
NM_000075	CDK4	Cyclin-dependent kinase 4	1.254511008
NM_058195	CDKN2A	Cyclin-dependent kinase inhibitor 2A (melanoma,	0.99740318
NM_001846	COL4A2	Collagen, type IV, alpha 2	3.323387465
NM_001903	CTNNA1	Catenin (cadherin-associated protein), alpha 1, 10	0.460525909
NM_000396	CTSK	Cathepsin K (pycnodysostosis)	2.03170137
NM_001912	CTSL	Cathepsin L	0.914700595
NM_003467	CXCR4	Chemokine (C-X-C motif) receptor 4	1.291646371
NM_003677	DENR	Density-regulated protein	0.737343367
NM_004442	EPHB2	EphB2	0.918158666
NM_001986	ETV4	Ets variant gene 4 (E1A enhancer binding protein,	1.074488969
NM_001987	ETV6	Ets variant gene 6 (TEL oncogene)	0.646942147
NM_005243	EWSR1	Ewing sarcoma breakpoint region 1	0.865250152
NM_005245	FAT	FAT tumor suppressor homolog 1 (Drosophila)	1.091593743
NM_002020	FLT4	Fms-related tyrosine kinase 4	1.377992262
NM_002026	FN1	Fibronectin 1	2.765638566
NM_014164	FXYD5	FXYD domain containing ion transport regulator 5	1.252226309
NM_002510	GPNMB	Glycoprotein (transmembrane) nmb	1.118058088
NM_004964	HDAC1	Histone deacetylase 1	0.710986617
NM_005343	HRAS	V-Ha-ras Harvey rat sarcoma viral oncogene hom	0.685132919
NM_006410	HTATIP2	HIV-1 Tat interactive protein 2, 30kDa	0.953462174
NM_000576	IL1B	Interleukin 1, beta	1.118740757
NM_001557	IL8RB	Interleukin 8 receptor, beta	0.881065489
NM_002206	ITGA7	Integrin, alpha 7	0.833608423
NM_000212	ITGB3	Integrin, beta 3 (platelet glycoprotein IIIa, antigen	0.859002464
NM_002231	KAI1	Kangai 1 (suppression of tumorigenicity 6, prostate	1.451101029
NM_004985	KRAS	V-Ki-ras2 Kirsten rat sarcoma viral oncogene hom	0.784300224
NM_002295	LAMR1	Ribosomal protein SA	1.523553848
NM_006500	MCAM	Melanoma cell adhesion molecule	1.02634255
NM_000245	MET	Met proto-oncogene (hepatocyte growth factor rec	0.997103474
NM_006838	METAP2	Methionyl aminopeptidase 2	0.655237824
NM_002410	MGAT5	Mannosyl (alpha-1,6-)-glycoprotein beta-1,6-N-ace	0.877793883
NM_005940	MMP11	Matrix metalloproteinase 11 (stromelysin 3)	3.16852346
NM_002427	MMP13	Matrix metalloproteinase 13 (collagenase 3)	0.944121757
NM_004530	MMP2	Matrix metalloproteinase 2 (gelatinase A, 72kDa g	1.43789686
NM_004689	MTA1	Metastasis associated 1	1.016238971
NM_005375	MYB	V-myb myeloblastosis viral oncogene homolog (av	0.482347815
NM_002467	MYC	V-myc myelocytomatosis viral oncogene homolog	0.801880853
NM_005376	MYCL1	V-myc myelocytomatosis viral oncogene homolog	0.798406227
NM_000268	NF2	Neurofibromin 2 (bilateral acoustic neuroma)	0.676584074
NM_000269	NME1	Non-metastatic cells 1, protein (NM23A) expresse	1.087439715
NM_002512	NME2	Non-metastatic cells 2, protein (NM23B) expresse	1.22172009
			Table A4/report page 29

NM_005009	NME4	Non-metastatic cells 4, protein expressed in	0.817067697
NM_006981	NR4A3	Nuclear receptor subfamily 4, group A, member 3	0.79437045
NM_002768	PCOLN3	Procollagen (type III) N-endopeptidase	0.749895086
NM_002659	PLAUR	Plasminogen activator, urokinase receptor	4.061094169
NM_002687	PNN	Pinin, desmosome associated protein	1.225185448
NM_000314	PTEN	Phosphatase and tensin homolog (mutated in mult	0.854592989
NM_002820	PTHLH	Parathyroid hormone-like hormone	0.889548262
NM_007079	PTP4A3	Protein tyrosine phosphatase type IVA, member 3	0.849480209
NM_000321	RB1	Retinoblastoma 1 (including osteosarcoma)	0.843738435
NM_021111	RECK	Reversion-inducing-cysteine-rich protein with kaza	0.693464907
NM_175744	RHOC	Ras homolog gene family, member C	1.17234167
NM_002961	S100A4	S100 calcium binding protein A4 (calcium protein,	3.598620514
NM_002639	SERPINB5	Serine (or cysteine) proteinase inhibitor, clade B (c	0.692595718
NM_003011	SET	SET translocation (myeloid leukemia-associated)	0.786029816
NM_003064	SLPI	Secretory leukocyte protease inhibitor (antileukopr	1.590686782
NM_005901	SMAD2	SMAD, mothers against DPP homolog 2 (Drosoph	0.778339808
NM_005417	SRC	V-src sarcoma (Schmidt-Ruppin A-2) viral oncoger	1.033034614
NM_000362	TIMP3	Tissue inhibitor of metalloproteinase 3 (Sorsby fun	1.318480186
NM_000546	TP53	Tumor protein p53 (Li-Fraumeni syndrome)	0.875703301
NM_006670	TPBG	Trophoblast glycoprotein	1.130637565
NM_003379	VIL2	Villin 2 (ezrin)	0.574163629
NM_002046	**GAPDH**	**Glyceraldehyde-3-phosphate dehydrogenase**	1.607503599
NM_004048	**B2M**	**Beta-2-microglobulin**	1.306666803
NM_007355	**HSPCB**	**Heat shock 90kDa protein 1, beta**	1.614917563
NM_007355	**HSPCB**	**Heat shock 90kDa protein 1, beta**	1.522843786
NM_001101	**ACTB**	**Actin, beta**	1.62115247
NM_001101	**ACTB**	**Actin, beta**	1.581194216

Table A 3 :Array results for metastasis associated genes/SUM149 cells and bone tumors

RefSeq Num	Symbol	Description	in vivo/cell line	selected/original cells
NM_002954	RPS27A	Ribosomal protein S27a	1.036118795	1.011087429
NM_001702	BAI1	Brain-specific angiogenesis inhibitor 1	1.387239102	0.802050964
NM_015399	BRMS1	Breast cancer metastasis suppressor	0.798186269	0.727763877
NM_001753	CAV1	Caveolin 1, caveolae protein, 22kDa	0.312701023	0.738300821
NM_000610	CD44	CD44 antigen (homing function and Ir	0.817341025	0.997767065
NM_021153	CDH19	Cadherin 19, type 2	8.573903982	1.689426027
NM_001796	CDH8	Cadherin 8, type 2	0.617217934	1.02506757
NM_000075	CDK4	Cyclin-dependent kinase 4	1.078298641	1.060105384
NM_001846	COL4A2	Collagen, type IV, alpha 2	0.48859293	0.739021916
NM_001903	CTNNA1	Catenin (cadherin-associated protein)	0.727826162	0.883347926
NM_000396	CTSK	Cathepsin K (pycnodysostosis)	12.90875341	1.993122334
NM_003467	CXCR4	Chemokine (C-X-C motif) receptor 4	0.489326305	0.558756323
NM_003677	DENR	Density-regulated protein	0.702479904	0.771442525
NM_004442	EPHB2	EphB2	0.670226001	0.795043811
NM_001986	ETV4	Ets variant gene 4 (E1A enhancer bin	0.825927141	1.055398898
NM_001987	ETV6	Ets variant gene 6 (TEL oncogene)	1.43413974	1.016002279
NM_005243	EWSR1	Ewing sarcoma breakpoint region 1	0.988513479	1.142810239
NM_005245	FAT	FAT tumor suppressor homolog 1 (Dr	3.095744128	1.249269329
NM_002026	FN1	Fibronectin 1	1.346319654	1.251025338
NM_014164	FXYD5	FXYD domain containing ion transpor	0.602659133	0.848065626
NM_002510	GPNMB	Glycoprotein (transmembrane) nmb	5.641536705	2.621493706
NM_004964	HDAC1	Histone deacetylase 1	1.15540772	0.700705619
NM_005343	HRAS	V-Ha-ras Harvey rat sarcoma viral onc	1.015151833	1.03846257
NM_006410	HTATIP2	HIV-1 Tat interactive protein 2, 30kDa	0.714193694	0.807128111
NM_001562	IL18	Interleukin 18 (interferon-gamma-indu	0.585268453	1.604347883
NM_000576	IL1B	Interleukin 1, beta	0.491227555	0.813740355
NM_001557	IL8RB	Interleukin 8 receptor, beta	0.456483606	0.774704313
NM_002206	ITGA7	Integrin, alpha 7	0.46489725	0.784356186
NM_000212	ITGB3	Integrin, beta 3 (platelet glycoprotein I	0.547654646	0.783327733
NM_002231	KAI1	Kangai 1 (suppression of tumorigenici	1.090027443	0.945327578
NM_004985	KRAS	V-Ki-ras2 Kirsten rat sarcoma viral on	0.871934962	1.085184327
NM_002295	LAMR1	Ribosomal protein SA	1.041637789	1.022646507
NM_006500	MCAM	Melanoma cell adhesion molecule	3.909268148	3.390379311
NM_000245	MET	Met proto-oncogene (hepatocyte grow	0.692790975	1.017625127
NM_006838	METAP2	Methionyl aminopeptidase 2	0.460231975	0.823058908
NM_005940	MMP11	Matrix metalloproteinase 11 (stromely	5.440006637	4.04555207
NM_002427	MMP13	Matrix metalloproteinase 13 (collagen	0.898114682	1.515413586
NM_004530	MMP2	Matrix metalloproteinase 2 (gelatinase	1.262775053	0.576356707
NM_002423	MMP7	Matrix metalloproteinase 7 (matrilysin,	1.175443743	0.227349522
NM_004994	MMP9	Matrix metalloproteinase 9 (gelatinase	0.948060261	1.613300626
NM_004689	MTA1	Metastasis associated 1	0.596574076	0.977918179
NM_005375	MYB	V-myb myeloblastosis viral oncogene	2.848481082	1.721126184
NM_002467	MYC	V-myc myelocytomatosis viral oncoge	0.412384419	0.715054869
NM_005376	MYCL1	V-myc myelocytomatosis viral oncoge	0.50894795	0.750682723
NM_000268	NF2	Neurofibromin 2 (bilateral acoustic ne	0.950862384	0.739994629
NM_000269	NME1	Non-metastatic cells 1, protein (NM23	0.813651327	0.82343043
NM_002512	NME2	Non-metastatic cells 2, protein (NM23	1.003560387	0.942626121
NM_005009	NME4	Non-metastatic cells 4, protein expres	0.7110152	1.049477162
NM_006981	NR4A3	Nuclear receptor subfamily 4, group A	0.766771593	1.341831475
				Table A3/report page 27

NM_002768	PCOLN3	Procollagen (type III) N-endopeptidas	0.673907121	1.099332334
NM_002659	PLAUR	Plasminogen activator, urokinase rece	1.243176913	1.080217923
NM_002687	PNN	Pinin, desmosome associated protein	1.654033931	0.735049246
NM_000314	PTEN	Phosphatase and tensin homolog (mu	0.611797248	0.778618976
NM_002820	PTHLH	Parathyroid hormone-like hormone	0.780791499	0.831235077
NM_007079	PTP4A3	Protein tyrosine phosphatase type IVA	0.366675825	1.06780857
NM_000321	RB1	Retinoblastoma 1 (including osteosarc	1.052730407	1.335504471
NM_175744	RHOC	Ras homolog gene family, member C	0.923347548	0.985528589
NM_006914	RORB	RAR-related orphan receptor B	1.94347417	1.044643128
NM_002961	S100A4	S100 calcium binding protein A4 (calc	1.845506537	0.697935619
NM_002639	SERPINB5	Serine (or cysteine) proteinase inhibit	1.7901562	0.683077552
NM_003011	SET	SET translocation (myeloid leukemia-	0.776945912	0.929170447
NM_003064	SLPI	Secretory leukocyte protease inhibitor	1.447809875	1.283302563
NM_005901	SMAD2	SMAD, mothers against DPP homolog	0.846745416	0.824090735
NM_005417	SRC	V-src sarcoma (Schmidt-Ruppin A-2)	1.470618872	2.154612436
NM_000546	TP53	Tumor protein p53 (Li-Fraumeni syndr	0.352088759	0.773137539
NM_006670	TPBG	Trophoblast glycoprotein	0.524361035	1.150128661
NM_002046	**GAPDH**	**Glyceraldehyde-3-phosphate dehyc**	1.036285458	0.915941078
NM_004048	**B2M**	**Beta-2-microglobulin**	0.354119452	0.658119212
NM_007355	**HSPCB**	**Heat shock 90kDa protein 1, beta**	0.94752449	0.964520573
NM_007355	**HSPCB**	**Heat shock 90kDa protein 1, beta**	0.968687961	0.924043074
NM_001101	**ACTB**	**Actin, beta**	1.033902818	0.976156364
NM_001101	**ACTB**	**Actin, beta**	1.014765954	0.982188733

Table A2: Array result for cytokines and receptors/MDA-MB-435 compared with bone tumor

RefSeq Num	Symbol	Description	in vivo/original cells
NM_002954	RPS27A	Ribosomal protein S27a	0.565754649
NM_001090	ABCF1	ATP-binding cassette, sub-family F (GCN	0.895085
NM_001706	BCL6	B-cell CLL/lymphoma 6 (zinc finger protei	2.155775117
NM_002986	CCL11	Chemokine (C-C motif) ligand 11	1.932262621
NM_004167	CCL15	Chemokine (C-C motif) ligand 15	2.282999029
NM_002987	CCL17	Chemokine (C-C motif) ligand 17	0.829164865
NM_004591	CCL20	Chemokine (C-C motif) ligand 20	0.326764304
NM_005624	CCL25	Chemokine (C-C motif) ligand 25	0.836002871
NM_006273	CCL7	Chemokine (C-C motif) ligand 7	1.089601178
NM_005194	CEBPB	CCAAT/enhancer binding protein (C/EBP	0.403908608
NM_001511	CXCL1	Chemokine (C-X-C motif) ligand 1 (melan	1.670791601
NM_001565	CXCL10	Chemokine (C-X-C motif) ligand 10	0.920622454
NM_002994	CXCL5	Chemokine (C-X-C motif) ligand 5	0.919261112
NM_003467	CXCR4	Chemokine (C-X-C motif) receptor 4	1.665635087
NM_000628	IL10RB	Interleukin 10 receptor, beta	0.311760537
NM_000641	IL11	Interleukin 11	5.93947951
NM_004512	IL11RA	Interleukin 11 receptor, alpha	1.506704413
NM_000882	IL12A	Interleukin 12A (natural killer cell stimulat	1.156971035
NM_002188	IL13	Interleukin 13	1.408090786
NM_001560	IL13RA1	Interleukin 13 receptor, alpha 1	0.598577789
NM_000576	IL1B	Interleukin 1, beta	0.78193983
NM_000584	IL8	Interleukin 8	0.57259074
NM_000634	IL8RA	Interleukin 8 receptor, alpha	0.606348352
NM_001557	IL8RB	Interleukin 8 receptor, beta	1.019206933
NM_181657	LTB4R	Leukotriene B4 receptor	0.361481372
NM_002415	MIF	Macrophage migration inhibitory factor (gl	0.560753633
NM_004757	SCYE1	Small inducible cytokine subfamily E, mer	1.075345956
NM_000582	SPP1	Secreted phosphoprotein 1 (osteopontin,	0.717880721
NM_001065	TNFRSF1A	Tumor necrosis factor receptor superfami	1.17208194
NM_001066	TNFRSF1B	Tumor necrosis factor receptor superfami	0.24519639
NM_019009	TOLLIP	Toll interacting protein	0.661198807
NM_002995	XCL1	Chemokine (C motif) ligand 1	4.023622034
NM_005283	XCR1	Chemokine (C motif) receptor 1	1.655621112
L08752	PUC18	PUC18 Plasmid DNA	1.523793482
NM_002046	GAPDH	Glyceraldehyde-3-phosphate dehydrog	0.561666514
NM_004048	B2M	Beta-2-microglobulin	0.828790343
NM_007355	HSPCB	Heat shock 90kDa protein 1, beta	0.556602084
NM_007355	HSPCB	Heat shock 90kDa protein 1, beta	0.563988551
NM_001101	ACTB	Actin, beta	0.560810618
NM_001101	ACTB	Actin, beta	0.561890768

Inhibition of Platelet-Derived Growth Factor Receptor Signaling Restricts the Growth of Human Breast Cancer in the Bone of Nude Mice

Dina Chelouche Lev, Sun Jin Kim, Amir Onn, Valerie Stone, Do-Hyun Nam, Sertac Yazici, Isaiah J. Fidler and Janet E. Price

Department of Cancer Biology, University of Texas M.D. Anderson Cancer Center and the Program in Cancer Biology, University of Texas Graduate School of Biomedical Sciences at Houston, Houston, Texas

ABSTRACT

Purpose: **Bone is a common site for breast cancer metastasis. Platelet-derived growth factor (PDGF) and PDGF receptors (PDGFR) are involved in the regulation of bone resorption. This study examined the effects of STI571 (imatinib mesylate), which inhibits PDGFR tyrosine kinase signaling, on the growth of human breast cancer cells in the bone of nude mice with consequent osteolysis.**

Experimental Design: **Human breast cancer MDA-MB-435 cells were injected into the tibia of female nude mice. Two weeks later the mice were treated with p.o. and injected water (control), daily p.o. STI571, weekly injection of paclitaxel, or daily STI571, plus weekly paclitaxel, for up to 8 weeks. Growth of tumors in bones and osteolysis were monitored by digital radiography and tumors were collected for histochemical analysis.**

Results: **Mice treated with STI571 or STI571 plus paclitaxel had smaller bone tumors with less lytic bone destruction than did mice treated with water or paclitaxel alone. The results of treatment with paclitaxel plus STI571 did not differ from those with STI571 alone. Immunohistochemistry showed that PDGF-A, PDGF-B, PDGFRα, and PDGFRβ were expressed in the bone tumors. STI571 treatment inhibited PDGFR phosphorylation in tumor cells and tumor-associated endothelial cells, coincident with increased apoptosis, reduced proliferation, and lower microvessel density in the tumors.**

Conclusions: **Activated PDGFRs are expressed by endothelial and tumor cells in breast cancer tumors growing in the bone of nude mice. Interfering with PDGFR signaling may be an approach to control the progressive growth of breast cancer cells and thus reduce bone lysis.**

INTRODUCTION

The skeleton is the most common site of breast cancer metastasis, with bone lesions found in approximately 70% of patients with metastatic disease (1). Although patients who have only bone metastases generally have a better prognosis and longer median survival time than patients with metastases in lung, liver, or brain do, they tend to suffer from long-term skeletal morbidity, leading to considerable reduction in quality of life (2). The complications of bone metastasis include pain, pathologic fractures, spinal cord compression, and hypercalcemia. Currently, no curative therapy exists for bone metastasis, and clinical management is generally palliative. Treatment options include surgery or radiation to prevent or repair fractures and the use of bisphosphonates and analgesics to reduce osteolysis and pain (1, 3).

Research is gradually leading to a better understanding of the molecular biology of breast cancer and the genotypic and phenotypic processes underlying the progression to metastasis (4–6). Identification of key molecules controlling the growth of breast cancer cells in the primary and metastatic sites can lead to the development of improved and potentially specific therapeutic strategies. Breast cancer cells produce various growth factors and cytokines that may contribute to malignant progression, through autocrine or paracrine mechanisms (7). One example is the family of platelet-derived growth factors (PDGF), which are multifunctional cytokines involved in the growth, survival, and differentiation of connective tissues (8, 9). The A and B isoforms of PDGF can form either homodimers or heterodimers that bind to and activate the protein tyrosine kinase PDGF receptors (PDGFRα and PDGFRβ; ref. 10). Immunohistochemical studies of breast cancer specimens have showed expression of PDGFs in cancer cells and expression of the receptors predominantly in stromal cells, notably the α smooth muscle–staining cells and vascular endothelial cells in the periepithelial stroma (7, 11). This expression of PDGF and PDGFRs suggests a paracrine mechanism for tumor development or maintenance. A key paracrine action of PDGFs that can affect the malignant phenotype is the promotion of tumor stroma and angiogenesis (8, 9). Elevated levels of PDGF in plasma and increased expression of PDGF in tumor tissues correlate with increased incidence of metastasis, lower response to chemotherapy, and shorter survival time of patients with breast cancer (12, 13).

In the bone microenvironment, osteoblasts both produce and respond to PDGF, which can promote proliferation, bone resorption, collagen degradation, and collagenase expression (14, 15). The presence of cancer cells in the bone microenvironment may shift the balance of bone homeostasis toward osteolysis (16). Because PDGF has been reported to stimulate

Received 5/28/04; revised 9/24/04; accepted 10/7/04.

Grant support: U.S. Army Medical Research and Material Command grant DAMD17-01-0445 (J.E. Price) and NIH/National Cancer Institute Cancer Center grant CA 16672.

The costs of publication of this article were defrayed in part by the payment of page charges. This article must therefore be hereby marked *advertisement* in accordance with 18 U.S.C. Section 1734 solely to indicate this fact.

Requests for reprints: Janet E. Price, Department of Cancer Biology, University of Texas M.D. Anderson Cancer Center, 1515 Holcombe Boulevard, Unit 173, Houston, TX 77030. Phone: 713-792-8577; Fax: 713-792-8747; E-mail: jprice@mdanderson.org.

bone resorption, by regulating expression of cytokines such as interleukin (IL)-6 by osteoblasts, or by direct action on osteoclasts (17), the release of PDGF by metastatic breast cancer cells may influence the development and progressive growth of bone metastases (18–20).

Identification of molecules responsible for paracrine interactions involved in promoting growth of metastases presents an opportunity to interfere with this process. Several small-molecule inhibitors of different signaling pathways, notably tyrosine kinase inhibitors, have shown therapeutic efficacy and are undergoing clinical trials (21). We previously reported that STI571 (imatinib mesylate, Gleevec, Novartis Pharma, Basel, Switzerland), a derivative of 2-phenylaminopyrimidine, developed as an inhibitor of the Abl protein tyrosine kinase, and a potent inhibitor of PDGFR and C-Kit tyrosine kinases (22), can slow the progressive growth of experimental bone metastases of a human prostate cancer (23). In this study we used the same strategy we used in that previous study to test the therapeutic effect of STI571, both alone and in combination with paclitaxel, against human breast cancer cells growing in the tibias of nude mice, to test the hypothesis that inhibiting PDGFR signaling can impair the growth of breast cancer in bone.

MATERIALS AND METHODS

Cell Line. The MDA-MB-435 breast cancer cell line was provided by Dr. Relda Cailleau (University of Texas M.D. Anderson Cancer Center, Houston, TX). Cells were maintained in monolayer culture in MEM supplemented with 5% fetal bovine serum, sodium pyruvate, L-glutamine, and vitamin solution (2× MEM; Life Technologies, Inc., Grand Island, NY) in a humidified incubator with 5% CO_2-95% air. For all *in vivo* experiments, tumor cells in exponential growth phase were harvested by brief exposure to 0.25% trypsin in 0.02% EDTA, then washed and resuspended in Ca^{2+}- and Mg^{2+}-free PBS.

Animals. Female athymic NCr-nu mice were purchased from the National Cancer Institute-Frederick Cancer Research Facility (Frederick, MD). The mice were housed in a specific pathogen-free facility and used at 7 to 8 weeks of age. The care and use of laboratory animals was in accordance with the principles and standards set forth in the Principles for Use of Animals (*NIH Guide for Grants and Contracts*), the *Guide for the Care and Use of Laboratory Animals* (DHEW, Public Health Service Publication 80-23, Rev. 1978), the provisions of the Animal Welfare Acts (P.L. 89-544 and its amendments). The study was approved by the Institutional Animal Care and Use Committee of the University of Texas M.D Anderson Cancer Center.

Intratibial Injections of MDA-MB-435 Cells. To establish bone tumors, the mice were anesthetized with Nembutal (0.5 mg/g body weight; Abbott Laboratories, North Chicago, IL). A percutaneous intraosseal injection was made by drilling a 27-gauge needle into the tibia immediately proximal to the tibial tuberosity (24). After penetration of the cortical bone, the needle was inserted farther into the tibial shaft to deposit 20 μL of the MDA-MB-435 cell suspension (5×10^5 cells) in the cortex with a calibrated, push button–controlled dispensing device (Hamilton Syringe Co., Reno, NV). A cotton swab was then held against the injection site for 1 minute to prevent leakage of the inoculum. The animals tolerated this procedure well.

Experimental Design. STI571 (imatinib mesylate, Gleevec). For each p.o. administration, STI571 was dissolved in distilled water (dH_2O) at 6.25 mg/mL. For each i.p. injection, paclitaxel (Taxol; Bristol-Myers Squibb, Princeton, NJ) was diluted in dH_2O at 1 mg/mL. Therapy was initiated 2 weeks after injection of the tumor cells, according to preliminary results showing that at this point the mice had tumors confined within the marrow space (Fig. 1). Mice (12-15 mice per treatment group) were randomly assigned to receive one of the following four treatments: (*a*) a daily p.o. dose of vehicle solution and weekly i.p. injection of dH_2O (control group); (*b*) no p.o. medication and weekly i.p. injection of 8.5 mg/kg paclitaxel (paclitaxel group); (*c*) a daily p.o. dose of 50 mg/kg STI571 and weekly i.p. injection of dH_2O (STI571 group); and (*d*) a daily p.o. dose of 50 mg/kg STI571 and weekly i.p. injection of 8.5 mg/kg paclitaxel (STI571 + paclitaxel). In the first experiment, the mice were treated for 6 weeks, and in the second, the treatment was extended to 8 weeks. Tumor size and osteolysis of the injected bone were evaluated by gross observation and by digital radiography as described below.

Digital Radiography and Harvesting of Bone Tumors. Progression of disease in the bone was monitored by digital radiography, starting 2 weeks after initiation of treatment and every second week thereafter. Mice were anesthetized and placed in a prone position, and their hind limbs were imaged using a digital radiography system (Faxitron X-ray Corp., Wheeling, IL). At the end of the study, the mice were euthanized and the hind limbs were imaged and then resected and weighed. The tumor weight was calculated as the difference between the weights of the tumor-bearing and tumor-free legs. A semiquantitative grading system of osteolysis, with numeric values ranging from 0 to 4+, was used to assess the extent of bone destruction (24). A grade of 0 represented no lysis, 1+ was minimal but visible bone lysis within the medullary canal, 2+ was moderate osteolysis in the medullary canal with preservation of the cortex, 3+ was severe osteolysis with cortical disruption, and 4+ was massive destruction with extension of the tumor into the soft tissue.

Fig. 1 Radiologic and histologic appearance of nude mouse tibia 2 weeks after injection of MDA-MB-435 human breast cancer cells. Digital radiograph of a noninjected tibia for reference (*A*) and of an injected tibia (*B*) shows no evidence of osteolysis. *C,* a histologic section of the tibia shown in *B* shows a representative focus of breast cancer cells growing in the bone marrow space (*arrowhead*), with no evidence of osteolysis. H&E stain, original magnification ×200.

Preparation of Tissues. Tumors harvested from the tibia and the surrounding muscles were cut into 2- to 3-mm pieces, fixed in 10% buffered formalin for 24 hours at room temperature, washed with PBS for 30 minutes, decalcified by incubation with 15% EDTA (pH 7.4) for 7 to 10 days at 4°C, and embedded in paraffin. Frozen sections of the tumors were prepared following the method described previously (23). Tumors cut into 2- to 3-mm pieces were fixed in 4% paraformaldehyde containing 0.075 mol/L lysine and 0.01 mol/L sodium periodate for 24 hours, washed with PBS containing 10% sucrose for 4 hours, then with PBS containing 15% sucrose for 4 hours, and finally with PBS containing 20% sucrose for 16 hours. All procedures were carried out at 4°C. The tissues were then embedded in ornithine carbamyl transferase compound (Miles, Inc., Elkhart, IN), rapidly frozen in liquid nitrogen, and stored at −70°C.

Immunohistochemistry and Single-Label Immunofluorescence. Paraffin-embedded tissues were sectioned (4 to 6 μm thick) and used to detect expression of PDGF, PDGFR, vascular endothelial growth factor (VEGF), basic fibroblast growth factor (bFGF), IL-8, and proliferating cell nuclear antigen (PCNA). Frozen sections were used for detecting activated PDGFR, CD31, and phosphorylated Akt. The following primary antibodies were used for immunohistochemistry and immunofluorescence: rabbit polyclonal anti-VEGF/VPF, anti-FGF-2 (which recognizes bFGF), anti-PDGF A, anti-PDGF B, anti-PDGFRα, and anti-PDGFRβ (Santa Cruz Biotechnology, Santa Cruz, CA); goat polyclonal anti-phospho-PDGFR (which recognizes activated PDGFR, Santa Cruz); rabbit polyclonal anti–IL-8 (Biosource International, Camarillo, CA); rat monoclonal anti-mouse CD31/platelet-endothelial cell adhesion molecule-1 (PECAM-1) (PharMingen, San Diego, CA); monoclonal anti-PCNA, clone PC-10 (Dako A/S, Copenhagen, Denmark), and rabbit polyclonal anti-phospho-Akt (Ser^{473}, Cell Signaling Technology, Beverly, MA). The tissue sections used to detect PCNA expression were microwaved at 1000 W for 5 minutes to improve antigen retrieval. All other paraffin-embedded tissues were treated with pepsin (Biomeda, Foster City, CA) for 15 minutes at 37°C and then washed with PBS.

Secondary antibodies used were horseradish peroxidase (HRP)–conjugated goat anti-rabbit immunoglobulin G, HRP-conjugated goat anti-rat immunoglobulin G, Texas Red–conjugated goat anti-rat immunoglobulin G, and FITC–conjugated goat anti-rabbit immunoglobulin G (Jackson ImmunoResearch Laboratories, West Grove, PA); HRP-conjugated rat anti-mouse IgG2a (Serotec, Harlan Bioproducts for Science, Inc., Indianapolis, IN); Alexa Fluor 594–conjugated goat anti-rabbit immunoglobulin G (Molecular Probes, Eugene, OR); and Biogenex multilink and Biogenex label used for enhancing antibody detection (San Ramon, CA).

Immunohistochemical procedures were performed as described previously (24). Positive antibody reactions in sections reacted with HRP-labeled antibodies were visualized by incubating the slides with stable 3,3′-diaminobenzidine for 10 to 20 minutes. The sections were rinsed with dH_2O, counterstained with Gill's hematoxylin for 1 minute, and mounted onto slides with the use of Universal Mount (Research Genetics, Huntsville, AL). Control samples, which were exposed to secondary antibody alone, showed no specific staining. The sections treated with Alexa Fluor were rinsed with dH_2O and mounted with medium with 4′,6-diamidino-2-phenylindole (Vectashield, Vector Laboratories, Inc., Burlingame, CA), which produced blue fluorescence in the cell nuclei.

Immunofluorescence Double Staining for CD31/PECAM-1 and PDGFR or Terminal Deoxynucleotidyl Transferase–Mediated Nick End Labeling. Frozen sections were incubated with a protein-blocking solution (5% normal horse serum and 1% normal goat serum in PBS) for 20 minutes at room temperature and then incubated for 18 hours at 4°C with a 1:400 dilution of rat monoclonal anti-mouse CD31/PECAM-1 antibody, which recognizes human and mouse PECAM-1. The samples were then rinsed four times with PBS for 3 minutes each, and the slides were incubated in the dark for 1 hour at room temperature with a 1:200 dilution of Texas Red–conjugated goat anti-rat antibody. Samples were then washed twice with PBS containing 0.1% Brij (Fisher Scientific, Pittsburgh, PA) and once for 5 minutes with PBS and then mounted onto slides with the use of Vectashield. The terminal deoxynucleotidyl transferase–mediated nick end labeling (TUNEL) assay was done using a commercial apoptosis detection kit (Promega Corp., Madison, WI), as described previously (24).

Immunofluorescence microscopy was done using an epifluorescence microscope (Carl Zeiss, Thornwood, NY) equipped with a 40× objective and narrow-bandpass excitation filters mounted on a filter wheel (Ludl Electronic Products, Hawthorne, NY). Images were captured with the use of a three-chip camera (Sony Corporation of America, Montvale, NJ) and Optimas Image Analysis software (Bioscan, Edmond, WA). Images were further processed with the use of Photoshop software (Adobe Systems, Mountain View, CA). Endothelial cells were identified by red fluorescence, and DNA fragmentation (i.e., TUNEL-positive apoptotic cells) was detected by green fluorescence localized within cell nuclei. The total number of TUNEL-positive tumor cells was determined in tissues at ×100 magnification. Quantification of apoptotic endothelial cells (yellow fluorescence) was expressed as the average of the ratio of apoptotic endothelial cells to the total number of endothelial cells in 5 to 10 random 0.011-mm^2 fields at ×400 magnification.

Quantification of Microvessel Density and PCNA-Expressing Cells. To quantify microvessel density, we captured the images (magnification ×100) of 10 randomly chosen 0.159-mm^2 microscope fields for each tumor and used those images to count microvessel-like structures consisting of endothelial cells that were stained with the anti-CD31/PECAM-1 antibody, as described previously (25). We also counted the number of cells that stained with the anti-PCNA antibody in the same 10 randomly chosen 0.159-mm^2 fields at ×100 magnification.

Statistical Analysis. Comparisons of tumor weight and numbers of TUNEL-positive, PCNA-positive, and CD31 positive cells were analyzed by Student's t tests. Differences between groups were considered statistically significant at $P < 0.05$.

RESULTS

Expression of PDGF and PDGFR in MDA-MB-435 Bone Tumors. Preliminary experiments[2] had shown that cultured MDA-MB-435 cells release PDGF-A and PDGF-B.

[2] D. Chelouche Lev and J. E. Price, Unpublished data.

In the work reported here, immunohistochemistry of the tumors in the mouse tibia showed expression of the ligands PDGF-A and PDGF-B (Fig. 2). Although the cultured cells did not express detectable levels of PDGFR (measured by immunoblotting, data not shown), both PDGFRα and PDGFRβ were detected in the MDA-MB-435 cells growing in bone (Fig. 2), suggesting that expression of the receptors can be regulated by the organ microenvironment.

Effect of STI571 on the Growth of MDA-MB-435 Tumors in the Bone of Nude Mice. We evaluated the effects of treatment with STI571 alone and in combination with paclitaxel on the growth of the tumors in the bone of nude mice in two experiments; the results were similar in the two experiments (Table 1). No significant differences in tumor incidence occurred between the groups of mice receiving the different treatments. The control mice had the largest bone tumors, and the weights of tumors in mice receiving paclitaxel alone did not differ significantly from tumors of the control animals ($P = 0.99$ and 0.7 in experiments 1 and 2, respectively). Mice treated with STI571 alone had significantly smaller tumors than the control animals ($P = 0.04$ and 0.003 in experiments 1 and 2, respectively) and the mice treated with paclitaxel alone ($P = 0.03$ and 0.045 in experiments 1 and 2, respectively). Mice receiving the combination of STI571 and paclitaxel had significantly smaller tumors than the control or paclitaxel-treated mice (control versus combination, $P = 0.007$ and 0.018 in experiments 1 and 2; paclitaxel versus combination; $P = 0.004$ and 0.10 in experiments 1 and 2, respectively). However, the tumor sizes in the mice treated with the combined agents did not differ significantly from those of mice treated with STI571 alone ($P = 0.44$ and 0.54 in experiments 1 and 2, respectively).

We assessed the extent of osteolysis in the different treatment groups using digital radiography (Fig. 3), and scoring by three observers using a semiquantitative scale already described. Control mice and those treated with paclitaxel alone developed obvious osteolytic lesions by week 4 of the experiments, whereas in those treated with STI571 or STI571 plus paclitaxel the appearance of osteolytic lesions was delayed by 2 or more weeks. At the end of experiment 1 (6 weeks of treatments) the average osteolysis scores for the control and paclitaxel groups were 2.1 and 1.7, respectively; in contrast, the scores for mice treated with STI571 or STI571 and paclitaxel were 1.2 and 0.8, respectively. Similar results were found in experiment 2. Thus, the use of STI571, either alone or in combination with paclitaxel, was associated with a substantial delay in the development and progression of osteolytic MDA-MB-435 tumors.

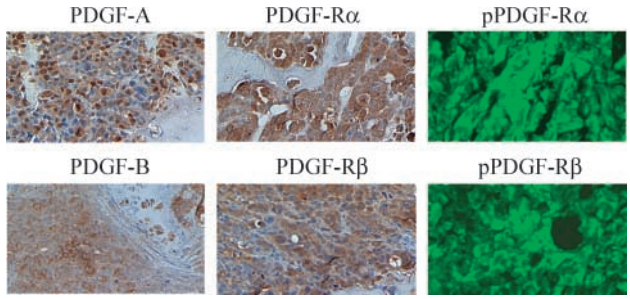

Fig. 2 Immunohistochemical detection of PDGF-A, PDGF-B, PDGFRα, and PDGFRβ (*brown*) and phosphorylated PDGFRα and PDGFRβ (*green fluorescence*) in MDA-MB-435 tumors growing in the bone of nude mice. (Original magnification ×100).

STI571 Treatment Inhibits the Phosphorylation of PDGFR in MDA-MB-435 Bone Tumors and Tumor-Associated Endothelial Cells. Specimens of the MDA-MB-435 bone tumors were processed and used for histologic and immunohistochemical studies. H&E staining of decalcified sections of tumors from mice treated with STI571, with or without paclitaxel, revealed prominent necrotic zones, notably within tumor lesions in the marrow cavity and, to a lesser extent, in tumor extending into the surrounding muscles (Fig. 3). On the other hand, the tumor samples from control and paclitaxel-treated mice revealed minimal or no necrosis.

Immunohistochemistry using antibodies specific for PDGFRα, PDGFRβ, and activated receptors was done to

Table 1 STI571 inhibits the growth of MDA-MB-435 in the bone of nude mice

Treatment group	Tumor incidence*	Mean tumor weight† ±SD (mg)	Lysis score‡
Experiment 1			
Control	15/15	281 ± 67	2.1 ± 0.3
Paclitaxel	14/15	282 ± 60	1.7 ± 0.1§
STI571	13/15	102 ± 40‖	1.2 ± 0.1¶
STI571 + paclitaxel	13/15	67 ± 24**	0.8 ± 0.1¶
Experiment 2			
Control	12/12	470 ± 77	2.5 ± 0.2
Paclitaxel	13/13	416 ± 102	2.1 ± 0.2
STI571	10/12	165 ± 37††	1.5 ± 0.2¶
STI571 + paclitaxel	10/12	211 ± 61‡‡	1.0 ± 0.4¶

*Number of mice with tumors/number of mice given injections.
†Difference in weight between the tumor-bearing and non–tumor-bearing hind legs.
‡Mean score for degree of lysis seen in radiographs of the tumors, with 0 = no lysis to 4 = extensive bone destruction.
§$P = 0.03$ versus control, Mann-Whitney test.
‖$P = 0.044$ versus control, Student's t test.
¶$P = 0.008$ versus control, Mann-Whitney test.
**$P = 0.007$ versus control, Student's t test.
††$P = 0.003$ versus control, Student's t test.
‡‡$P = 0.018$ versus control, Student's t test.

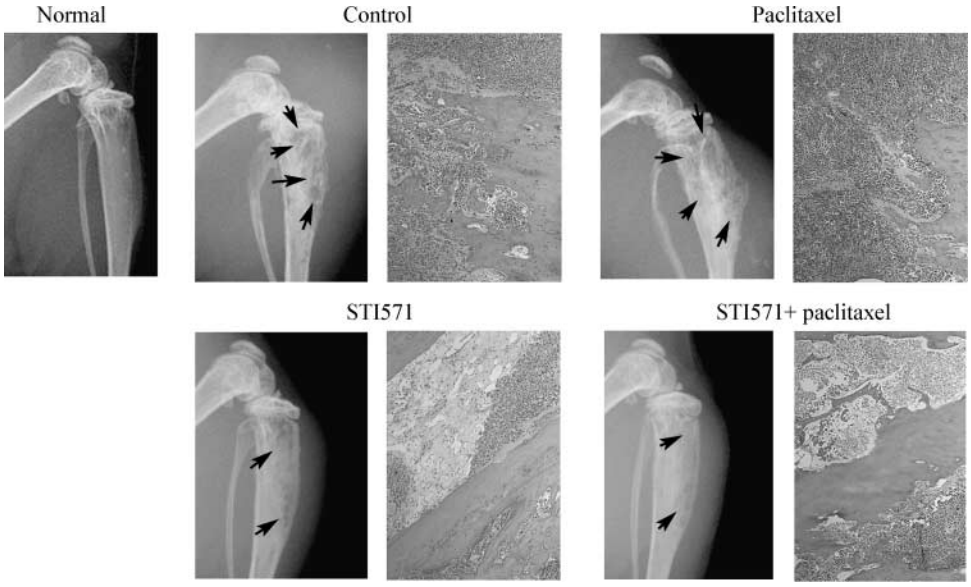

Fig. 3 Digital radiographic and histologic appearance of MDA-MB-435 tumors in the tibias of nude mice at the end of 6 weeks of therapy with paclitaxel, STI571, or STI571 plus paclitaxel. The radiographs (*left of each pair of images*) were taken at necropsy; *arrowheads,* areas of lysis. An image from a noninjected tibia is included for reference. In the micrographs (*right of each pair of images*), substantial areas of necrosis were seen only in tumors of mice treated with STI571, with or without paclitaxel. H&E stain, original magnification ×100.

determine the effect of STI571 on phosphorylation of the receptors in the tumors. No differences were found in the abundance of PDGF-A or PDGF-B or of the two forms of PDGFR in the tumors from the four treatment groups, suggesting that neither STI571 nor paclitaxel affected the expression of these proteins in the MDA-MB-435 tumors. However, treatment with STI571 alone or in combination with paclitaxel greatly reduced the expression of phosphorylated PDGFR (Fig. 4). Thus, p.o. administration of STI571 inhibited PDGFR activity in the MDA-MB-435 tumors. The activation of Akt, a signaling molecule downstream of PDGFR was also substantially reduced in the tumors of mice treated with STI571.

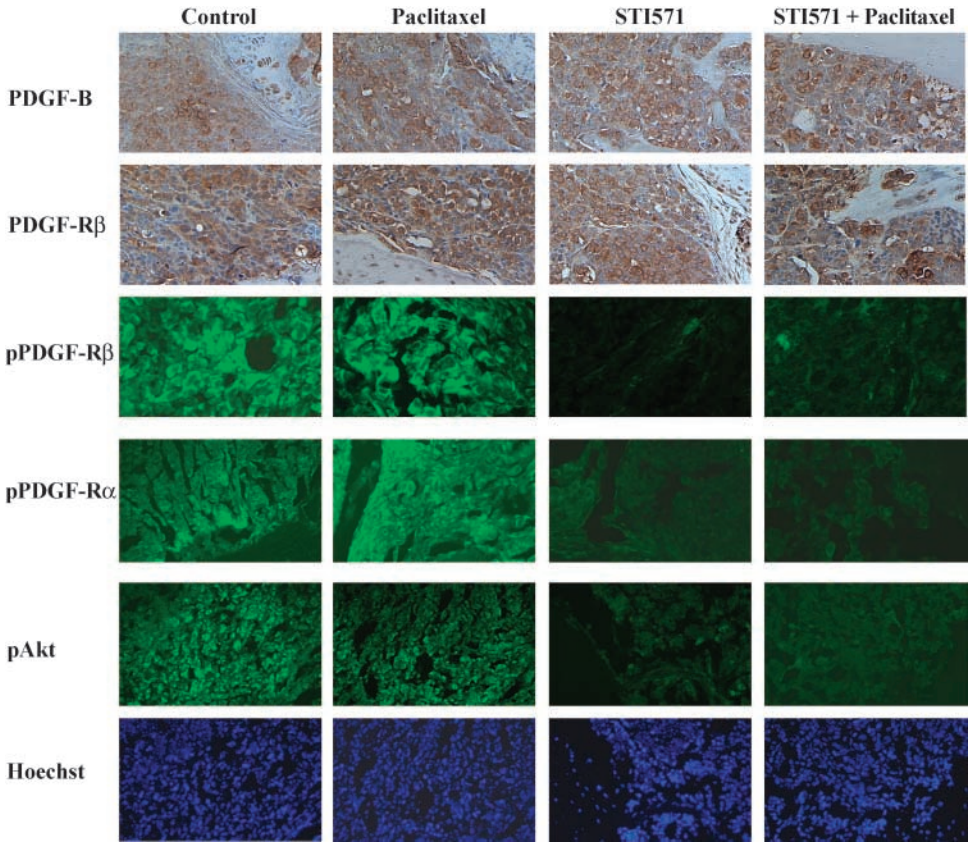

Fig. 4 Immunohistochemical detection of PDGF-B, PDGFRβ, phosphorylated PDGFRβ and PDGFRα, and phosphorylated Akt in MDA-MB-435 tumors growing in the tibias of nude mice, treated with paclitaxel, STI571, or STI571 plus paclitaxel. *First and second rows,* representative staining (*brown*) for PDGF-B and PDGFRβ, respectively. *Third row,* representative images of fluorescent immunohistochemistry for phosphorylated (*p*) PDGFRβ (*green*). *Fourth row,* fluorescent immunohistochemistry for phosphorylated PDGFRα. *Fifth and sixth rows,* fluorescent immunohistochemistry for phosphorylated Akt and corresponding Hoechst stain of the same fields, respectively. Treatment with STI571, alone or in combination with paclitaxel, reduced PDGFR and Akt activity in the tumors. Original magnification ×100.

To investigate whether inhibition of PDGFR phosphorylation was restricted to the tumor cells or was also seen in stromal cells within the tumors, we used double-immunofluorescence staining to examine PDGFR activation on tumor-associated endothelial cells. Endothelial cells were identified by staining for CD31, and colocalization of this marker and phosphorylated PDGFR was apparent in tumor specimens from control and paclitaxel-treated animals (Fig. 5). In contrast, in tumors from mice treated with STI571 or STI571 plus paclitaxel, endothelial cells did not express phosphorylated PDGFR. The effects of STI571 in inhibiting the growth of MDA-MB-435 bone tumors may therefore be through a direct effect on the tumor cells and also through inhibition of PDGFR signaling in the tumor-associated endothelial cells.

STI571 Inhibits Tumor Cell Proliferation and Induces Apoptosis. Inhibition of tumor growth in the STI571-treated mice could be the consequence of decreased tumor cell division, increased tumor cell death, or both. The proportion of cells expressing PCNA, a marker of proliferating cells, and the number of apoptotic cells indicated by the TUNEL reaction were determined in the bone tumors from the different treatment groups (Table 2). The mean percentage of PCNA-positive cells was 59.2% in control tumors and 48.9% in paclitaxel-treated tumors ($P = 0.01$; Table 2). More substantial reductions in the proportion of proliferating cells was found in tumors from STI571-treated mice, with 27.5% PCNA positive cells in the STI571-treated tumors ($P < 0.001$ versus control) and 23.85% in tumors from mice treated with STI571 plus paclitaxel ($P < 0.001$). The difference between the proportions of proliferating cells in the tumors from mice treated with STI571 and those from mice treated with STI571 plus paclitaxel was significant ($P = 0.0037$), suggesting that the combination treatment had an additive effect in inhibiting cellular proliferation.

Few TUNEL-positive cells were detected in the tumors from control mice (mean number 5.1 per 100× field), with a modest increase in those from the paclitaxel-treated mice (8.0, $P = 0.01$; Table 2; Fig. 6). The tumors from mice treated with STI571, alone or in combination with paclitaxel, had significantly more TUNEL-positive cells than did those from control and paclitaxel-treated mice ($P < 0.001$). The combination of the two agents produced an additive induction of apoptosis ($P = 0.039$, STI571 versus STI571 + paclitaxel).

STI571 Induces Apoptosis in Tumor-Associated Endothelial Cells and Reduces Tumor Microvessel Density. Immunohistochemical testing for CD31 (for measurement of microvessel density) and immunofluorescence double labeling for CD31 and TUNEL were used to evaluate the effects of STI571 on tumor-associated endothelial cells. Paclitaxel treatment alone had no effect on microvessel density in the tumors (Table 2), whereas treatment with STI571, alone and in combination with paclitaxel, resulted in a significant reduction in the number of CD31 positive cells ($P < 0.001$). Immunofluorescence showed CD31 expression (red fluorescence, Fig. 6) TUNEL positivity (green fluorescence), and colocalization of the signals (yellow fluorescence) in endothelial cells in the tumors of mice treated with STI571 or STI571 plus paclitaxel. No colocalization of the red and green fluorescence was detected in tumors from the control or paclitaxel-treated mice. These results suggested that STI571 can induce apoptosis in both MDA-MB-435 and endothelial cells. Immunohistochemical staining of the bone tumors for VEGF, IL-8, and bFGF did not reveal differences between the four treatment groups (data not shown), suggesting that the STI571-mediated apoptosis

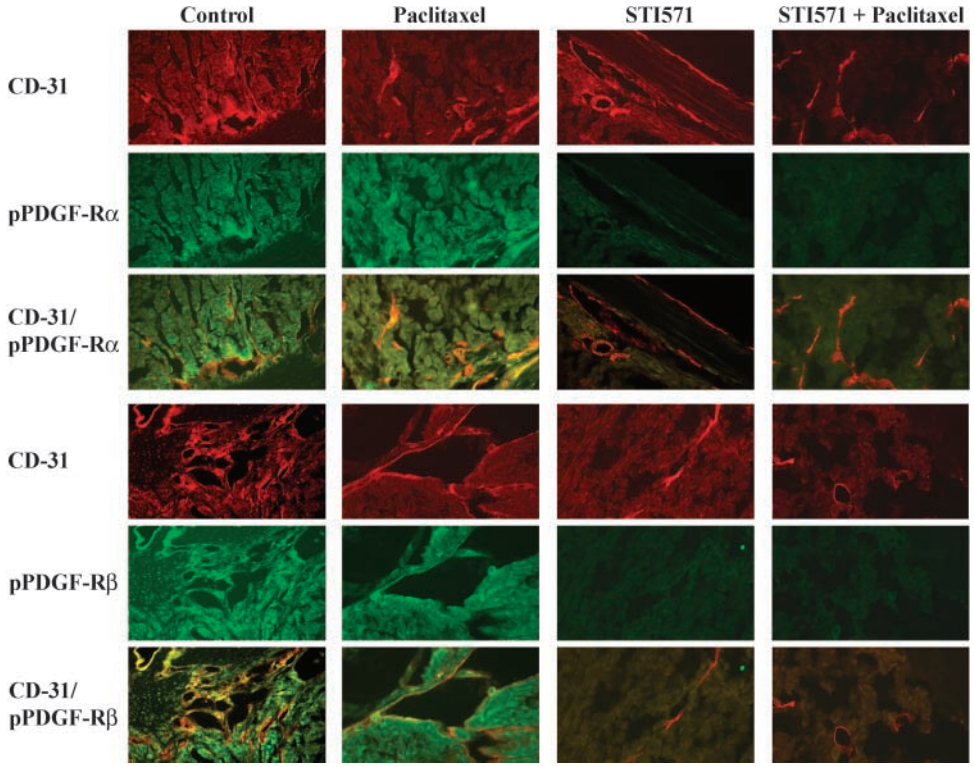

Fig. 5 Immunofluorescence histochemical detection of tumor-associated endothelial cells with antibodies against CD31 and phosphorylated PDGFRβ and PDGFRα (pPDGFRβ and pPDGFRα) in MDA-MB-435 tumors growing in the bone of nude mice, treated with paclitaxel, STI571, or STI571 plus paclitaxel. Staining with CD31 antibodies was detected with Texas Red–conjugated goat anti-rat antibody, and FITC-conjugated goat anti-rabbit antibody detected phosphorylated PDGFRβ staining. Colocalization of the signals (*yellow*) showed that CD31 positive cells also expressed pPDGFR in tumors from control and paclitaxel-treated mice, whereas treatment with STI571, with or without paclitaxel, inhibited PDGFR activity. Original magnification ×100.

Table 2 Effects of STI571 and paclitaxel treatment on proliferation, apoptosis, and microvessel density in MDA-MB-435 bone tumors

Treatment	Mean counts (±SD)*		
	TUNEL positive	% PCNA positive	CD31 positive
Control	5.1 ± 2.8	59.2 ± 6.9	26.9 ± 10.4
Paclitaxel	8.0 ± 4.6†	48.9 ± 7.3‡	27.8 ± 9.9
STI571	34.1 ± 13.6	27.5 ± 3.4‡	9.6 ± 3.9‡
STI571 + paclitaxel	42.2 ± 1.7‡	23.8 ± 3.9‡	10.75 ± 5.8‡

*Mean values of positively stained cells counted in 10 randomly selected fields of 3 tumor samples from each treatment group. Values for TUNEL positive and CD31 positive cells are the numbers of stained cells per field. Values for PCNA positive cells are expressed as the percentage of PCNA positive cells counted per field.

†$P = 0.01$ versus control, Student's t test.

‡$P = 0.001$ versus control, Student's t test.

of endothelial cells was not due to diminished expression of these proangiogenic factors in MDA-MB-435 tumor cells growing in the bone.

DISCUSSION

As originally described by Stephen Paget in 1889 (26), the characteristic patterns of metastasis seen in patients with breast cancer and other cancers are the result of multiple interactions between the metastasizing cancer cells (the "seeds") and the compatible organ environment (the "soil"). The mediators of interactions between tumor and normal cells include cytokines and growth factors, which act in an autocrine or paracrine manner (4, 27). Identifying the mechanisms of these tumor-host interactions, notably those involved in the promotion of tumor angiogenesis, offers opportunities for therapeutic intervention.

Metastasis to the bone is a common complication for patients with breast cancer. The predominantly lytic nature of breast cancer bone metastases is thought to be a consequence of the "vicious cycle" described by Chirgwin and Guise (16), in which metastatic cells in the bone microenvironment release factors and cytokines that promote osteoclast activation and bone destruction. In turn, this liberates factors from the bone matrix, notably transforming growth factor-β, which provide feedback that further enhances the osteolysis-promoting phenotype in the breast cancer cells (16, 28). Among the cytokines and growth factors thought to contribute to the regulation of bone turnover are the PDGFs (14), which are expressed by many types of cancer, including breast cancers (7, 11). High levels of PDGF in plasma or tumor tissues from patients with breast cancer have been correlated with a higher incidence of metastasis and, hence,

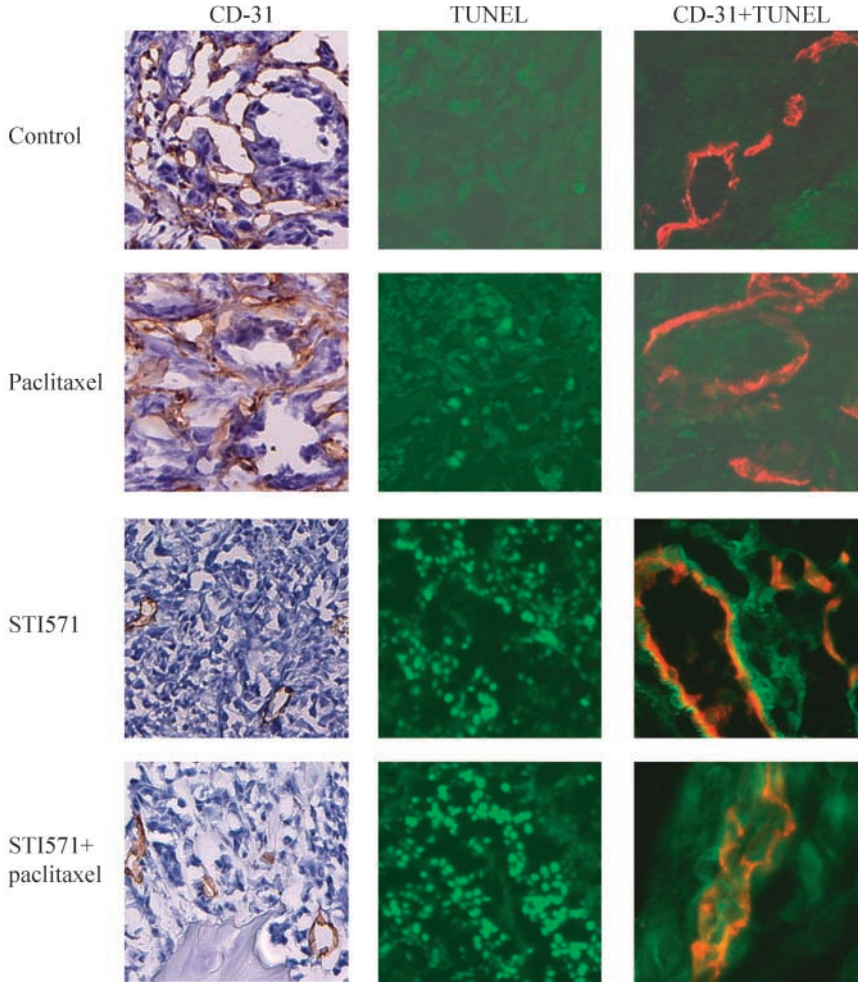

Fig. 6 Immunohistochemical detection of CD31 positive cells and apoptotic cells in MDA-MB-435 tumors growing in the bone of nude mice, treated with paclitaxel, STI571, or STI571 plus paclitaxel. Treatment with STI571 reduced the numbers of CD31 positive cells (*left*), detecting the primary antibody with horseradish peroxidase-conjugated antibody and increased apoptosis (*center*), detected with the TUNEL reaction. Colocalization of signals for TUNEL positive cells, and antibody to CD31 detected with Texas Red–conjugated goat anti-rat antibody (*right*) was seen only in tumors from mice treated with STI571, with or without paclitaxel. Original magnification ×200.

shorter survival (13, 29). Our study tested whether p.o. administration of STI571, a small-molecule inhibitor of PDGFR tyrosine kinase, would inhibit the growth of human breast cancer cells implanted into the tibias of nude mice as an experimental model of cancer growing in the bone environment. The data from immunohistochemistry showed that the breast cancer cells growing in the bone of mice expressed PDGF-A and PDGF-B as well as PDGFRα and PDGFRβ. Because the MDA-MB-435 cells do not express detectable levels of these receptors when grown in tissue culture, these *in vivo* findings suggest up-regulation by factors present in the tissue environment. Transforming growth factor β, which is found in abundance in bone matrix, can promote PDGF expression in breast cancer cells *in vitro* (30).[3] The expression level of PDGFR can be modulated by various conditions and factors in the tissue microenvironment (9). We previously reported that endothelial cells in prostate cancer bone lesions express high levels of PDGFR, whereas endothelial cells in unaffected bone or in tumors growing in muscle did not express PDGFR (23). Similarly, endothelial cells present in the MDA-MB-435 bone tumors expressed the receptors for PDGF, and the receptors were phosphorylated.

Treatment with STI571 blocked activation of PDGFR and also substantially reduced Akt activation in the tumors, thus blocking a signal transduction pathway that is important for tumor growth and survival (31). Growth of the MDA-MB-435 tumors was significantly inhibited and bone structure was preserved in the STI571-treated mice. These results suggested that signaling through PDGFR is important for the development of osteolytic breast cancer lesions and that inhibiting this pathway may be an effective method of controlling the progression of skeletal metastasis. Our current findings are similar to a previous report, demonstrating that STI571 inhibited the growth of human prostate cancer cells in mouse bone (23). In both these studies, STI571 blocked PDGFR phosphorylation in tumor cells in bone lesions and in tumor-associated endothelial cells, coincident with the appearance of apoptotic cells and reduced microvessel density within the tumors. STI571 targets cells expressing phosphorylated PDGFR, and in the microenvironment of bone metastases, these include tumor cells and tumor-associated endothelial cells, osteoblasts (32) and osteoclasts (17). Our study documented a significant reduction in proliferation and an increase in apoptosis in the breast cancer cells, and apoptosis in tumor-associated endothelial cells in STI571-treated mice. The study did not determine whether STI571 interfered with the actions of tumor-derived PDGF on osteoblasts or osteoclasts. STI571 treatment reduced the extent of osteolysis, but the current study cannot distinguish whether this effect was primarily by inhibiting the growth and survival of the breast cancer cells or whether STI571 inhibited the release of osteolytic factors by MDA-MB-435 cells.

The progressive growth of primary tumors and metastases depends on the development and maintenance of vasculature (4, 33). The function, proliferation, and survival of endothelial cells depend on expression of receptors responding to various factors, including bFGF, VEGF, epithelial growth factor, and PDGF (9, 34). Blocking the interactions between these factors and their receptors or inhibiting the receptor function can lead to endothelial cell apoptosis, resulting in the loss of vasculature and leading to tumor necrosis. Our study provides another example of a potential antivascular action from blocking PDGF-mediated signaling in the MDA-MB-435 tumors in the tibias of nude mice. The inhibition of different receptor tyrosine kinases in tumor-associated endothelial cells has been shown to be an effective therapeutic strategy in several preclinical models of human cancer and metastasis (25, 35, 36).

Systemic administration of STI571 has been shown to enhance antitumor effects of chemotherapy by reducing interstitial hypertension and increasing drug uptake (37). Although we found evidence of impaired PDGFR signaling in the bone tumors of STI571-treated mice, our results did not demonstrate any enhancement of paclitaxel's antitumor in the tumors. The dose of paclitaxel we used was lower than the maximal tolerated dose for mice, and was deliberately chosen to show a potential additive effect when combined with STI571. In preliminary studies,[4] we found that the same dose and administration schedule of paclitaxel used in this work significantly inhibited the growth of MDA-MB-435 tumors in the mammary fat pads of nude mice, yet our data from this study showed a minimal effect of the paclitaxel alone on the MDA-MB-435 tumor cells growing in the bone. This may be an example of the effect of different organ environments on modulation of drug sensitivity of cancer cells (38, 39), and the possibility that the organ microenvironment can regulate P glycoprotein levels in tumor cells is currently being investigated.

In summary, we found that human breast cancer cells growing in the bone of nude mice express PDGF and that both tumor cells and tumor-associated endothelial cells express activated PDGFR. Systemically administered STI571 inhibited PDGFR activation, induced apoptosis in the endothelial and breast cancer cells, and significantly decreased tumor size and osteolysis. These results suggest that interfering with the PDGFR signaling pathway may be a useful approach for controlling the progressive growth of breast cancer cells within the bone microenvironment. The data reported here are potentially significant for developing additional therapeutic strategies for breast cancer that has metastasized to bone.

ACKNOWLEDGMENTS

We thank Dr. Corazon Bucana for her expert advice, Donna Reynolds and Joseph Douglas for their technical assistance with histology and immunohistochemistry used in this study, and Karen Phillips for expert editorial assistance.

REFERENCES

1. Plunkett TA, Smith P, Rubens RD. Risk of complications from bone metastases in breast cancer: implications for management. Eur J Cancer 2000;36:476–82.

2. Hortobagyi GN. Novel approaches to the management of bone metastases in patients with breast cancer. Semin Oncol 2002;29:134–44.

3. Theriault RL, Hortobagyi GN. The evolving role of bisphosphonates. Semin Oncol 2001;28:284–90.

[3] D. Chelouche Lev and J. E. Price, Unpublished data.

[4] D. Chelouche Lev and J. E. Price, Unpublished data.

4. Fidler IJ. Critical determinants of metastasis. Semin Cancer Biol 2002;12:89–96.

5. Chambers AF, Naumov GN, Vantyghem SA, Tuck AB. Molecular biology of breast cancer metastasis: clinical implications of experimental studies on metastatic inefficiency. Breast Cancer Res 2000;2:400–7.

6. Welch DR, Steeg PS, Rinker-Schaeffer CW. Molecular biology of breast cancer metastasis. Genetic regulation of human breast carcinoma metastasis. Breast Cancer Res 2001;2:408–16.

7. De Jong JS, van Diest PJ, van der Valk P, Baak JPA. Expression of growth factors, growth inhibiting factors, and their receptors in invasive breast cancer. I. An inventory in search of autocrine and paracrine loops. J Pathol 1998;184:44–52.

8. Dirks RPH, Bloemers HPJ. Signals controlling the expression of PDGF. Mol Biol Rep 1996;22:1–24.

9. Heldin CH, Westermark B. Mechanism of action and *in vivo* role of platelet-derived growth factor. Physiol Rev 1999;79:1283–316.

10. Claesson-Welsh L. Platelet-derived growth factor receptor signals. J Biol Chem 1994;269:32023–6.

11. Bhardwaj B, Klassen J, Cossette N, et al. Localization of platelet-derived growth factor beta receptor expression in the periepithelial stroma of human breast carcinoma. Clin Cancer Res 1996;2:773–82.

12. Ariad S, Seymour L, Bezwoda WR. Platelet-derived growth factor (PDGF) in plasma of breast cancer patients: correlation with stage and rate of progression. Breast Cancer Res Treat 1991;20:11–7.

13. Seymour L, Dajee D, Bezwoda WR. Tissue platelet derived-growth factor (PDGF) predicts for shortened survival and treatment failure in advanced breast cancer. Breast Cancer Res Treat 1993;26:247–52.

14. Canalis E, Varghese S, McCarthy TL, Centrella M. Role of platelet derived growth factor in bone cell function. Growth Regul 1992;2:151–5.

15. Roodman GD. Role of stromal-derived cytokines and growth factors in bone metastasis. Cancer 2003;97:733–8.

16. Chirgwin JM, Guise TA. Molecular mechanisms of tumor-bone interactions in osteolytic metastases. Crit Rev Eukaryot Gene Expr 2000;10:159–78.

17. Zhang Z, Chen J, Jin D. Platelet-derived growth factor (PDGF)-BB stimulates osteoclastic bone resorption directly: the role of receptor β. Biochem Biophys Res Commun 1998;251:190–4.

18. Franchimont N, Canalis E. Platelet-derived growth factor stimulates the synthesis of interleukin-6 in cells of the osteoblast lineage. Endocrinology 1995;136:5469–75.

19. Kubota K, Sakikawa C, Katsumata M, Nakamura T, Wakabayashi K. Platelet-derived growth factor BB secreted from osteoclasts acts as an osteoblastogenesis inhibitory factor. J Bone Miner Res 2002;17:257–65.

20. Yi B, Williams PJ, Niewolna M, Wang Y, Yoneda T. Tumor-derived platelet-derived growth factor-BB plays a critical role in osteosclerotic bone metastasis in an animal model of human breast cancer. Cancer Res 2002;62:917–23.

21. Traxler P, Bold G, Buchdunger E, et al. Tyrosine kinase inhibitors: from rational design to clinical trials. Med Res Rev 2001;21:499–512.

22. Buchdunger E, Zimmermann J, Mett H, et al. Inhibition of the Abl protein tyrosine kinase *in vitro* and *in vivo* by a 2-phenylaminopyrimidine derivative. Cancer Res 1996;56:100–4.

23. Uehara H, Kim SJ, Karashima T, et al. Effects of blocking platelet-derived growth factor-receptor signaling in a mouse model of experimental prostate cancer bone metastases. J Natl Cancer Inst 2003; 95:558–70.

24. Weber KL, Doucet M, Price JE, Baker C, Kim SJ, Fidler IJ. Blockade of epidermal growth factor receptor signaling leads to inhibition of renal cell carcinoma growth in the bone of nude mice. Cancer Res 2003;63:2940–7.

25. Baker CH, Kedar D, McCarty MF, et al. Blockade of epidermal growth factor receptor signaling on tumor cells and tumor-associated endothelial cells for therapy of human carcinomas. Am J Pathol 2002; 161:929–38.

26. Paget S. The distribution of secondary growths in cancer of the breast. Lancet 1889;1:571–3.

27. Liotta LA, Kohn EA. The microenvironment of the tumour-host interface. Nature 2001;411:375–9.

28. Kang Y, Siegel PM, Shu W, et al. A multigenic program mediating breast cancer metastasis to bone. Cancer Cell 2003;3:537–49.

29. Seymour L, Bezwoda WR. Positive immunostaining for platelet derived growth factor (PDGF) is an adverse prognostic factor in patients with advanced breast cancer. Breast Cancer Res Treat 1993; 26:247–52.

30. Chen C-R, Kang Y, Massague J. Defective repression of c-*myc* in breast cancer cells: a loss at the core of the transforming growth factor β growth arrest program. Proc Natl Acad Sci U S A 2001;98:992–9.

31. Vivanco I, Sawyers CL. The phosphatidylinositol 3-kinase-AKT pathway in human cancer. Nat Rev Cancer 2002;2:489–501.

32. Horner A, Bord S, Kemp P, Grainger D, Compston JE. Distribution of platelet-derived growth factor (PDGF) A chain mRNA, protein and PDGF-α-receptor in rapidly forming human bone. Bone 1996;19: 353–62.

33. Folkman J. Role of angiogenesis in tumor growth and metastasis. Semin Oncol 2002;29:15–8.

34. Tonini T, Rossi F, Claudio PP. Molecular basis of angiogenesis and cancer. Oncogene 2003;22:6549–56.

35. Bruns CJ, Solorzano CC, Harbison M, et al. Blockade of the epidermal growth factor receptor by a novel tyrosine kinase inhibitor leads to apoptosis of endothelial cells and therapy of human pancreatic carcinoma. Cancer Res 2000;60:2926–35.

36. Xu L, Yoneda J, Herrera C, Wood J, Killion JJ, Fidler IJ. Inhibition of malignant ascites and growth of human ovarian carcinoma by oral administration of a potent inhibitor of the vascular endothelial growth factor receptor tyrosine kinases. Int J Oncol 2000;16:445–54.

37. Pietras K, Rubin K, Sjöblom T, Buchdunger E, Heldin CH, Östman A. Inhibition of PDGF receptor signaling in tumor stroma enhances antitumor effect of chemotherapy. Cancer Res 2002;62:5476–84.

38. Wilmanns C, Fan D, O'Brian CA, et al. Modulation of doxorubicin sensitivity and level of p-glycoprotein expression in human colon carcinoma cells by ectopic and orthotopic environments in nude mice. Int J Oncol 1993;3:413–8.

39. Holden SA, Emi Y, Kakeji Y, Northey D, Teicher BA. Host distribution and response to antitumor alkylating agents of EMT-6 tumor cells from subcutaneous tumor implants. Cancer Chemother Pharmacol 1997;40:87–93.

Clinical & Experimental Metastasis (2005) 22: 39–46
DOI 10.1007/s10585-005-3222-y

Chemokine receptor CXCR4 expression in breast cancer as a potential predictive marker of isolated tumor cells in bone marrow

Neslihan Cabioglu[1], Aysegul Sahin[2], Michele Doucet[1], Ekrem Yavuz[3], Abdullah Igci[4], Engin O. Yildirim[5], Esin Aktas[5], Sema Bilgic[5], Bayram Kiran[5], Gunnur Deniz[5] & Janet E. Price[1]
[1]*Department of Cancer Biology; and* [2]*Department of Pathology, The University of Texas M.D. Anderson Cancer Center, Houston, Texas, USA;* [3]*Department of Pathology,* [4]*Department of General Surgery, Istanbul Faculty of Medicine and* [5]*Institute of Experimental Medical Research, Instanbul University, Istanbul, Turkey*

Received 2 September 2004; accepted in revised form 24 February 2005

Key words: bone marrow micrometastases, breast cancer, chemokine receptors, CXCR4, EGFR, HER2/neu

Abstract

Interactions between the CXCR4 chemokine receptor in breast cancer cells and the ligand CXCL12/SDF-1α are thought to play an important role in breast cancer metastases. In this pilot study, CXCR4 expression along with other biomarkers including HER2-neu and EGFR, were measured in primary tumor samples of patients with operable breast cancer to test whether any of these biomarkers alone and in combination could indicate breast cancer with high likelihood of metastasizing to bone marrow. Cytokeratin (CK) positive cells in bone marrow were identified by flow-cytometry following enrichment with CK 7/8 antibody-coupled magnetic beads. Primary tumors (n = 18) were stained with specific antibodies for CXCR4, HER2-neu, EGFR, and PCNA using an indirect avidin–biotin horseradish peroxidase method. The majority of the patients had T2/T3 tumors (72%), or lymph node involvement (67%) as pathologic characteristics that were more indicative of high-risk breast cancer. High CXCR4 cytoplasmic expression was found in 7 of 18 patients (39%), whereas 6 of 18 patients (33%) were found to have CK positivity in bone marrow. The median number of CK^+ cells was 236 (range, 20–847) per 5×10^4 enriched BM cells. The presence of CK^+ cells in bone marrow was found to be associated with increased expression of CXCR4 alone or in addition to EGFR and/or HER2-neu expression ($P = 0.013$, $P = 0.005$, and $P = 0.025$, respectively) in primary tumors. Furthermore, three patients with high CK positivity (>236 CK^+ per 5×10^4 enriched bone marrow cells) in bone marrow exclusively expressed high levels of CXCR4 with EGFR/HER2-neu ($P = 0.001$). Our data suggest that high CXCR4 expression in breast cancer may be a potential marker in predicting isolated tumor cells in bone marrow. CXCR4 coexpression with EGFR/HER2-neu might further predict a particular subset of patients with high CK positivity in bone marrow.

Abbreviations: BM – bone marrow; CK – cytokeratin; EGFR – epidermal growth factor receptor; ER – estrogen receptor; HG – histologic grade; ITC – isolated tumor cell; PBS – phosphate buffered saline; PCNA – proliferating cell nuclear antigen; PR – progesteron receptor; TNM – tumor node metastasis

Introduction

Numerous clinical studies have shown the presence of isolated tumor cells (ITC) in bone marrow (BM) to be an independent factor of poor prognosis in breast cancer [1–5]. However, there have been only limited data about the characteristics of the primary tumor in patients with ITC in BM. Increased expression of laminin receptor levels of the primary breast cancer were reported to be associated with the presence of ITC in BM, while no associations were found with other markers, including c-erb-1 oncogene products, p-53, and cathepsin D levels [6, 7].

Nevertheless, controversial findings were obtained in terms of HER2-neu expression. Naume et al. [6] reported increased expression of HER2-neu in patients with ITC in BM detected by immunocytochemistry following immunomagnetic enrichment, whereas others [7, 8] could not demonstrate such a relationship between HER2-neu expression in primary tumor and BM involvement using standard immunocytochemistry in BM aspirates of patients with breast cancer.

Correspondence to: Neslihan Cabioglu, UT M.D. Anderson Cancer Center, 1515 Holcombe Blvd., Unit 85, Houston, TX 77030, USA. Tel: +1-713-745-5709; Fax: +1-713-745-5709; E-mail: neslicab@yahoo.com

Breast cancer is characterized by a distinct metastatic pattern involving the regional lymph nodes, BM, liver, and lung; it was recently suggested that this is influenced by CXCR4 chemokine receptor expression [9, 10]. The expression of CXCR4 has also been reported to be associated with disseminated tumor cells in BM in other malignancies, including neuroblastoma, prostate cancer, and leukemia [11–14]. Migration of breast cancer cells in response to conditioned medium from human BM was significantly reduced after CXCR4 blocking, suggesting SDF-1α is an important component in the BM environment for tumor–host interactions. Furthermore, Braun et al. [15] demonstrated that patients with breast cancer developed fatal metastatic relapses in the presence of HER2-neu positive micrometastatic cells in BM. This calls into question whether factors in BM microenvironment, such as SDF-1α, might give a survival advantage to HER2-neu overexpressing micrometastatic cells.

We recently showed a crosstalk between CXCR4 and HER2-neu or EGFR, and demonstrated the transactivation of HER2-neu and EGFR by SDF-1α through CXCR4 chemokine receptor [16]. Therefore, we tested whether CXCR4 expression alone or in combination with HER2-neu and/or EGFR, can indicate breast cancer with high likelihood of metastasizing to bone marrow.

Materials and methods

Patients

Between October 2000 and March 2001, 18 patients with a diagnosis of breast carcinoma and a clinically negative axilla who had undergone surgery at the Department of General Surgery, Faculty of Medicine, Istanbul University (Istanbul, Turkey), were included in this study. Histologic grade of the primary tumors was determined according to the Richardson–Bloom grading system [17].

BM assessment

BM (10 cc) was aspirated from the sternum and both upper iliac crests before initial removal of the primary carcinoma under general anesthesia, a procedure approved by the institutional ethical boards. Presence of ITC in BM was determined by detection of CK^+ by flow-cytometry (FACSCalibur; Becton Dickinson, San Jose, CA) following a positive enrichment technique using a MACS Carcinoma Cell Enrichment and Detection Kit (Miltenyi Biotec GmbH, Bergisch Gladbach, Germany) [18].

Briefly, BM samples spun at 300 g for 10 min were permeabilized with MACS CellPerm Solution (Miltenyi Biotec), PBS containing 0.5% bovine serum albumin and 0.1% saponin, for 5 min, that was also a lysis step for erythrocytes. Thereafter, cells were fixed upon addition of MACS CellFix Solution (Miltenyi Biotec) containing 37% formaldehyde for 30 min. To block the Fc receptor, 100 μl of FcR Blocking Reagent (Miltenyi Biotec) was added; and epithelial tumor cells were directly magnetically labeled by incubating the cells with Cytokeratin 7/8 MicroBeads (Miltenyi Biotec) for 45 min. At this step, half of the sample of each patient was used as unstained control to adjust the settings of flow-cytometry according to the autofluorescence of the cells. To detect and quantify CK-expressing tumor cells, the rest of the sample was further incubated with anti-CK-7/8 fluorescein isothiocyanate (clone: CAM5.2) and CD45-phycoerythrin monoclonal antibodies (Miltenyi Biotec) for 15 min. For magnetic enrichment of epithelial tumor cells, magnetically labeled cells were applied to a MACS MS separation column (Miltenyi Biotec). All solutions and MACS MS separation columns were kept cold at 4 °C before using in the assay to avoid nonspecific binding of the immunobeads.

BM samples spiked with MCF-7 cells were used as positive controls when adjusting the settings for forward scatter (distribution of the cells according to the size) and side scatter (distribution of the cells according to the granularity) so that the CK^+ cells were located in the upper-right corner of the forward scatter vs. side scatter dotplot as described previously [19]. Furthermore, the settings for FL-1 (fluorescein isothiocyanate) and FL-2 (phycoerythrin) were adjusted so that $CK^+/CD45^-$ tumor cells were located in the lower-right corner and unspecifically retained $CK^-/CD45^+$ leukocytes were located in the upper-left corner (Figures 1c–d). Data of 2×10^4 to 5×10^4 cells per sample were analyzed using Cell Quest software program (Becton Dickinson, San Jose, CA). For each sample, a gate including all enriched BM cells (Figure 1a, $gate_{enriched\ BM\ cells}$) and a specific gate for MCF-7 breast cancer cells (Figure 1b, $gate_{MCF\text{-}7\ cells}$) were both evaluated [19]. Positivity of ITC in BM was considered as the presence of $CK^+/CD45^-$ cells located in the lower-right corner in both gates (Figures 1c–d).

Immunohistochemistry

Avidin–biotin complex method was used for immunohistochemical staining. After deparaffinization of tissue sections (5 μm), antigen retrieval was required for all stainings except CXCR4. For blocking endogen peroxidase of samples for PCNA staining, 0.3% H_2O_2 in absolute methanol was used, whereas all other sections were immersed in 0.3% H_2O_2 in PBS. Nonspecific binding was blocked by incubation in protein-blocking solution containing 5% normal horse serum and 1% normal goat serum in PBS for 20 min at room temperature. The primary antibodies and the staining procedure are summarized in Table 1. Color was developed with diaminobenzidine, and sections were counterstained with haematoxylin. As negative controls for all primary antibodies, sections were incubated with protein-blocking solution.

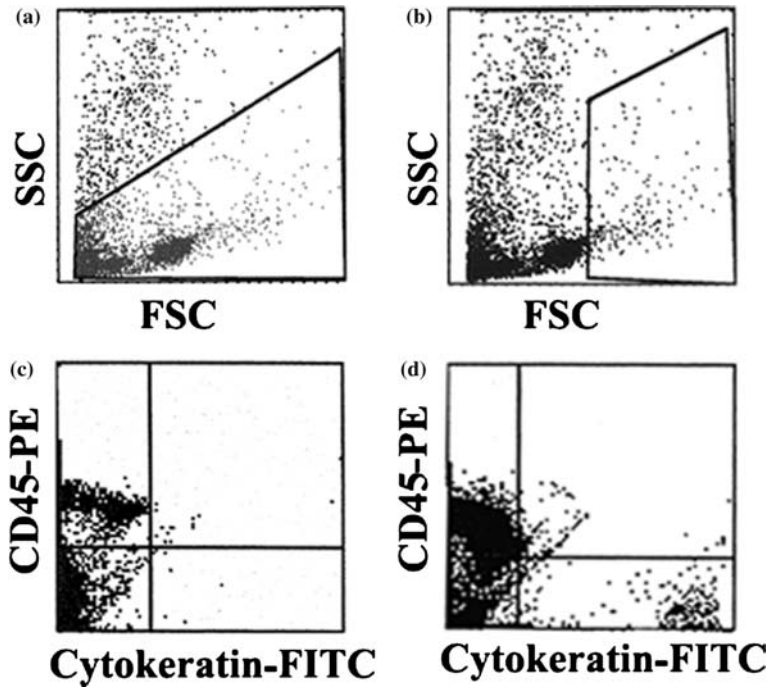

Figure 1. (a) A gate including all enriched BM cells; (b) The MCF-7 gate of enriched BM cells; (c) Flow-cytometric analysis of a BM sample of a patient with low CK^+ cells (<236 CK^+ per 5×10^4 enriched BM cells); (d) Flow-cytometric analysis of a BM sample of a patient with high CK^+ cells (>236 CK^+ per 5×10^4 enriched BM cells). BM, bone marrow; CK, cytokeratin; FSC, forward scatter; SSC, side scatter.

Table 1. Primary antibodies and immunohistochemical procedure.

Primary antibody	Manufacturer	Clone	Antibody dilution	Primary antibody incubation
ER	Novo Castra (New Castle, UK)	NCL-ER-6F11	1:50	60 min at room temperature
PR	Neomarkers	hPRa2 + hPRa3	1:50	60 min at room temperature
HER2/neu	Neomarkers	AB8	1:300	60 min at room temperature
[a]HER2/neu	Santa Cruz Biotechnology (Santa Cruz, CA)	Neu, c18	1:200	Overnight at 4 °C
EGF-R	Santa Cruz Biotechnology (Santa Cruz, CA)	Sc 03	1:200	Overnight at 4 °C
CXCR4	R&D Systems	44717.111	1:150	Overnight at 4 °C
PCNA	DAKO (Dako Corporation, Glostrup, Denmark)	Clone PC 10	1:50	Overnight at 4 °C

[a]Used in immunofluorescence.

Immunohistochemical scoring

The staining for CXCR4 was predominantly cytoplasmic. A nuclear and membranous staining was occasionally detected with the cytoplasmic staining in some cases. A scoring system was used for this marker according to the intensity (low, intermediate, strong) and percentage of cytoplasmic staining distribution in the tumor sections to define low-, moderate- and high-expression patterns, respectively (Figure 2a). Low expression was considered if no staining was detected or less than 30% of tumor cells showed a cytoplasmic staining pattern with low intensity. Moderate expression was considered if invasive tumor cells with a range from 30 to 50% revealed low or intermediate cytoplasmic staining. CXCR4 expression was considered high when >30% or >50% of the tumor cells showed strong or moderate cytoplasmic staining, respectively. High expression of cytoplasmic CXCR4 was regarded positive in the statistical analyses based on our previous observations [20].

ER, PR, and PCNA were considered positive if the nuclear staining was >10% per at least 1000 invasive tumor cells. For EGFR, any complete membranous staining was considered positive regardless of the intensity of the staining in concordance with previous studies [21]. HER2-neu expression was evaluated by using the United States Food and Drug Administration-approved scoring system as defined in the HerceptTest kit scoring guidelines. HER2-neu overexpression was considered positive in the statistical analyses if more than 10% of the tumor cells showed a complete and strong membranous staining (HerceptTest 3+).

Immunofluorescence double staining for CXCR4, and HER2-neu or EGFR

Following deparaffinization of formalin-fixed and paraffin-embedded slides, samples were washed three times with PBS, incubated with protein-blocking solution for 20 min at room temperature, and with mouse anti-

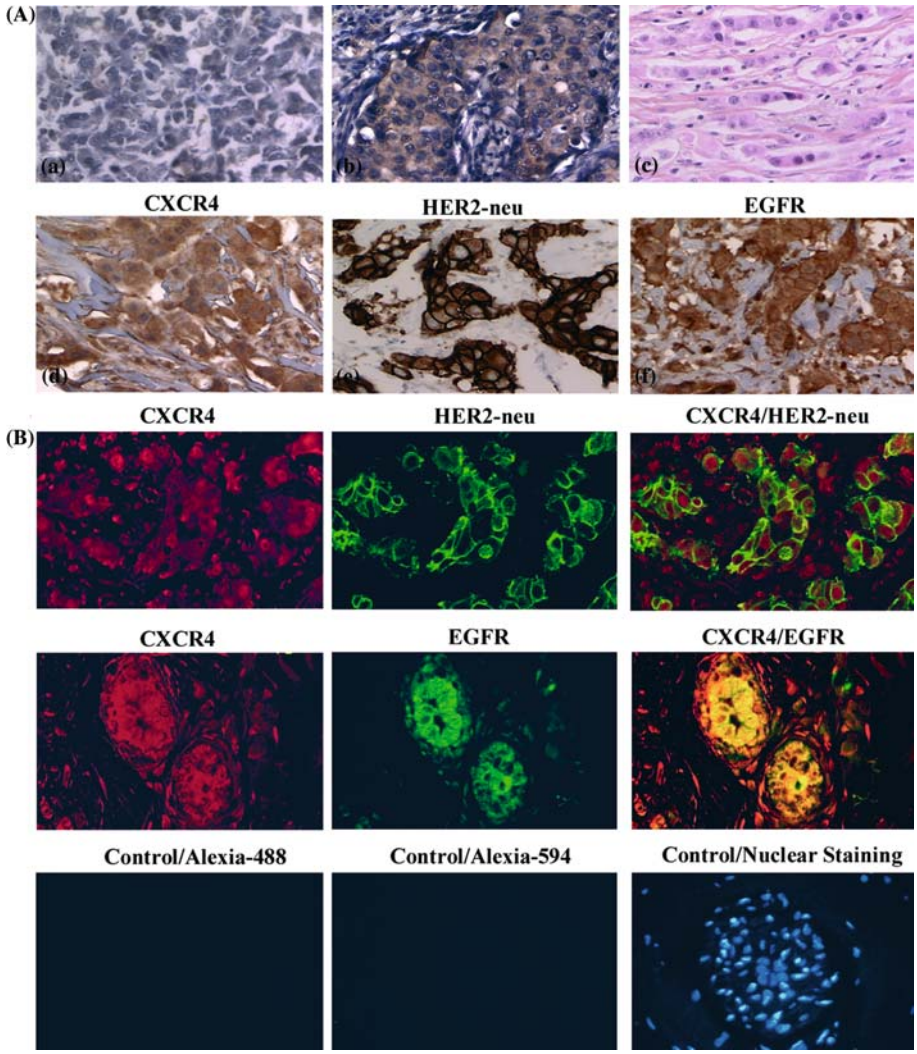

Figure 2. A: (a) A cytoplasmic staining pattern for "low expression" of CXCR4; (b) A cytoplasmic staining pattern for "moderate expression" of CXCR4; (c) H&E staining of a breast tumor showing high CXCR4 and EGFR expression and HER2-neu overexpression in a patient with high CK^+ cells in BM (>236 CK^+ per 5×10^4 enriched BM cells); (d–f), Immunohistochemical staining of (d) high CXCR4 expression, and (e) HER2-neu overexpression, and (f) high EGFR expression in the same patient sample. B: Immunofluorescence double staining of CXCR4 and HER2-neu and EGFR in a patient with high CK^+ cells in BM (>236 CK^+ per 5×10^4 enriched BM cells) with high CXCR4 and HER2-neu and EGFR expression. "$CXCR4^+/HER2\text{-}neu^+$" cells were demonstrated as cells with colocalized green fluorescence in membrane and red fluorescence in cytoplasm, whereas "$CXCR4^+/EGFR^+$" cells were shown predominantly as localized yellow fluorescence within the membrane and cytoplasm. BM, bone marrow; CK, cytokeratin; EGFR, epidermal growth factor receptor.

human CXCR4 Mab at dilution 1:150 for 18 h at 4 °C. After the samples were washed with PBS, the slides were blocked again with protein-blocking solution, and incubated with secondary mouse antibody conjugated to goat anti-mouse antibody conjugated to Alexia-488-FITC (Molecular Probe, Eugene, OR) at a 1:400 dilution. For double staining of CXCR4 with other markers, sections were further incubated with rabbit anti-human EGFR, or HER2-neu at 1:400 and 1:200 dilutions, respectively. After incubation with the primary antibodies, samples were applied to a goat anti-rabbit antibody conjugated with Alexia-594 (Molecular Probe) at a 1:600 dilution for 1 h at room temperature in the dark, and incubated with 300 μg/ml Hoechst stain (Sigma Chemical Co., St Louis, MO) for 10 min at room temperature to identify cell nuclei. As negative controls for all primary antibodies, sections were incubated with protein-blocking solution.

Immunofluoresence microscopy was performed using 20× objective (Carl Zeiss, Inc., Thornwood, NY) on an epifluoresence microscopy equipped with narrow-band-pass excitation filters mounted in a filter wheel (Ludl Electronic Products, Hawthorne, NY) to individually select for green, red, and blue fluorescence. Images were captured using a cooled 3 CCD camera (Photometrics, Tucson, AZ) mounted on a Zeiss universal microscope (Carl Zeiss) and Optimus Image Analysis software (Bioscan, Edmond, WA) installed on a Compaq computer with a Pentium chip, a frame grabber, an optical disk storage system, and a Sony Mavigraph UP-D7000 Digital Color Printer (Tokyo, Japan). Images were further processed using Adobe Photoshop software (Adobe Systems, Mountain View, CA). For the CXCR4 and EGFR double staining, CXCR4-positive cells were identified by red fluorescence, and the EGFR and

HER2-neu were identified by green fluorescence. Cells with localized yellow fluorescence within the cytoplasm and membrane were considered "$CXCR4^+/EGFR^+$" cells, and cells with colocalized green fluorescence in membrane and red fluorescence in cytoplasm were considered $CXCR4^+$/HER2-neu cells.

Statistical methods

The SPSS 10.1 software package (SPSS, Inc., Chicago, IL) was used in statistical analysis. Expression of biomarkers in primary tumors was correlated with the presence of ITC in BM and histopathologic characteristics by chi-square test or two-tailed Fisher's exact test. A *P*-value of less than 0.05 was considered to be statistically significant.

Results

BM aspirates were obtained from 18 patients with primary breast cancer. Median age was 45 (38–76). Among those, 13 patients (72%) had T2 or T3 tumors (> 2 cm), and 12 patients (67%) had axillary lymph node involvement. Therefore, the majority of patients were of a high-risk patient population. In the current study, CK positivity in BM was found to be 33% (6/18), and the median number of CK^+ cells was 236 (20–847) per 5×10^4 enriched BM cells.

High expression of CXCR4 was demonstrated in 39% of our patient population (7/18). No significant associations could be found between the presence of ITC in BM, and tumor characteristics including histological type, high NG or HG along with biomarker expressions including ER or PR positivity, PCNA, HER2-neu or EGFR positivity (Table 2). However, ITC positivity in BM was found to be significantly associated with increased expression of CXCR4 alone (CXCR4 with ITC positivity in BM, 83% vs. other 17%, $P = 0.013$). Similarly, tumors of patients with ITC positivity in BM were more likely to coexpress CXCR4/EGFR ($P = 0.005$), CXCR4/HER2-neu ($P = 0.025$) or CXCR4/HER2-neu/EGFR ($P = 0.025$).

Tumors of the three patients with high numbers of CK^+ cells in BM (> 236 CK^+ per 5×10^4 enriched BM cells), exclusively expressed high levels of CXCR4 with EGFR/HER2-neu, whereas this expression pattern was not observed in other patients. Therefore, primary tumors of patients with high numbers of CK^+ cells in BM were more likely to coexpress CXCR4/HER2-neu/EGFR or CXCR4/HER2-neu compared with the other tumors in this study ($P = 0.001$). Figure 2 shows coexpression of CXCR4 with HER2/neu or EGFR in a primary tumor specimen of a patient with high CK positivity in BM by immunofluorescence double staining.

Furthermore, tumor size and axillary lymph node status of the patients, and tumor characteristics including NG and HG were correlated with biomarker expressions including ER/PR, PCNA, EGFR, HER2-neu, CXCR4, CXCR4/HER2-neu, CXCR4/EGFR, and CXCR4/HER2-neu/EGFR. Tumors with high NG or HG were more likely to have high PCNA positivity than tumors with intermediate NG (11/11 vs. 4/7, $P = 0.043$) or HG positivity (10/10 vs. 5/8, $P = 0.069$), respectively. No other statistical associations could be found in this small series (data not shown).

Discussion

In this study, we found that CXCR4 overexpression in primary tumors alone or coexpressed with HER2-neu

Table 2. Tumor characteristics of patients with/without ITC in bone marrow.

Variable	ITC (−) (n = 12)	ITC (+) (n = 6)	*P*-value
Invasive ductal	9 (75%)	5 (83%)	0.999
NG 3	7 (58%)	4 (67%)	0.999
HG 3	8 (75%)	2 (33%)	0.321
ER positivity	7 (58%)	5 (83%)	0.600
PR positivity	6 (50%)	5 (83%)	0.316
PCNA	10 (83%)	5 (83%)	0.999
HER2/neu overexpression	4 (33%)	3 (50%)	0.627
EGFR expression	2 (17%)	4 (67%)	0.107
High CXCR4 expression	2 (17%)	5 (83%)	0.013
CXCR4/EGFR coexpression	0 (0%)	4 (67%)	0.005
CXCR4/HER2/neu coexpression	0 (0%)	3 (50%)	0.025
CXCR4/EGFR/HER2/neu coexpression	0 (0%)	3 (50%)	0.025

ITC, isolated tumor cells; NG, nuclear grade; HG, histologic grade; ER, estrogen receptor; PR, progesterone receptor; EGFR, epidermal growth factor receptor; PCNA, proliferating cell nuclear antigen. Presence of ITC was determined by CK^+ by flow-cytometry per 5×10^4 enriched BM cells. HG was determined according to Richardson–Bloom Classification. ER, PR, and PCNA were considered as positive if the nuclear staining was >10%. HER2-neu was considered positive, if more than 10% of the tumor cells showed a complete and strong membranous staining. For EGFR, any positive membranous staining was considered as positive. High expression of CXCR4 was considered positive, if >30% or >50% of the tumor cells showed strong or moderate cytoplasmic staining, respectively.

and/or EGFR could predict the presence of ITC in BM in patients with breast cancer. CXCR4 is a G protein-coupled chemokine receptor for the ligand SDF-1α, which plays a critical role in leukocyte trafficking, and HIV-1 infection. A role in metastasis of breast carcinoma has been suggested more recently [9, 10]. The ligand SDF-1α was found in high levels in organs representing the major sites of breast-cancer metastases, i.e. the lymph node, lung, liver, and BM. Furthermore, the migration of breast-cancer cells in response to conditioned medium from human BM was shown to be significantly reduced in the presence of CXCR4-blocking antibodies [9].

SDF-1α/CXCR4 interactions were also shown to play an important role in homing of other malignant cells, including neuroblastoma, leukemia cells and prostate cancer cells to BM [11–14]. SH-SY5Y neuroblastoma cells were shown to interact at multiple levels with BM components, as evidenced by the fact that conditioned medium derived from MBA2.1 BM stromal cells promoted SH-SY5Y cell migration, adhesion to BM stromal cells, and proliferation [11]. Furthermore, Russell et al. [12] recently reported that high expression of CXCR4 in primary tumors was associated with bone and bone marrow metastases in patients with neuroblastoma. Prostate cancer cells were also observed migrating across BM endothelial cell monolayers in response to SDF-1α [14]. Pretreatment of the prostate cancer cells with SDF-1α significantly increased their adhesion and invasion *in vitro* to BM endothelial cell lines, which could be inhibited by antibody to CXCR4. All these results suggest that interactions between CXCR4 expressed in cancer cells and SDF-1α secreted by the BM microenvironment may play an important role in the development of BM metastases.

Both EGFR and HER2-neu have been implicated in malignant progression in many human cancers including breast, gastric, glioblastoma, and squamous cell carcinomas [22–24]. Based on our previous observations of SDF-1α-induced HER2-neu and EGFR transactivation through CXCR4 in breast cancer cells [16], we also evaluated the value of coexpression of CXCR4 with HER2-neu or EGFR in primary tumors. Li et al. [25] recently reported a correlation between CXCR4 and HER2-neu, and found that HER2-neu overexpression increased the expression of the chemokine receptor CXCR4, and reduced ligand-induced CXCR4 degradation. Our findings in the present study suggest that patients with CXCR4 coexpression with HER2-neu and/or EGFR in primary breast tumors were more likely to have high CK-positivity in BM. HER2-neu overexpression has frequently been found in CK-positive ITCs in the BM of breast cancer patients [15, 26, 27], and has been reported as a poor prognostic factor in breast cancer [15]. Similarly, EGFR expression has been demonstrated in CK-positive cells in BM of breast cancer and colorectal cancer patients [28, 29]. CXCR4 has been suggested to be critical for the outgrowth of micrometastatic colon carcinoma cells [30]. We similarly found that SDF-1α increased tumor colony formation of MDA-MB-231 breast cancer cells (unpublished, Cabioglu and Price). These results suggest an increased tumorigenic potential through SDF-1α stimulation of CXCR4 that might give a survival advantage to CXCR4 and HER2-neu and EGFR coexpressing micrometastatic cancer cells. Since increased number of ITCs in the BM in breast cancer patients have been reported as a poor prognostic factor [31], CXCR4 coexpressed with HER2-neu and/or EGFR might be also a poor prognostic indicator in breast cancer that further merits investigation.

In the present study, one third of the patients with operable breast cancer were found to have ITCs in BM detected by an immunomagnetic enrichment technique followed by flow-cytometry. This rate is comparable with other studies of operable breast cancer patients, which reported an ITC incidence between 29 and 43% by immunocytochemistry [1–5], or between 16 and 25% by immunomagnetic enrichment and immunocytochemistry techniques [6, 32, 33]. The flow-cytometric procedure combined with immunomagnetic enrichment in the current study has been demonstrated to be a more sensitive technique than immunocytochemistry alone as has been shown to identify one tumor cell in 10^7–10^8 mononuclear cells [18, 34]. However, the anti-cytokeratin antibody CAM5.2 against cytokeratin 7/8 that was used for this procedure has been reported to show CK-positive circulating peripheral blood cells in some healthy samples [34, 35]. We therefore considered the positivity of ITC as the presence of CK^+ cells in both of the gates including the entire enriched BM cells and a specific gate for MCF-7 breast cancer cells in flow-cytometric evaluation as we reported before [19] and illustrated in Figure 1. This approach can also eliminate any false positivity due to the nonspecific binding that might occur during magnetic enrichment or the possible artifacts during flow-cytometric assessment [34]. Even though the median number of CK-positive cells appears to be higher (236 per 5×10^4 enriched BM cells) in our study than previous studies reporting 1–9 CK-positive cells per BM sample by using immunocytochemistry alone or combined with an enrichment procedure [2, 6, 36], it may not be relevant to compare our findings with those studies due to the following reasons: First, we evaluated the entire BM sample (10 cc), which corresponds to $2.5–5 \times 10^7$ mononuclear cells before enrichment, unlike other studies using buffy coat upon Ficoll density gradient separation and/or evaluating 2×10^6 mononuclear cells. Second, cell loss might occur in samples upon cytocentrifugation by immunocytochemistry techniques alone or combined with enrichment. Finally, the median number of CK^+ cells given is a proportional flow-cytometric estimate per 5×10^4 BM cells enriched with CK 7/8 antibody-coupled magnetic beads that could be approximately obtained from 10 cc BM cells. It appears that although flow-cytometry does not provide morphological evidence of tumor cells as does immunocytochemistry, careful adjustments of the flow-cytometric settings according to

the negative and positive controls may improve its feasibility in detection of ITCs without the use of additional diagnostic techniques.

In conclusion, our preliminary findings support the hypothesis that increased CXCR4 expression in breast cancer cells may play an important role in homing to BM, where its ligand SDF-1α is expressed in high levels. Coexpression of HER2/neu and/or EGFR with CXCR4 in primary tumors may increase the invasive and tumorigenic capacity of these potentially dormant ITC in BM. Whether CXCR4 alone, or coexpressed with HER2-neu and/or EGFR is associated with poor prognosis in breast cancer, should be investigated in a larger of patients.

Acknowledgements

This work was supported by DAMD17-02-0455 and NIH/NCI Cancer Center Support Grant CA 16672 (to J.E.P.) and by the Research Fund of the University of Istanbul (T-753/251099, to A.I. and E.O.Y.).

References

1. Diel IJ, Costa SD, Holle R et al. Micrometastatic breast cancer cells in bone marrow at primary surgery: Prognostic value in comparison with nodal status. J Natl Cancer Inst 1996; 88:1652–64.
2. Braun S, Pantel K, Müller P et al. Cytokeratin-positive cells in the bone marrow and survival of patients with stage I, II, or III breast cancer. N Engl J Med 2000; 343(4): 525–33.
3. Solomayer EF, Diel IJ, Salanti G et al. Time independence of the prognostic impact of tumor cell detection in the bone marrow of primary breast cancer patients. Clin Cancer Res 2001; 74102–8.
4. Braun S, Cevatli BS, Assemi C et al. Comparative analysis of micrometastasis to the bone marrow and lymph nodes of node-negative breast cancer patients receiving no adjuvant therapy. J Clin Oncol 2001; 19(5): 1468–75.
5. Gerber B, Krause A, Müller H et al. Simultaneous immunohistochemical detection of tumor cells in lymph nodes and bone marrow aspirates in breast cancer and its correlation with other prognostic factors. J Clin Oncol 2001; 19(4): 960–71.
6. Naume B, Borgen E, Kvalheim G et al. Detection of isolated tumor cells in bone marrow in early-stage breast carcinoma patients: comparison with preoperative clinical parameters and primary tumor characteristics. Clin Cancer Res 2001; 7(12): 4122–29.
7. Menard S, Squicciarini P, Luini A et al. Immunodetection of bone marrow micrometastases in breast carcinoma patients and its correlation with primary tumour prognostic features. Br J Cancer 1994; 69(6): 1126–9.
8. Schindlbeck C, Janni W, Shabani N et al. Comparative analysis between the HER2 status primary breast cancer tissue and the detection of isolated tumor cells in the bone marrow. Breast Cancer Res Treat 2004; 87: 65–74.
9. Muller A, Homey B, Soto H et al. Involvement of chemokine receptors in breast cancer metastases. Nature 2001; 410(6824): 50–6.
10. Smith MCP, Luker KE, Garbow JR et al. CXCR4 regulates growth of both primary and metastatic breast cancer. Cancer Res 2004; 64: 8604–12.
11. Geminder H, Sagi-Assif O, Goldberg L et al. A possible role for CXCR4 and its ligand, the CXC chemokine stromal cell-derived factor-1, in the development of bone marrow metastases in neuroblastoma. J Immunol 2001; 167(8): 4747–57.
12. Russell HV, Hicks J, Okcu MF, Nuchtern JG. CXCR4 expression in neuroblastoma primary tumors is associated with clinical presentation of bone and bone marrow metastases. J Pediatr Surg 2004; 39(10): 1506–11.
13. Shen W, Bendall LJ, Gottlieb DJ, Bradstock K. The chemokine receptor CXCR4 enhances integrin-mediated *in vitro* adhesion and facilitates engraftment of leukemic precursor-B cells in the bone marrow. Exp Hematol 2001; 29(12): 1439–47.
14. Taichman RS, Cooper C, Keller ET et al. Use of the stromal cell-derived factor-1/CXCR4 pathway in prostate cancer metastasis to bone. Cancer Res 2002; 62(6): 1832–7.
15. Braun S, Schlimock G, Heumos I et al. Erb2 overexpression on occult metastatic cells in bone marrow predicts poor clinical outcome of stage I-III breast cancer patients. Cancer Res 2001; 61(5): 1890–5.
16. Cabioglu N, Miller C, Parikh N et al. Crosstalk between CXCR4 and HER2-neu in breast cancer: transactivation of HER2-neu by stromal derived factor-1 alpha through Src kinase activation. Proceedings of 95th American Association for Cancer Research, 95th Annual Meeting, 2004; p. 907.
17. Bloom HJG, Richardson WW. Histologic grading and prognosis in breast cancer. Br J Cancer 1957; 11(3): 359–77.
18. Martin VM, Siewert C, Scharl A et al. Immunomagnetic enrichment of disseminated epithelial tumor cells from peripheral blood by MACS. Exp Hematol 1998; 26(3): 252–64.
19. Cabioglu N, Igci A, Yildirim EO et al. An ultrasensitive tumor enriched flow-cytometric assay for detection of isolated tumor cells in bone marrow of patients with breast cancer. Am J Surg 2002; 184: 414–7.
20. Cabioglu N, Yazici MS, Arun BK et al. Expression of CXCR4 predicts lymph node metastasis in early breast cancer. Annual Meeting Proceedings; the 40th Annual Meeting of the American Society of Clinical Oncology, 2004, p. 9525.
21. Chen B, van den Brekel MWM, Buschers W et al. Validation of tissue array technology in head and neck squamous cell carcinoma. Head Neck 2003; 25:922–30.
22. Niu Y, Fu X, Lv A et al. Potential markers predicting distant metastasis in axillary node-negative breast carcinoma. Int J Cancer 2002; 98(5): 754–60.
23. Suo Z, Risberg B, Kalsson MG et al. EGFR family expression in breast carcinomas. c-erbB-2 and c-erbB-4 receptors have different effects on survival. J Pathol 2002; 196(1): 17–25.
24. Tsutsui S, Ohno S, Murakami S et al. Prognostic value of the combination of epidermal growth factor receptor and c-erbB-2 in breast cancer. Surgery 2003; 133(2): 219–21.
25. Li YM, Pan Y, Wei Y et al. Upregulation of CXCR4 is essential for HER2-mediated tumor metastasis. Cancer Cell 2004; 6:459–69.
26. Braun S, Hepp F, Sommer HL, Pantel K. Tumor-antigen heterogeneity of disseminated breast cancer cells: implications for immunotherapy of minimal residual disease. Int J Cancer (Pred Oncol) 1999; 84:1–5.
27. Forus A, Høifødt HK, Øverli GET et al Sensitive fluorescent in situ hybridisation method for the characterisation of breast cancer cells in bone marrow aspirates. J Clin Pathol Mol Pathol 1999; 52:68–74.
28. Schlimock G, Riethmuller G. Detection, characterization and tumorigenicity of disseminated tumor cells in human bone marrow. Semin Cancer Biol 1990; 1:207–15.
29. Schlimock G, Funke I, Bock B et al. Epithelial tumor cells in bone marrow of patients with colorectal cancer: Immunocytochemical detection, phenotypic characterization, and prognostic significance. J Clin Oncol 1990; 8:831–7.
30. Zeelenberg IS, Ruuls-Van Stalle L, Roos E. The chemokine receptor CXCR4 is required for outgrowth of colon carcinoma micrometastases. Cancer Res 2003; 63(13): 3833–9.
31. Janni W, Gastroph S, Hepp F et al. Prognostic significance of an increased number of micrometastatic tumor cells in the bone marrow of patients with first recurrence of breast carcinoma. Cancer 2000; 88:2252–9.

32. Naume B, Boregen E, Nesland JM et al. Increased sensitivity for detection of micrometastases in bone-marrow/peripheral-blood stem-cell products from breast-cancer patients by negative immunomagnetic seperation. Int J Cancer 1998; 78: 556–60.
33. Kasimir-Bauer S, Oberhoff C, Sliwinska K et al. Evaluation of different methods for the detection of minimal residual disease in blood and bone marrow of patients with primary breast cancer: importance for clinical use? Breast Cancer Res Treat 2001; 69: 123–32.
34. Racilla E, Euhus D, Weiss AJ et al. Detection and characterization of carcinoma cells in the blood. Proc Natl Acad Sci USA 1998; 95: 4589–94.
35. Molnar B, Ladanyi A, Tanko L et al. Correspondence re: circulating tumor cell clusters in the peripheral blood of colorectal cancer patients. Clin Cancer Res 2001; 7: 4080–5.
36. Weihrauch MR, Skibowski E, Draube A et al. Immunomagnetic enrichment and detection of isolated tumor cells in bone marrow of patients with epithelial malignancies. Clin Exp Metast 2002; 19: 617–21.

CXCL-12/Stromal Cell–Derived Factor-1α Transactivates HER2-neu in Breast Cancer Cells by a Novel Pathway Involving Src Kinase Activation

Neslihan Cabioglu,[1] Justin Summy,[1] Claudia Miller,[1] Nila U. Parikh,[1] Aysegul A. Sahin,[2] Sitki Tuzlali,[3] Kevin Pumiglia,[4] Gary E. Gallick,[1] and Janet E. Price[1]

Departments of [1]Cancer Biology and [2]Pathology, The University of Texas M.D. Anderson Cancer Center, Houston, Texas; [3]Department of Pathology, Istanbul Faculty of Medicine, Istanbul University, Istanbul, Turkey; and [4]Center for Cell Biology and Cancer Research, Albany Medical College, Albany, New York

Abstract

Experimental evidence suggests that CXCR4, a G_i protein–coupled receptor for the ligand CXCL12/stromal cell–derived factor-1α (SDF-1α), plays a role in breast cancer metastasis. Transactivation of HER2-neu by G protein–coupled receptor activation has been reported as a ligand-independent mechanism of activating tyrosine kinase receptors. We found that SDF-1α transactivated HER2-neu in the breast cancer cell lines MDA-MB-361 and SKBR3, which express both CXCR4 and HER2-neu. AMD3100, a CXCR4 inhibitor, PKI 166, an epidermal growth factor receptor/HER2-neu tyrosine kinase inhibitor, and PP2, a Src kinase inhibitor, each blocked SDF-1α–induced HER2-neu phosphorylation. Blocking Src kinase, with PP2 or using a kinase-inactive Src construct, and inhibiting epidermal growth factor receptor/HER2-neu signaling with PKI 166 each inhibited SDF-1α–stimulated cell migration. We report a novel mechanism of HER2-neu transactivation through SDF-1α stimulation of CXCR4 that involves Src kinase activation. (Cancer Res 2005; 65(15): 6493-7)

Introduction

HER2-neu (ErbB2) is recognized as an indicator of poor prognosis in breast cancer, and substantial evidence exists to suggest that signaling through this receptor contributes to malignant progression. Unlike other members of this receptor family [HER1 (ErbB1 or epidermal growth factor receptor, EGFR), HER3 and HER4] that bind specific ligands [the epidermal growth factor receptor (EGF)-related peptide growth factors] and form heterodimers with HER-2neu, HER2-neu does not seem to have a ligand (1). Increasing evidence suggests that the primary function of HER2-neu is that of a coreceptor (2). Transactivation of EGFR and HER2-neu by endothelin-1, thrombin, and lysophosphatidic acid through activation of seven-transmembrane G protein–coupled receptors has been reported as a ligand-independent mechanism in various types of cancer cells (3). In several studies, the phosphorylation of EGFR by activation of certain G protein–coupled receptors was found to depend on Src kinase activity (4). Chemokine receptors are also members of the G protein–coupled receptor family, which initiate chemotactic and growth signals following interaction with their ligands. Stimulation of CXCR-1/2 chemokine receptors by interleukin-8 has been shown to induce transient phosphorylation of EGFR in ovarian cancer cells, causing rapid activation of the p44/42 mitogen-activated protein kinase (5). Another chemokine receptor, CXCR4, a pertussis toxin–sensitive, G_i protein–coupled receptor for CXCL12/stromal cell–derived factor-1α (referred to as SDF-1α), has recently been shown to have an important role in breast cancer metastasis (6). Given what has been reported on G protein–coupled receptor transactivation, we investigated whether SDF-1α-CXCR4 interactions would increase HER2-neu signaling. We report in this study that SDF-1α induced HER2-neu tyrosine kinase transactivation in breast cancer cells, and that this transactivation involved the activation of Src kinase.

Materials and Methods

Cell culture and reagents. Breast cancer cell lines MDA-MB-361, SKBR3, T47D, and MCF-7 were obtained from the American Type Culture Collection (Manassas, VA). Human recombinant SDF-1α was purchased from R&D Systems (Minneapolis, MN); EGF, pertussis toxin and AMD3100 were purchased from Sigma Chemical Co. (St. Louis, MO); PP2 was purchased from Calbiochem (La Jolla, CA). PKI 166 was provided by Novartis Pharmaceutical (through Dr. I.J. Fidler, University of Texas M.D. Anderson Cancer Center).

Immunohistochemistry for CXCR4 and immunofluorescence staining for CXCR4 and HER2-neu. Primary tumor tissue samples of invasive ductal carcinoma were obtained after informed consent, and approval from institutional ethics committees. Deparaffinized slides of tissues were incubated with mouse anti-human CXCR4 monoclonal antibody (44173.111, IgG_{2b}, R&D Systems) at 1:150 dilution for 18 hours at 4°C. Color was developed with diaminobenzidine after incubation with a rat anti-mouse-IgG_{2b}-horseradish peroxidase (Serotec, Inc., Raleigh, NC). CXCR4 expression was considered high when >50% of tumor cells showed strong cytoplasmic staining.

For immunofluorescence double staining, samples were incubated with the primary antibody as described above, and then with goat anti-mouse antibody conjugated to Alexia-488-FITC (Molecular Probes, Eugene, OR) at 1:400 dilution. The sections were then incubated with rabbit anti-human HER2-neu (Santa Cruz Biotechnology, Santa Cruz, CA) at 1:200 dilution, then with goat anti-rabbit antibody conjugated with Alexia-549 (Molecular Probes) at 1:600 dilution at room temperature for 1 hour. Immunofluorescence staining of MDA-MB-361 cells cultured on glass slides, then fixed in acetone, used the same primary antibodies and Cy5-conjugated anti-mouse IgG, and Cy3-conjugated anti-rabbit IgG (Jackson ImmunoResearch Laboratories, Inc., West Grove, PA). Confocal microscopy was used to examine the localization of CXCR4 and HER2-neu. As negative controls for all staining, replicate samples were incubated with protein-blocking solution instead of primary antibodies.

The HER2-neu-expressing cell lines MDA-MB-361 and SKBR3 were analyzed for CXCR4 and HER2-neu expression by flow cytometry using

Note: N. Cabioglu is currently at the Istanbul Haseki Research Hospital, Istanbul, Turkey.

Requests for reprints: Janet E. Price, Department of Cancer Biology, Unit 173, The University of Texas M.D. Anderson Cancer Center, 1515 Holcombe Boulevard, Houston, TX 77030. Phone: 713-563-5484; Fax: 713-792-8747; E-mail: jprice@mdanderson.org.

anti-HER2-neuFITC and anti-human CXCR4CyChrome and the corresponding isotypic monoclonal control antibodies (BD Biosciences, San Jose, CA).

Quantitative real-time PCR. Total RNA was isolated using TriReagent (Sigma) and reverse-transcribed with random primers from the high capacity cDNA archive kit (Applied Biosystems, Foster City, CA). cDNA was amplified in duplicate samples using the ABI 7000 sequence detection system for the expression of CXCR4 and 18S using predeveloped TaqMan assay reagents (Applied Biosystems) following the manufacturer's recommended amplification procedure. Results were recorded as mean threshold cycle, and relative expression was determined using the comparative threshold cycle method, using human placenta RNA (Promega, Madison, WI) as a calibrator sample.

Immunoblot analysis for HER2-neu, epidermal growth factor receptor, Src, extracellular signal-regulated kinase-1/2, and Akt phosphorylation. Breast cancer cells were plated in culture plates and grown to 50% to 80% confluence. The cultures were serum-starved for 48 hours then stimulated with SDF-1α (10-50 ng/mL) after treatment with AMD3100 (10 μmol/L), pertussis toxin (0.25 μg/mL), PKI 166 (0.5 μmol/L), or PP2 (1 and 2.5 μmol/L) in different combinations. Lysates were prepared from the cells, and aliquots of protein were separated on SDS-polyacrylamide gels and transferred to nitrocellulose membranes. The membranes were hybridized with antibodies in 5% bovine serum albumin (BSA) in TBS and 0.1% Tween 20. Antibodies against phospho-HER2/ErbB2 (Tyr^{1248}), HER2/ErbB2, phospho-EGFR (Tyr^{845}), EGFR, phospho-extracellular signal–regulated kinase (ERK)-1/2, ERK1/2, phospho-Akt, Akt and phospho-Src (Tyr^{416}) were purchased from Cell Signaling Technology (Beverly, MA); antibodies against phospho-Src (Tyr^{215}) and pan-Src were purchased from Biosource (Camarillo, CA). The secondary antibody was horseradish peroxidase–conjugated goat anti-rabbit (Amersham Corp., Arlington Heights, IL), which was detected with the Amersham enhanced chemiluminescence system, following the manufacturer's recommended procedure. Immunoreactive bands were quantified by densitometry using ImageQuant software (Molecular Dynamics, Sunnyvale, CA).

Migration assays. SDF-1α-induced migration was measured using 24-well cell culture inserts with membranes with 8 μm pores (Becton Dickinson, Bedford, MA). Breast cancer cells were suspended in serum-free medium with 0.1% BSA and 1×10^5 cells in 0.5 mL plated in the top part of the insert. PP2 (2.5 μmol/L), PKI 166 (0.5 μmol/L), or DMSO (0.01% v/v) was added to the cell suspension; DMSO was the solvent for stock solutions of the inhibitors. The inserts were placed in wells containing serum-free medium with 0.1% BSA, with or without SDF-1α. After incubation at 37°C for 24 hours, residual cells were wiped off the top of the membranes with cotton swabs, and migrated cells on the underside of the membranes were fixed and stained using the HEMA-3 kit (Fisher Diagnostics, Middletown, VA). Cells were counted in 10 microscope fields of each filter, from three inserts per experimental condition.

SDF-1α-induced migration was measured in MDA-MB-361 cells infected with adenovirus expressing a kinase inactive Src (7), or with a control adenovirus Ad PU1 (8). Cells plated in 35 mm plates were infected with adenovirus at the indicated multiplicity of infection, as described previously (8), then harvested after 48 hours of incubation for the migration assays.

Results

The expression of CXCR4 and HER2-neu in MDA-MB-361 and SKBR3 breast cancer cells was evaluated with double-staining flow cytometry. MDA-MB-361 showed the highest expression of CXCR4 and HER2-neu (Fig. 1*A*). We also examined expression in primary tumor specimens from patients with stage II or stage III breast cancer by immunohistochemistry. Four of 24 patients (17%) showed high CXCR4 and HER2-neu expression. Expression of

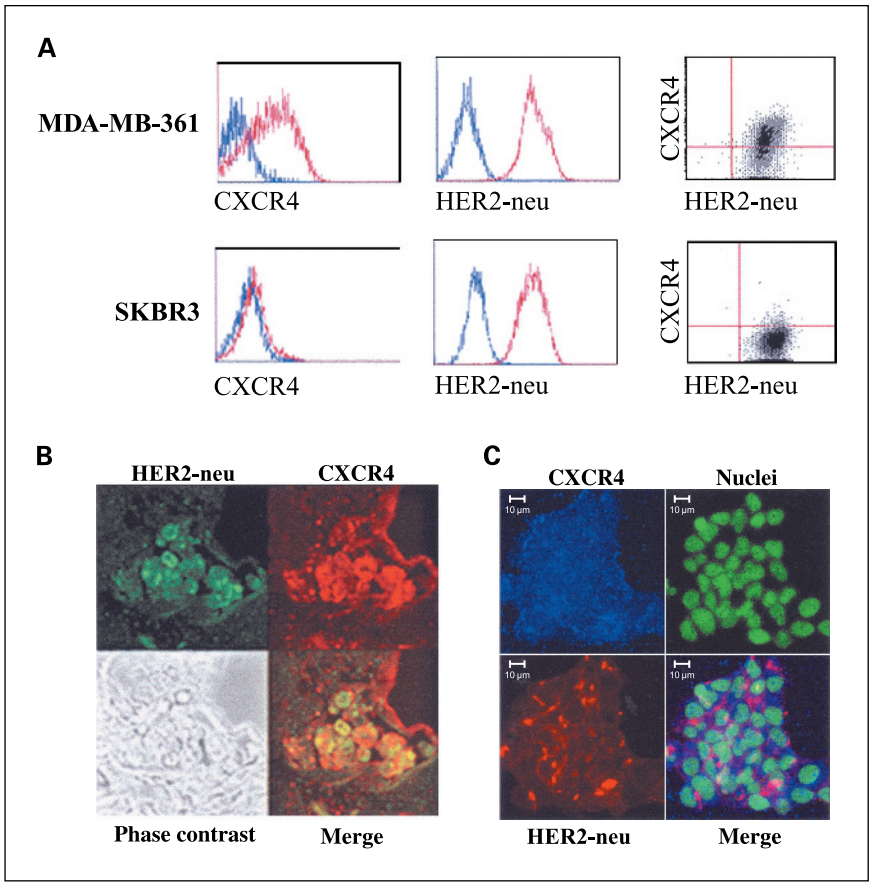

Figure 1. Coexpression of CXCR4 and HER2-neu in breast cancer cells. *A,* flow cytometric analysis shows coexpression of CXCR4 and HER2-neu in MDA-MB-361 and SKBR3, cells with the high CXCR4 and HER2-neu expression. Blue lines, cells incubated with control IgG; red lines, cells incubated with the indicated antibody. *B,* confocal microscopy series of a representative slide showing CXCR4 and HER2-neu coexpression in cells from a primary breast tumor by double immunofluorescence staining. HER2-neu expression was indicated by green fluorescence, and CXCR4 by red fluorescence. Bottom right, yellow fluorescence shows coexpression of the proteins (180× original magnification). *C,* confocal microscopy showing CXCR4 and HER2-neu coexpression in MDA-MB-361 cells *in vitro.* Diffuse and punctate CXCR4 expression is shown by blue fluorescence and HER2-neu expression is shown by red fluorescence. Nuclei were stained with Cytox green (green fluorescence).

CXCR4 and HER2-neu in breast cancer cells in a sample from a patient who developed bone and lung metastases is shown in Fig. 1*B*. Confocal microscopy of MDA-MB-361 cells showed coexpression but not colocalization of HER2-neu and CXCR4 (Fig. 1*C*). This result was the same whether or not the cells were stimulated with SDF-1α (data not shown).

MDA-MB-361 cells were used for *in vitro* studies of responses to SDF-1α as these cells had the highest expression of CXCR4 of a panel of breast cancer cell lines, measured by flow cytometry (Fig. 1*A*) and real-time PCR (data not shown); the PCR results were consistent with a previous report using some of the same cell lines (6). Stimulation with SDF-1α increased the phosphorylation of HER2-neu and Akt in serum-starved cells (Fig. 2*A* and *E*). To show whether the activation of HER2-neu occurred through G protein–dependent mechanisms, MDA-MB-361 cells were preincubated with pertussis toxin (0.25 μg/mL) for 18 hours; this inhibited the SDF-1α-induced HER2-neu phosphorylation (Fig. 2*A*).

To investigate the participation of Src kinase activity in SDF-1α-induced HER2-neu phosphorylation, we examined the phosphorylation of Src in lysates of SDF-1α-treated MDA-MB-361 cells. SDF-1α stimulation increased phosphorylation of Src-Tyr^{416} and Src-Tyr^{215} (Fig. 2*B*), in parallel with induction of HER2-neu phosphorylation. Pretreatment with pertussis toxin inhibited the SDF-1α-induced Src phosphorylation. In separate experiments, treating MDA-MB-361 cells with the Src kinase inhibitor PP2 for 1 hour before stimulation with SDF-1α led to inhibition of SDF-1α-induced HER2-neu phosphorylation (Fig. 2*C*). To confirm the specificity of the action of the SDF-1α and CXCR4, we added AMD3100, an inhibitor of ligand binding to CXCR4 (9), which inhibited the SDF-1α/CXCR4-mediated transactivation of HER2-neu (Fig. 2*D*).

SDF-1α-induced transactivation of receptor tyrosine kinases was shown in SKBR3 cells (Fig. 3*A* and *B*), in which both HER2-neu and EGFR showed increased phosphorylation following treatment with the chemokine. These cells express moderate levels of CXCR4, compared with MDA-MB-361 cells and both EGFR and HER2-neu (10). Stimulation with SDF-1α also increased the phosphorylation of ERK1/2 (Fig. 3*C*). When SKBR3 cells were stimulated with both SDF-1α and EGF, the level of HER2-neu phosphorylation was more than that in cells treated with either ligand alone. Addition of the tyrosine kinase inhibitor PKI 166 inhibited the HER2-neu phosphorylation induced in cells stimulated with either EGF or

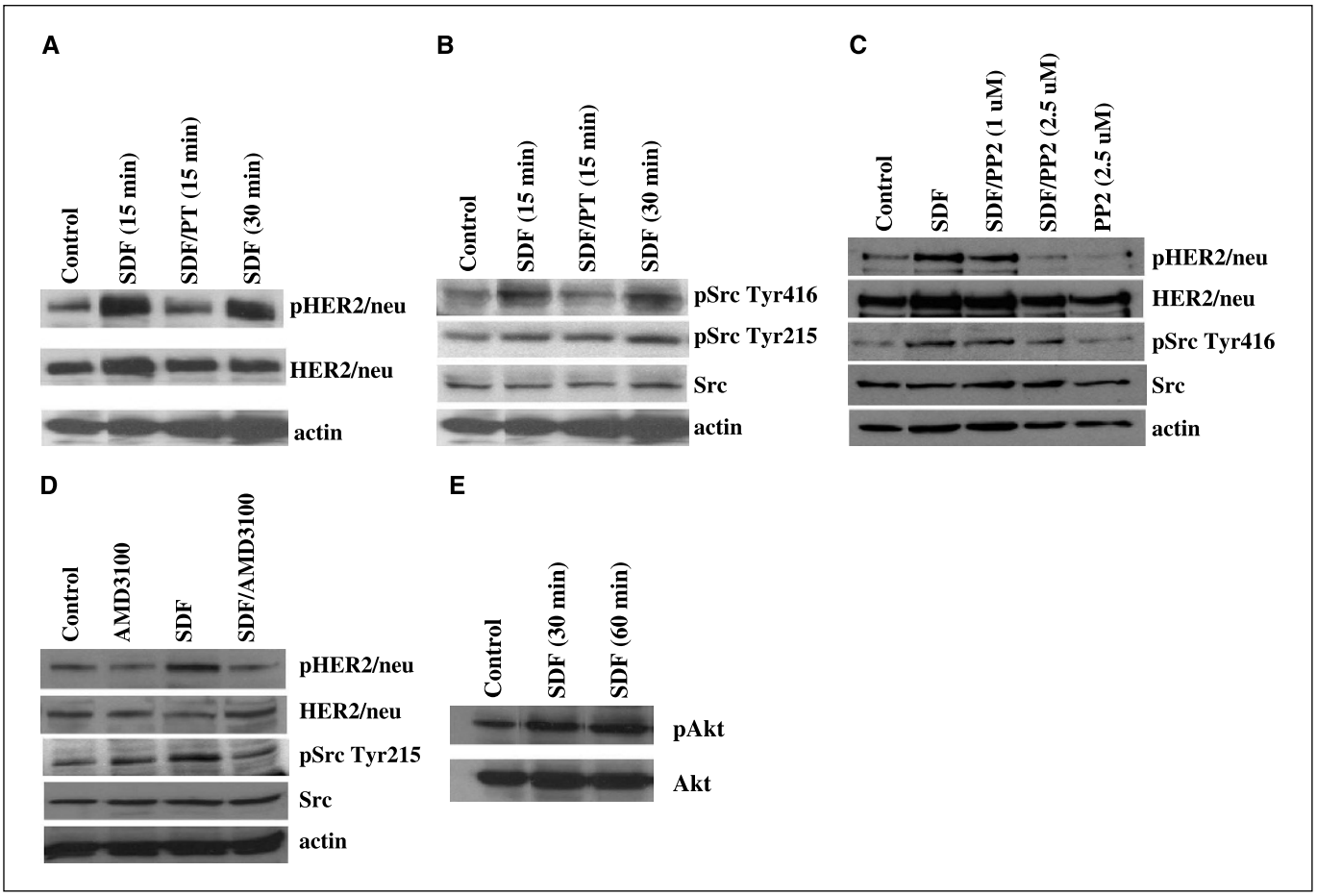

Figure 2. *A,* the effect of pertussis toxin (PT), G_i protein inhibitor, on SDF-1α-induced HER2-neu phosphorylation in MDA-MB-361 breast cancer cells. Western blot analysis shows that phosphorylation of HER2-neu by SDF-1α (10 ng/mL) was inhibited by pretreatment with pertussis toxin (0.25 μg/mL). SDF-1α increased the phosphorylation of HER2-neu by a factor of 7 and 4.1, at 15 and 30 minutes incubation, respectively, based on densitometric analysis; pretreatment with pertussis toxin abrogated this response. *B,* phosphorylation of Tyr^{416} and Tyr^{215} of Src kinase upon stimulation with SDF-1α in MDA-MB-361 cells. The addition of SDF-1α increased the phosphorylation of Src Tyr^{416} by a factor of 6.5, and Tyr^{215} by a factor of 2.4, compared with control. *C,* pretreatment of MDA-MB-361 cells with 1 or 2.5 μmol/L PP2, a Src kinase inhibitor, inhibited SDF-1α-induced phosphorylation of HER2-neu and Src (Tyr^{416}) in MDA-MB-361 cells. *D,* pretreatment of MDA-MB-361 cells with 10 μmol/L AMD3100, a CXCR4 inhibitor, for 1 hour inhibited SDF-1α-induced phosphorylation of HER2-neu and Src (Tyr^{416}). *E,* the addition of SDF-1α increased the phosphorylation of Akt (Ser^{473}) by a factor of 1.6 to 2 in MDA-MB-361 cells after 30 and 60 minutes, respectively.

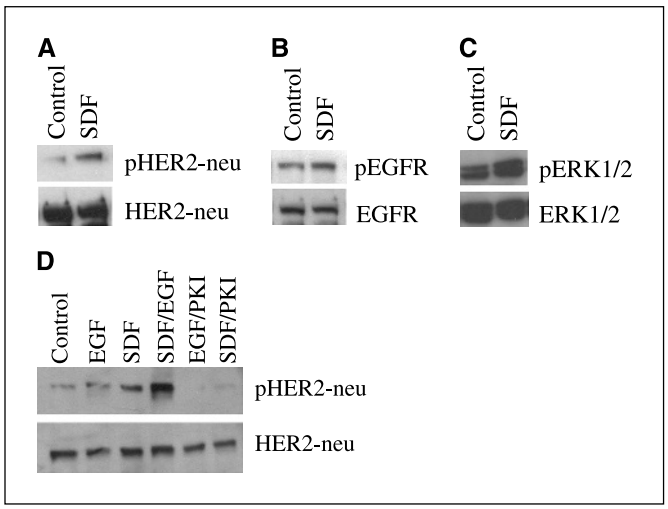

Figure 3. Immunoblot analysis of lysates from SKBR3 cells showing the SDF-1α-induced increases in phosphorylation of HER2-neu (*A*), by a factor of 6.4; EGFR by a factor of 3.4 (*B*), ERK1/2 by a factor of 2.8 (*C*). *D,* EGF and SDF-1α increased phosphorylation of HER2-neu by a factor of 4 and 3, respectively, and the combination of the ligands results in increased phosphorylation by a factor of 13. Addition of PKI 166 (0.5 μmol/L) inhibited phosphorylation induced by either EGF or SDF-1α.

SDF-1α (Fig. 3*D*). In two additional breast cancer cell lines, T47D and MCF-7, which express moderate levels of CXCR4 and relatively less HER2-neu, stimulation with SDF-1α did not induce HER2-neu phosphorylation (data not shown).

A biological response stimulated by SDF-1α was shown in migration assays. SDF-1α promoted the migration of MDA-MB-361 in a dose-dependent manner (Fig. 4*A*). The SDF-1α-induced increase in migration was completely inhibited by the Src kinase inhibitor PP2, or the HER2-neu/EGFR tyrosine kinase inhibitor PKI 166 (Fig. 4*B*), using concentrations of the inhibitors that blocked SDF-1α-induced HER2-neu phosphorylation. Infection of cells with a kinase-inactive Src adenovirus construct substantially reduced the baseline migration of cells and abrogated SDF-1α-induced migration, whereas the migration of cells infected with control adenovirus was significantly increased by the addition of SDF-1α (Fig. 4*C*).

Discussion

This study shows the expression of CXCR4 and HER2-neu in breast cancer specimens and cell lines, and describes a novel mechanism of HER2-neu transactivation induced by SDF-1α/CXCR4 interactions in HER2-neu- and CXCR4-expressing breast cancer cells through a pertussis toxin–sensitive, G protein–dependent signal transduction mechanism. Previous reports (11, 12) similarly showed that stimulation of chemokine receptors resulted in phosphorylation of certain tyrosine kinase receptors, triggered by $G_{i\alpha}$ protein–dependent and -independent signaling pathways, despite the lack of intrinsic tyrosine kinase activity in the chemokine receptors.

Transactivation of EGFR, unlike that of HER2-neu, is a well-documented pathway (3). A recent report suggested crosstalk between EGFR and CXCR4 based on the observation that an inhibitor of the EGFR kinase (AG1478) blocked both SDF-1α-dependent proliferation and ERK1/2 activation (13). Consistent with this report, our results show EGFR transactivation in SKBR3 cells, which express EGFR and HER2-neu, following stimulation with SDF-1α. The few studies addressing HER2-neu receptor kinase transactivation by G protein–coupled receptor used normal prostate stromal cells, or head and neck cancer cells (14, 15). Most previous studies have focused on the mechanisms underlying EGFR transactivation, and members of the Src family of cytoplasmic tyrosine kinases were examined as potential mediators. Src has been reported to induce EGFR tyrosine phosphorylation after stimulation by various different ligands (4). In contrast to EGFR, less is known about the relationship between HER2-neu and c-Src. HER2-neu has been shown to associate with the SH_2 domain of c-Src in a tyrosine phosphorylation–dependent manner, raising the possibility that phosphorylation of HER2-neu increases Src kinase activity as a downstream signaling pathway (10). Transgenic mouse

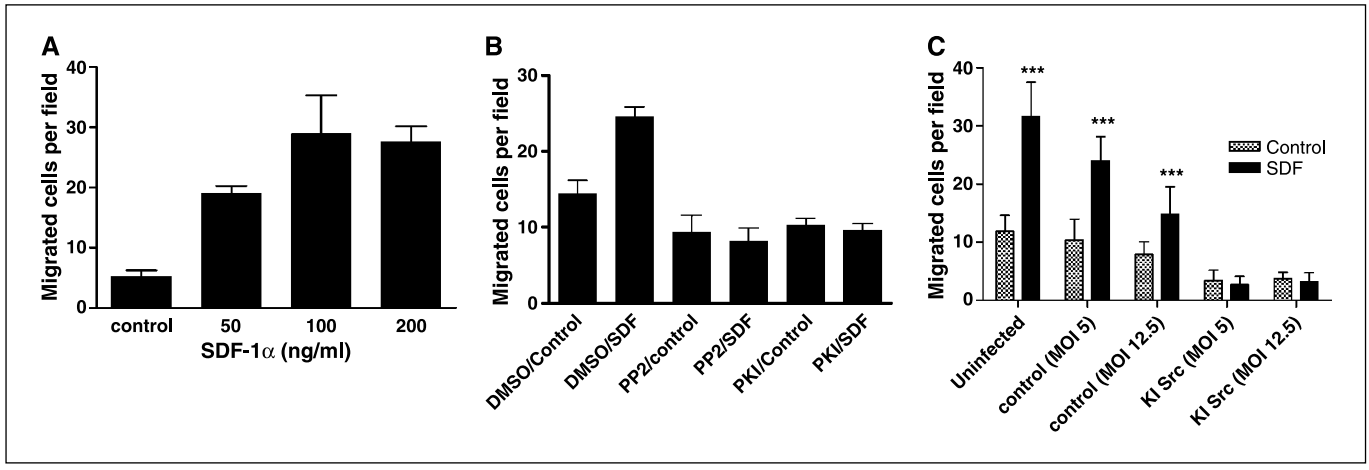

Figure 4. *A,* migration of MDA-MB-361 was stimulated by SDF-1α (50-200 ng/mL) in medium with 0.1% BSA. Cells were plated in the upper chamber of culture well inserts with membranes with 8 μm pores, and with SDF-1α in the lower chamber. After 24 hours of incubation, the membranes were fixed and stained, and cells counted on the underside of the membranes. *B,* the addition of PP2 (2.5 μmol/L) or PKI 166 (0.5 μmol/L) significantly inhibited the migration of cells towards SDF-1α ($P < 0.0001$, Student's *t* test), compared with the control condition, cells treated with 0.01% DMSO. The results shown are the mean and SD from 10 fields counted in triplicate filters, and are representative of repeated experiments. *C,* infection of MDA-MB-361 with adenovirus expressing kinase-inactive Src (KI) abrogated the SDF-1α-induced migration. The cells were incubated for 48 hours with 5 or 12.5 multiplicity of infection of the kinase inactive virus or control adenovirus before plating in culture well inserts. ***, significant increase ($P < 0.0001$, Student's *t* test) in numbers of cells migrating to the underside of the filter in the presence of SDF-1α (100 ng/mL), seen only in uninfected, or control virus–infected cells, but not those expressing kinase-inactive Src.

mammary tumors expressing mutant-activated Neu exhibit a correlative increase in c-Src activity (16). Our results are evidence that Src kinase activation is a component of HER2-neu activation. We showed that SDF-1α/CXCR4 signaling activated Src kinase in breast cancer cells, findings similar to those reported recently with oral squamous cell carcinoma cells (17). As in previous reports, we found that the increase in Src kinase phosphorylation at Tyr^{416} and Tyr^{215} residues correlated with SDF-1α-induced HER2-neu phosphorylation. Even though the biological significance of induction of Src Tyr^{215} is not well understood, ligands such as platelet-derived growth factor and heregulin were shown to induce phosphorylation of this residue (18). Inhibition of Src kinase abolished the SDF-1α-induced HER2-neu phosphorylation, as well as the increased motility of SDF-1α-stimulated MDA-MB-361 cells; the latter was shown using a kinase-inactive Src construct and the PP2 kinase inhibitor. Therefore, the induction of Src kinase by SDF-1α might be important for activating downstream signaling pathways involved in the migration and invasion of cancer cells. SDF-1α has been shown to promote migration and chemoinvasion of breast cancer cells by additional mechanisms. Fernandis et al. showed SDF-1α-induced activation of phosphatidylinositol-3-kinase and focal adhesion complex components (19). Lee et al. showed the involvement of phosphoinositide-3-kinase/Akt and calcium-mediated signaling in SDF-1α-induced breast cancer migration through endothelial cell monolayers (20). Both of these studies used CXCR4-expressing breast cancer cell lines (MDA-MB-231 and DU4475) that do not express high levels of HER2-neu. Thus, different signaling pathways may be activated in breast cancer cells that express CXCR4, but differ in ErbB receptor expression.

We showed SDF-1α-induced HER2-neu phosphorylation in breast cancer cells that express relatively high levels of HER2-neu and either high or moderate CXCR4 expression (MDA-MB-361 and SKBR3, respectively), but not in breast cancer cells with moderate levels of expression, such as T47D and MCF-7. This may suggest that the abundance of HER2-neu may be more critical than that of CXCR4 for SDF-1α-induced transactivation. Confocal microscopy and coimmunoprecipitation of lysates from MDA-MB-361 cells (data not shown) did not show a physical interaction between the two proteins, implying key roles for other intracellular mediators. However, further studies are needed to understand the molecular mechanisms involved in SDF-1α-induced HER2-neu transactivation, including whether the conserved three–amino acid cytoplasmic domain required for ligand-dependent HER2-neu transactivation (21) is essential for chemokine-stimulated transactivation.

In conclusion, our data suggest a novel mechanism of HER2-neu transactivation, through SDF-1α stimulation of the CXCR4 chemokine receptor that involves Src kinase activation. SDF-1α is expressed in organs that are some of the major sites of breast cancer metastasis (6), and signaling through CXCR4 may contribute to critical pathways that determine the survival, invasion, or growth of disseminated HER2-neu-expressing breast cancer cells. Another observation with significance for breast cancer progression is the finding that HER2-neu could enhance the expression of CXCR4, which was required for metastatic colonization by HER2-neu expressing cells (22). Whether the inhibition of CXCR4-mediated signaling with novel CXCR4 targeting drugs can improve HER2-neu targeted therapies merits further study.

Acknowledgments

Received 4/13/2004; revised 5/11/2005; accepted 6/2/2005.

Grant support: In part by DAMD17-02-0455 (to J.E. Price) and NIH/National Cancer Institute Cancer Center Support grant CA 16672.

The costs of publication of this article were defrayed in part by the payment of page charges. This article must therefore be hereby marked *advertisement* in accordance with 18 U.S.C. Section 1734 solely to indicate this fact.

The authors thank Dr. I.J. Fidler for providing PKI 166, Karen Ramirez for expert assistance with flow cytometry, and Christine F. Wogan for editorial assistance. We also gratefully acknowledge the assistance of Dr. Corazon Bucana for confocal microscope images.

References

1. Karunagaran D, Tzahar E, Beerli RR, et al. ErbB-2 is a common auxiliary subunit of NDF and EGF receptors: implications for breast cancer. EMBO J 1996;15:254–64.
2. Klapper LN, Glathe S, Vaisman N, et al. The ErbB-2/HER2 oncoprotein of human carcinomas may function solely as a shared coreceptor for multiple stroma-derived growth factors. Proc Natl Acad Sci U S A 1999;96:4995–5000.
3. Fischer OM, Hart S, Gschwind A, Ullrich A. EGFR signal transactivation in cancer cells. Biochem Soc Trans 2003;31:1203–8.
4. Luttrell DK, Luttrell LM. Not so strange bedfellows: G-protein-coupled receptors and Src family kinases. Oncogene 2004;23:7969–78.
5. Venkatakrishnan G, Salgia R, Groopman JE. Chemokine receptors CXCR-1/2 activate mitogen-activated protein kinase via the epidermal growth factor receptor in ovarian cancer cells. J Biol Chem 2000;275:6868–75.
6. Muller A, Homey B, Soto H, et al. Involvement of chemokine receptors in breast cancer metastasis. Nature 2001;410:50–6.
7. McMullen M, Keller R, Sussman M, Pumiglia K. Vascular endothelial growth factor-mediated activation of p38 is dependent upon Src and RAFTK/Pyk2. Oncogene 2004;23:1275–82.
8. Kim SJ, Johnson M, Koterba K, Herynk MH, Uehara H, Gallick GE. Reduced c-met expression by an adenovirus expressing a c-met ribozyme inhibits tumorigenic growth and lymph node metastases of PC3-LN4 prostate tumor cells in an orthotopic nude mouse model. Clin Cancer Res 2003;9:5161–70.
9. Hatse S, Princen K, Bridger G, De Clercq E, Schols D. Chemokine receptor inhibition by AMD3100 is strictly confined to CXCR4. FEBS Lett 2002;527:255–62.
10. Belsches-Jablonski AP, Biscardi JS, Peavy DR, Tice DA, Romney DA, Parsons SJ. Src family kinases and HER2 interactions in human breast cancer cell growth and survival. Oncogene 2001;20:1465–75.
11. Ganju RK, Brubaker SA, Meyer J, et al. The α-chemokine, stromal cell-derived factor-1α, binds to the transmembrane G-protein-coupled CXCR4 receptor and activates multiple signal transduction pathways. J Biol Chem 1998;273:23169–75.
12. Vlahakis SR, Villasis-Keever A, Gomez T, Vanegas M, Vlahakis N, Paya CV. G protein-coupled chemokine receptors induce both survival and apoptotic signaling pathways. J Immunol 2002;169:5546–54.
13. Porcile C, Bajetto A, Barbero S, Pirani P, Schettini G. CXCR4 activation induces epidermal growth factor receptor transactivation in an ovarian cancer cell line. Ann N Y Acad Sci 2004;1030:162–9.
14. Lin J, Freeman MR. Transactivation of ErbB1 and ErbB2 receptors by angiotensin II in normal human prostate stromal cells. Prostate 2003;54:1–7.
15. Gschwind A, Prenzel N, Ullrich A. Lysophosphatidic acid-induced squamous cell carcinoma cell proliferation and motility involves epidermal growth receptor signal transactivation. Cancer Res 2002;62:6329–36.
16. Muthuswamy SK, Siegel PM, Dankort DL, Webster MA, Muller WJ. Mammary tumors expressing the neu proto-oncogene possess elevated c-src tyrosine kinase activity. Mol Cell Biol 1994;14:735–43.
17. Uchida D, Begum NM, Almofti A, et al. Possible role of stromal-cell-derived factor-1/CXCR4 signaling on lymph node metastasis of oral squamous cell carcinoma. Exp Cell Res 2003;290:289–302.
18. Vadlamudi RK, Sahin AA, Adam L, Wang R, Kumar R. Heregulin and HER2 signaling selectively activates c-src phosphorylation at tyrosine 215. FEBS Lett 2003;543:76–80.
19. Fernandis AZ, Prasad A, Band H, Klösel R, Ganju RK. Regulation of CXCR4-mediated chemotaxis and chemoinvasion of breast cancer cells. Oncogene 2004;23:157–67.
20. Lee B-C, Lee T-H, Avraham S, Avraham HK. Involvement of the chemokine receptor CXCR4 and its ligand stromal cell-derived factor 1α in breast cancer cell migration through human brain microvascular endothelial cells. Mol Cancer Res 2004;2:327–38.
21. Penuel E, Schaefer G, Akita RW, Sliwkowski MX. Structural requirements for ErbB2 transactivation. Semin Oncol 2001;28:36–42.
22. Li YM, Pan Y, Wei Y, et al. Upregulation of CXCR4 is essential for HER2-mediated tumor metastasis. Cancer Cell 2004;6:459–69.